Aalto University
School of Chemical
Engineering

Nelli Jämsä

MODEL PREDICTIVE CONTROL FOR THE TENNESSEE EASTMAN PROCESS

Master's Programme in Chemical, Biochemical and Materials Engineering
Major in Chemical and Process Engineering

Master's thesis for the degree of Master of Science in Technology submitted for inspection, Espoo, 22 January, 2017.

Supervisor	Professor Sirkka-Liisa Jämsä-Jounela
Instructor	D.Sc. (Tech.) Markus Kettunen
Instructor	D.Sc. (Tech.) Yancho Todorov

Aalto University
School of Chemical Engineering

Aalto University, P.O. BOX 11000, 00076 AALTO
www.aalto.fi

Abstract of bachelor's thesis

Author Nelli Jämsä	
Title of thesis Model Predictive Control for the Tennessee Eastman Process	
Degree programme Master's Programme in Chemical, Biochemical and Materials Engineering	
Major Chemical and Process Engineering	
Supervisor Professor Sirkka-Liisa Jämsä-Jounela	
Thesis advisor(s) D.Sc. (Tech.) Markus Kettunen, D.Sc. (Tech.) Yancho Todorov	
Date 22.01.2018 **Number of pages** 68	**Language** English

Abstract

This thesis aims to design a multivariable Model Predictive Control (MPC) scheme for a complex industrial process. The focus of the thesis is on the implementation and testing of a linear MPC control strategy combined with fault detection and diagnosis methods.

The studied control methodology is based on a linear time invariant state-space model and the quadratic programming optimization procedure. The control scheme is realized as a supervisory one, where the MPC is used to calculate the optimal set point trajectories for the lower level PI controllers, thus aiming to decrease the fluctuations in the end product flows.

The Tennessee Eastman (TE) process is used as the testing environment. The TE process is a benchmark based on a real process modified for testing. It has five units, four reactants, an inert, two products and a byproduct. The control objective is to maintain the production rate and the product quality at the desired level. To achieve this, the MPC implemented in this thesis gives setpoints to three stabilizing PI control loops around the reactor and the product stripper. The performance of the designed control systems is evaluated by inducing process disturbances, setpoint changes, and faults for two operational regimes. The obtained results show the efficiency of the adopted approach in handling disturbances and flexibility in control of different operational regimes without the need of retuning. To suppress the effects caused by faults, an additional level that provides fault detection and controller reconfiguration should be developed as further research.

Keywords MPC, FTC, Tennessee Eastman

Tekijä Nelli Jämsä

Työn nimi Malliprediktiivinen säädin Tennessee Eastman prosessille

Koulutusohjelma Master's Programme in Chemical, Biochemical and Materials Engineering

Pääaine Chemical and Process Engineering

Työn valvoja Professori Sirkka-Liisa Jämsä-Jounela

Työn ohjaaja(t)/Työn tarkastaja(t) TkT Markus Kettunen, TkT Yancho Todorov

Päivämäärä 22.01.2018 **Sivumäärä** 68 **Kieli** englanti

Tiivistelmä

Tämän diplomityön tavoite on suunnitella monimuuttujainen-malliprediktiivinen säädin (MPC) teolliselle prosessille. Diplomityö keskittyy toteuttamaan ja testaamaan lineaarisen MPC strategian, joka yhdistettynä vikojen havainnointiin ja tunnistukseen sekä uudelleen konfigurointiin voidaan laajentaa vikasietoiseksi.

Tutkittu säätöstrategia perustuu lineaariseen ajan suhteen muuttumattomaan tilataso-malliin ja neliöllisen ohjelmoinnin optimointimenetelmään. Säätö on toteutettu nk. ylemmän tason järjestelmänä, eli MPC:tä käytetään laskemaan optimaaliset asetusarvot alemman säätötason PI säätimille, tavoitteena vähentää vaihtelua lopputuotteen virroissa.

Tennessee Eastman (TE) prosessia käytetään testiympäristönä. TE on testiprosessi, joka perustuu todelliseen teollisuuden prosessiin ja jota on muokattu testauskäyttöön sopivaksi. Prosessissa on viisi yksikköä, neljä lähtöainetta, inertti, kaksi tuotetta ja yksi sivutuote. Säätötavoite on ylläpitää haluttu taso tuotannon määrässä ja laadussa. Tämän saavuttamiseksi tässä diplomityössä toteutettu MPC antaa asetusarvoja kolmelle stabiloivalle PI-säätimelle reaktorin ja stripperin hallinnassa. Säätösysteemin suorituskykyä arvioitiin aiheuttamalla prosessiin häiriöitä, asetusarvon muutoksia ja vikoja eri operatiivisissa olosuhteissa. Saavutetut tulokset osoittavat valitun menetelmän tehokkuuden häiriöiden käsittelyyn ja joustavaan säätöön eri olosuhteissa. Tutkimuksen jatkokehityksenä vikojen vaikutuksen vaimentamiseksi säätöön tulisi lisätä taso, joka havaitsee viat ja uudelleen konfiguroi säätimen sen mukaisesti.

Avainsanat MPC, FTC, Tennessee Eastman

Preface

After almost a year of work the thesis is finally done. I would like to thank both my advisors D.Sc. Yancho Todorov and D.Sc. Markus Kettunen for all their patience and help. I would also like to thank my thesis supervisor Professor Sirkka-Liisa Jämsä-Jounela for giving me this opportunity and enough time to reach a version we could be satisfied with. Last but not least, I would like to thank my family and friends for their support during my whole studies.

22nd January 2018, Espoo

Nelli Jämsä

Contents

LIST OF ABBREVIATIONS

CSTR	Continuous Stirred Tank Reactor
FDD	Fault Detection and Diagnosis
FDI	Fault Detection and Isolation
FTC	Fault Tolerant Control
PFTCS	Passive Fault Tolerant Control System
AFTCS	Active Fault Tolerant Control System
MPC	Model Predictive Control
DMPC	Distributed Model Predictive Control
PCA	Principal Component Analysis
PLS	Partial Least Squares
RHC	Receding horizon control
SCP	Shell Control Problem
SMI	Subspace Model Identification
TE	Tennessee Eastman
TS	Takagi-Sugeno

LIST OF SYMBOLS

A, C, D, E	TE reactants
B	TE inert
G, H	TE products
F	TE byproduct
$r(t+k)$	Reference signal
$u(t\|t)$	First control signal
$u(t+k\|t)$	Future control signals
$w(t+k)$	Reference trajectory
$y(k)$)	Measured process output
$\hat{y}(k)$	Predicted output
N_1	Minimum cost horizon
N_2	Maximum cost horizon
N_u	Control horizon
$\delta(j)$	Coefficient (cost function)
$\lambda(j)$	Coefficient (cost function)
T_c	Critical reaction time
T_f	Time of fault
T_r	Time the FDD and control reconfiguration take

Literature part

1 Introduction

Model predictive control (MPC) was first advocated in the late seventies by (Richalet, Rault et al. 1976), but it was preceded by necessary concepts such as optimality that were discussed for example by (Bellman 1957) and (Lee, Markus 1967). A closely related methodology called generalized predictive control was developed in the eighties by (Clarke, Mohtadi et al. 1987) and others.

Model predictive control has experienced explosive growth especially in the process industry, where it has proved to be a highly successful method of multivariable control. This success is mostly due to the fact that the MPC is conceptually simple and able to control complex multivariable systems. (Mayne 2014)

Industrial processes must be reliable, profitable, and safe. Processes rely on automation, which increases the vulnerability to faults. A fault is a failure of a control or process element that affects the behavior of the plant. The fault could be for example a faulty sensor or a stuck valve, and it can cause physical damage to equipment, increased energy usage, process downtime, and hazard to environment or personnel. Because of this, research into fault detection and diagnosis, and fault tolerant control systems have received much attention in recent years.

The Tennessee Eastman process (Downs, Vogel 1993) is a simulated complex industrial process. It is based on a real process and its properties were modified for use as a test problem. It can be used to study applications such as plant-wide control strategy, multivariable control, predictive control, and diagnostics.

The focus of this thesis is the design and evaluation of the performance of a MPC, which can later be combined with fault detection and diagnosis methods and reconfigured into fault tolerant control for a complex industrial processes.

The thesis consists of separate literature and experimental parts. The literature part introduces the important aspects of both MPC and fault tolerance in Chapters 2 and 3. Chapter 4 introduces some examples of the previous work in the field. In the experimental part the Tennessee Eastman process is described in Chapter 5. Chapter 6 describes the implementation of the MPC. Chapters 7 and 8 show the dynamic behavior of the process, and the effect of faults. Chapter 9 presents a summary of the experimental part and Chapter 10 outlines the main findings and conclusions.

2 Receding horizon principle and model predictive control

The term MPC does not describe a specific control strategy, but rather any type of control that uses a process model for calculation of the control signal (Camacho, Bordons 2007). Instead of a laborious offline computation to obtain a control law ($u = k(x)$), the MPC solves online a constrained dynamic optimal control problem.

The different MPC methods lead to controllers with the same basic structure and adequate degrees of freedom. All predictive controllers have the following ideas to varying degrees:

- The explicit use of a process model for prediction of the process outputs
- The calculation of the control sequence that minimizes the objective function
- Receding horizon control.

These methods differ from each other only in the model they use to describe the process and its disturbances, and the objective function to be minimized. (Camacho, Bordons 2007)

Receding horizon control (RHC) is a concept where the optimization problem is solved over a number of future samples at the current time, and the first step of the resulting control law is implemented on the system. This is repeated at every instant the controller is run. (Park, Lee et al. 1999) The optimized control sequence is an open loop control, but it becomes closed loop because only the first element is applied, and every new instant has new measurements from the process. (Seron, Goodwin et al. 2003) See Figure 1.

The main advantage of receding horizon over infinite horizon control is its ability to handle constraints on the inputs, states, or outputs of the system. The constraints are treated simply as conditions that must be satisfied in solving the optimization problem. This makes it particularly suitable for time-varying systems and has been a key feature for its success in industry. (Park, Lee et al. 1999, Seron, Goodwin et al. 2003)

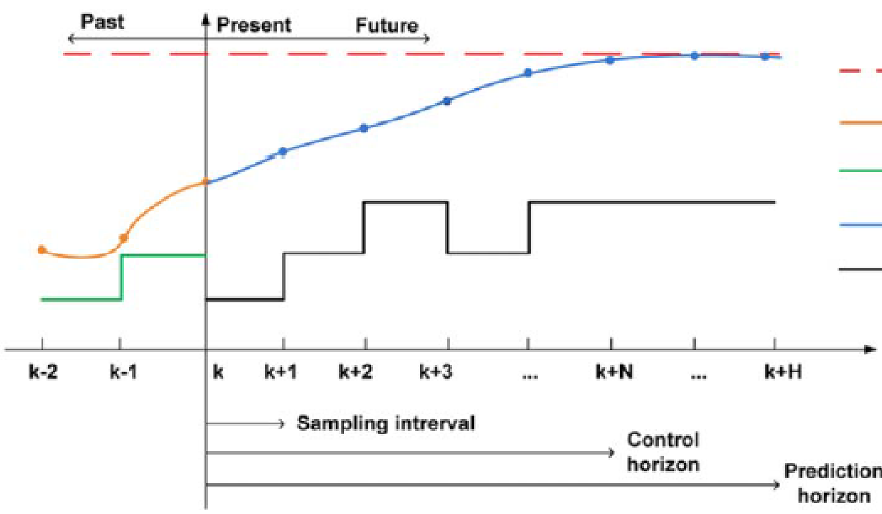

Fig. 1. Receding Horizon control (Charitopoulos, Dua 2016)

Model predictive control has several advantages over other control methods, these include:

- its attractiveness to personnel with limited control knowledge (the concept is intuitive and the controller easy to tune)
- its suitability for a wide variety of processes, from simple to complex dynamics, and even long delays and instability
- its suitability for multivariable processes

- its intrinsic ability to compensate for dead times
- its ability to use feed forward control to compensate for measured disturbances
- its ability to handle constraints
- its openness which allows for new extensions and applications.

(Camacho, Bordons 2007)

However, as is always the case, the MPC also has drawbacks:

- *Derivation of the controller*: In MPC the control law is usually easy to implement and does not require rigorous computation, but deriving it is often very complex in comparison with classical PID controllers.
    - In a process with unchanging dynamics, the controller can be derived beforehand, but with adaptive control it has to be done at every calculation.
    - If the MPC also has constraints, the required amount of computation is even higher.
    - Modern computing power negates most effects of this drawback, but it should be kept in mind that the computers used in the process industry are often not operating at their best. Process computers may also need to perform tasks other than control (alarms, recording, communications, etc.). (Camacho, Bordons 2007)
- *Requirement for an accurate model*: The design algorithm is independent of the model, but it is based on previous knowledge of it. It is fairly obvious that any benefits to be obtained by using MPC depend on the accuracy of the model. Even small discrepancies between the model and the process can cause issues. (Camacho, Bordons 2007)

The process model is discussed further later in this chapter.

All predictive controllers have the same basic methodology, and they differ only in their implementation of the main elements. (Camacho, Bordons 2007, Ogunnaike, Ray 1994) These elements are:

1. Specification of the reference trajectory $w(t+k)$, which can be a step or a smooth approximation to the set-point.

2. The process outputs are predicted to a prediction horizon N at each time instant t when there are no further control actions. The predicted outputs $\hat{y}(t+k|t)$ where $k = 1 \ldots N$ depend on all past inputs and outputs up to time t.
3. The future control signals $u(t+k|t), k = 0 \ldots N-1$ are calculated to optimize a predetermined criterion. The objective of the optimization can be for example to minimize the deviation between the reference trajectory and the predicted outputs, or to minimize the required control effort. In some cases, an explicit solution can be found (quadratic criterion, linear model, no constraints), but usually an iterative optimization method is needed.
4. The first control signal $u(t|t)$ is applied to the process, and the following signals are rejected, because the calculation uses the receding horizon method and the previous steps are repeated at each sampling instant.

The basic structure of the controller is shown in Figure 2. The model is used for the output prediction, and the optimizer is used calculate the control signals.

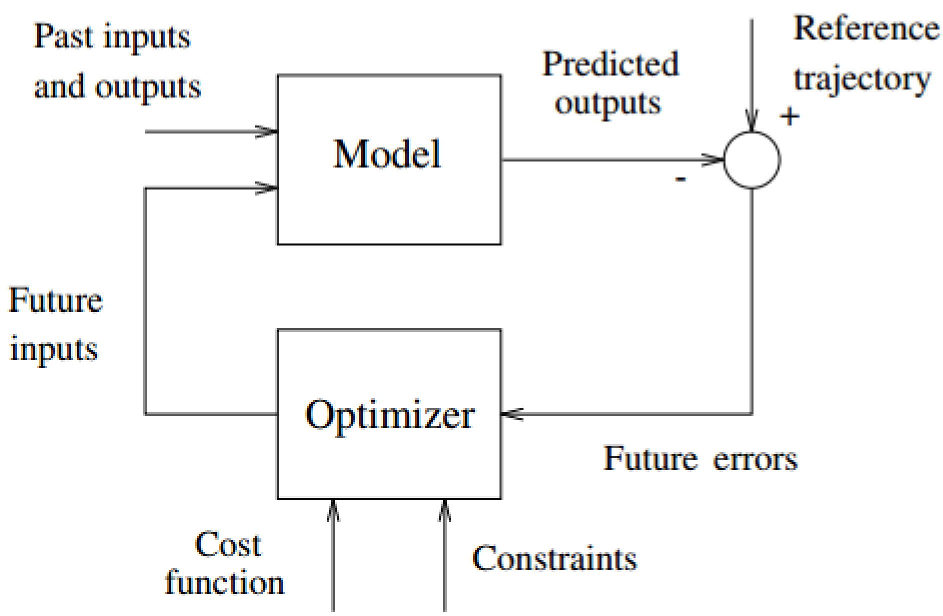

Fig. 2. Basic structure of MPC (Camacho, Bordons 2007)

2.1 Process model for the MPC

According to (Denn 1986) “A mathematical model of a process is a system of equations whose solution, given specified input data, is representative of the response of the process to a corresponding set of inputs.”

The model has a crucial role in the MPC. The model needs to be able to describe the process dynamics sufficiently to accurately predict the outputs, while remaining simple enough to implement. Model predictive control is not a specific technique but rather a set of different methods, so the model can be of several forms. For example an impulse or step response model, or a state space model. The different models have different ways of representing the relationship between the measurable inputs and the outputs. The inputs can be considered either manipulated variables or measurable disturbances. The measurable disturbances are compensated by feedforward action. The process can also have disturbances that are not measurable, or noise in the measurements, and these can be taken into account with disturbance models. The models used by the controller are usually separated into the process model and the disturbance model, which are both necessary for successful control. (Camacho, Bordons 2007)

A basic rule in modeling is not to estimate values that are already known. There are different levels of prior knowledge used in creating models, and these levels are called by colors:

- White-box models
- Gray-box models
- Black-box models

(Sjöberg, Zhang et al. 1995)

A white-box model is a model that is entirely constructed from prior knowledge of the system’s underlying physical, chemical, and thermodynamic processes. Models like this are also referred to as first-principles models. For complex industrial processes these are often expensive and difficult to develop, but they have become increasingly common. (Sjöberg, Zhang et al. 1995) (Maciejowski 2002)

A black-box model is a model where no prior knowledge of the process is available or used (Sjöberg, Zhang et al. 1995). The modeling is done by performing tests on the process. These tests involve stimulating the process with known signals (steps, multi-sines, etc.) and measuring the plant outputs. Alternatively, the data can be historical data from running the process. From this data the model can be obtained by system identification. There are several different techniques for this ranging from simple curve-fitting to complex statistically based methods. Models obtained this way are called black box models. They describe only the input-output behavior and tell nothing of the internal structure of the process. (Maciejowski 2002)

A grey-box model is a hybrid of white- and black-box models. They are created when some insight is available, but there are parameters that will require estimation. Sjöberg, Zhang et al. (1995) divide these into two subcases. Physical modeling means building a model on physical grounds, with a number of parameters estimated from data. An example could be a state-space model with specific structure and order. Semi-physical modeling means using physical insight to suggest specific nonlinear combinations of the data. These combinations are then used akin to black-box modeling. (Sjöberg, Zhang et al. 1995)

2.2 Tuning the controller

All predictive controllers have adjustable parameters such as weights, horizons, disturbance model, observer dynamics, and reference trajectory. Adjusting these parameters is called tuning the controller. Tuning can be done based on theorems, but is more commonly based on previous experience. Model predictive control uses feedback for the same reason all controllers do; to combat the effects of uncertainty. What should be remembered is that feedback should always be treated with caution. This is because improperly used feedback can turn a stable system into an unstable one. (Maciejowski 2002)

2.2.1 Horizons

The horizons that need to be chosen for MPC are prediction horizon N and control horizon N_u. The length of the prediction horizon affects the stability of the system. A small N responds fast, but the robustness of the system suffers. If a longer horizon is chosen, the system's dynamic response will be slower and more stable, but the computational burden will increase. Therefore, the chosen prediction horizon should be a compromise between speed and stability. (Jiang, Jutan 2000)

The control horizon N_u also requires compromise. A longer horizon increases the controlling scope, but decreases the robustness and stability. Tuning this parameter is usually done by trial and error because no general method for it exists. This value is also often left as a so-called safe value because it could be close to an optimal value and changing it unnecessarily might even result in instability. (Jiang, Jutan 2000)

2.2.2 Weights

One tuning method is control weighting. There are several ways of using it. For example, increasing the weights on the control moves compared to the weights on the tracking errors reduces the control activity. Increasing them indefinitely would reduce the control activity to zero, which would essentially mean switching off the feedback control. Therefore with a stable plant, a stable closed-loop system can be obtained by sufficiently increasing the control weights. However, the higher the weights, the slower the system responds to disturbances. For an unstable system increasing the weights too much will result in an unstable closed-loop system. (Maciejowski 2002)

2.2.3 Disturbance model and observer dynamics

Two important choices for tuning are disturbance model and observer dynamics. To achieve offset-free tracking in a system with constant output disturbances, the poles of the disturbance model must become the poles of the controller. This is an example of a phenomenon called

Internal Model Principle. Suppose a disturbance that won't decay to zero affects the system; this can often be approximated by sinusoidal, ramp or constant signals in practice. In this case, the feedback controller can only compensate for the disturbance perfectly if the disturbance signal poles are among the controller poles. In other words, the controller's internal model must have the same structure as the disturbance. This is the reason a disturbance model is added to the controller. (Maciejowski 2002)

The function of the observer is to filter the measured outputs before they affect the controller. Choosing the dynamics of the observer affects the system's response to disturbances. Deadbeat dynamics give a fast response, but some magnitudes of disturbance can then lead to frequent saturation of actuators. Therefore, it is sometimes better to choose a slower response, and reserve the saturation of actuators for exceptionally large disturbances. Especially in cases with an appreciable amount of measurement noise, it is usually better to use slower dynamics, to achieve some low-pass filtering of the measurement noise. (Maciejowski 2002)

2.3 Process optimization with MPC

The optimizer is the part of the controller that calculates the future control actions. It does this by minimizing the cost function. In the case of a quadratic cost function, the minimum can be found explicitly as a linear function of the reference trajectory and past inputs and outputs. However, in cases with constraints or nonlinearity, the cost function must be minimized numerically. (Camacho, Bordons 2007) The optimizer also needs to keep track of the prediction error, which is the difference between the measured process output $y(k)$) and the predicted output $\hat{y}(k)$. The error is updated on every calculation and used to correct future predictions. (Ogunnaike, Ray 1994)

Different MPC algorithms use different cost functions to acquire the control law. The general goal is for the future output (*y*) to follow the reference signal (*w*), while the control effort (Δu) is penalized. Equation 1 describes the general form of the cost function. (Camacho, Bordons 2007)

$$J(N_1, N_2, N_u) = \sum_{j=N_1}^{N_2} \delta(j)[\hat{y}(t+j|t) - w(t+j)]^2 + \sum_{j=1}^{N_u} \lambda(j)[\Delta u(t+j-1)]^2 \qquad (1)$$

where N_1 and N_2 are the cost horizons (minimum and maximum), N_u is the control horizon, and $\delta(j)$ and $\lambda(j)$ are the coefficient (sequences) that consider the future outputs of the process. The cost horizons define the limits of the sample times where it is advantageous for the output to match the reference. A high value of N_1 means that the early instants are not important, for example processes with dead time or inverse response. The maximum cost horizon N_2 always has a higher value than the control horizon N_u. The coefficients can be for example used to find an exponential weight along the horizon: $\delta(j) = \alpha^{N_2-j}$, where by choosing a value for α the smoothness or tightness of the control can be given (the more the first errors are penalized, the tighter the control).

The reference trajectory $w(t+k)$ was mentioned briefly earlier, and is also considered in the cost function. This is an advantage of predictive control, and it is especially useful in cases where the evolution of the reference $r(t+k)$ is known beforehand. Such applications include robotics and batch processes. Noticeable performance improvement can also be achieved in cases where the reference is constant, when the instant of the change in its value is known. The reference trajectory is usually a smooth approximation of the reference instead of following the actual reference. (Camacho, Bordons 2007)

2.4 Additional aspects to consider

In reality all processes have constraints that have to be taken into account in the minimization of the cost function. The constraints can be caused by a variety of things. Actuators have limited fields of action (e.g. a valve is limited by totally closed and totally open), safety and environmental reasons limit allowable tank levels, flows in pipes, and process pressures and temperatures. The operational conditions are often determined by the intersection of particular constraints, so the system will be operating close to the boundaries. Adding constraints to the cost function makes the minimization more complex so the solution has to be obtained numerically. (Camacho, Bordons 2007)

Most processes are nonlinear at least to some degree. In many cases this does not cause any problems since the process is operated at a steady state and can be approximated as a linear process. However, there are processes that either spend long periods of time away from the steady state or have transient dynamics during the whole operation. There are also processes where the nonlinearity is so severe that it must be taken into account even in steady state operation. The concept of MPC causes no problems with the use of nonlinear models, provided that a sufficiently accurate model can be found. Though it should be kept in mind that a mathematical model of a real process is never perfect. For effective control, the models require simplifying assumptions to ensure sufficient speed for the calculation of the control actions. Control models are always approximations of the real process. (Camacho, Bordons 2007)

Because the model is not exact and external disturbances can affect the process, the controller needs feedback. The feedback is used to ascertain that the model predictions are accurate and, as will be discussed later, to recognize when faults occur in the process. (Camacho, Bordons 2007)

3 Fault tolerant control

Industrial processes are faced with increasing requirements for reliability, profitability, and safety. These processes rely on highly automated controllers. Automation in itself, however, increases the vulnerability of the process to various faults. (Gani, Mhaskar et al. 2007) Often encountered faults are the failures of key control or process elements. These failures affect the performance of the plant, but can also lead to critical problems and risk of instability and breakdown. The faults can be for example a faulty sensor, a stuck valve, a burned-out thermocouple, or a broken transducer. (Mahmoud, Xia 2013) According to (Gani, Mhaskar et al. 2007) faults can cause

- physical damage to equipment
- increased use of energy and raw materials
- process downtime, which will result in production losses
- hazard to the environment and plant personnel.

These increasing demands have motivated significant amounts of research into fault detection and diagnosis (FDD), and fault tolerant control (FTC). A fault tolerant control system (FTCS) is a system that can maintain stability and a level of performance even during faults in the system. (Jiang, Yu 2012) The performance of the process is relative to the failure severity. This is an advantage compared to conventional control systems, where even a minor fault can cause breakdown. (Mahmoud, Xia 2013) Fault tolerance is exceedingly important in safety critical systems such as aircraft, industrial plants (with hazardous materials), and space vehicles. The achievable performance of an FTCS depends on the redundancies available in the control system, and on the design approach used. FTCSs are classified into two categories based on how they employ the redundancies. These categories are active FTCS and passive FTCS, which differ only in their design methods to reach the same control objective. Both approaches lead to similar results considering the main control objectives, but their distinctive design methods lead to certain unique properties, which will be discussed later in this chapter. (Jiang, Yu 2012)

A prerequisite of (active) fault tolerant control is the detection and isolation of faults. Existing methods for the design of fault-detection filters include those using plant data and those using process models. The methods using plant data use statistical and pattern recognition, and use the analyzed data to calculate indicators to detect faults. (Gani, Mhaskar et al. 2007) Both types of methods have been extensively studied in existing literature and, will not be discussed within this thesis.

According to Jiang & Yu (2012) “The main objectives of an FTCS are to preserve the stability of the overall system and to maintain an acceptable level of performance in the event of system component malfunctions.” These component failures are divided into two types. First, those that are anticipated during the design stage, and second, those that only occur during the operation of the system. This part of the chapter discusses two different approaches to handling faults. A passive approach to fault-tolerance means making the system failure-proof for a specifically defined set of faults at the design stage; this is done by built-in system redundancies. An active approach means responding to failures by reconfiguring the remaining elements online to ensure the necessary control capabilities. (Jiang, Yu 2012)

3.1 Passive fault tolerance

In passive fault tolerant control systems (PFTCS), the controllers are designed to be robust against a set of previously known faults, and they are fixed. The advantage to this approach is that it does not require an FDD component nor reconfiguration of the controller. The disadvantage is its limited capabilities for fault tolerance. The controller in a PFTCS remains fixed for the entire duration of the process operation. It should be able to sustain the designed system performance, even when a fault occurs. (Mahmoud, Xia 2013) The scheme is called "passive" because no additional control actions need to be taken. The main idea of a PFTCS is to obtain a controller in the intersection of all admissible solutions. There are several limiting situations for a PFTCS where no single intersection for all solutions can be found. This may lead to the necessity of optimality sacrifices even during normal operation. The architecture of a PFTCS is shown in Figure 3. (Jiang, Yu 2012)

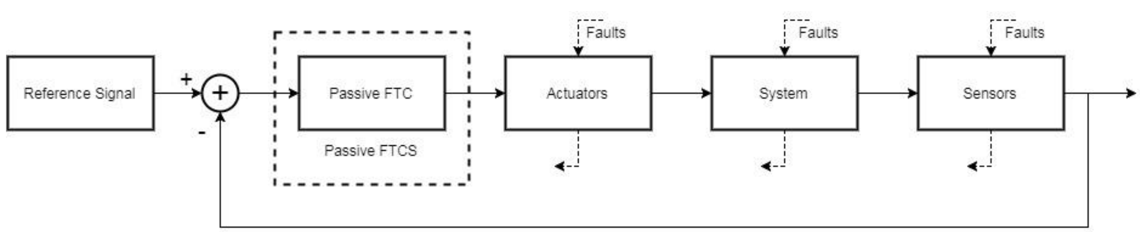

Fig. 3. Architecture of a passive FTCS. Adapted from (Jiang, Yu 2012)

3.2 Active fault tolerance

In active fault tolerant control systems (AFTCS), the controller reacts to faults by actively reconfiguring its actions to maintain the stability and satisfactory performance for the system. There are several terms that essentially describe an AFTCS, such as self-repairing, reconfigurable, restructurable, and self-designing. The AFTCS consistently has the same basic components: a fault detection and diagnosis (FDD) scheme, a restructurable controller, and a mechanism for the restructuring. (Mahmoud, Xia 2013) Since there are three main components to the AFTCS, there are also three design objectives for the system.

1. The development of an FDD system that provides accurate and timely information about any faults that occur in the system.
2. The reconfiguration of the control scheme to maintain the stability and acceptable performance of the closed-loop system.
3. The assignment of the restructured controller into the system smoothly.

The architecture of an AFTCS is shown in Figure 4. (Jiang, Yu 2012)

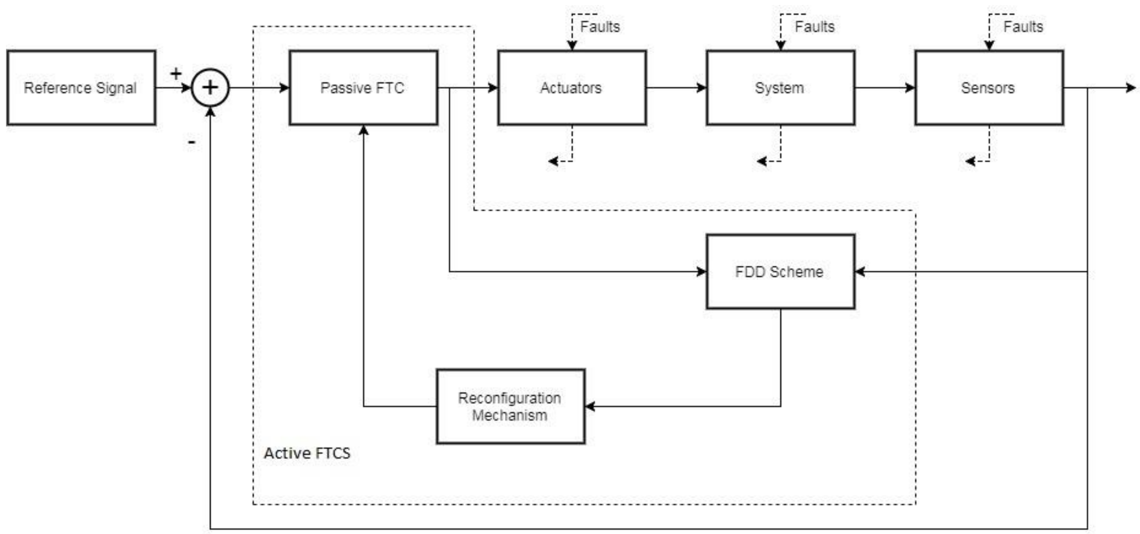

Fig. 4. Architecture of an active FTCS. Adapted from (Jiang, Yu 2012)

The AFTCS considers both normal and fault cases. It is assumed that for each case there is an admissible solution space, and in that space, a controller. The existence of an optimal solution within this space depends on the constraints of the process and the optimization techniques used. In a fault case, when a solution is found, the controller is reconfigured to compensate for the effects of the fault. The search algorithm for the solution can be made to find the optimal solution. However, it is often better to settle for a sufficient but sub-optimal controller, because obtaining the optimal solution requires more time. The controller must react to faults fast, so the time for finding the solution is limited. (Jiang, Yu 2012)

Though the concept sounds simple in theory, in practice there are issues that can decrease the ability of the controller to perform as desired. Problems can be caused for example by the accuracy of fault detection and the time it takes, and the time it takes to obtain and assign the new controls. The fault detection depends on the type of the faults, and the selected FDD methods. The AFTCS only has a limited time frame to react to faults, because faults can often render the process or system unstable. The time between the occurrence of the fault and the system becoming unstable is referred to as critical reaction time. If in practice the AFTCS takes longer to reconfigure itself than the critical reaction time, the process will become unrecoverable. Figure 5 shows both situations. T_c refers to the critical reaction time, T_f is the time the fault occurs, and T_r is the time the FDD and control reconfiguration take. (Jiang, Yu 2012)

In a general case of fault tolerant control the term reconfiguration refers to reacting to faults by switching off the faulty part of the process, and attempting to achieve desirable performance with the remaining control options (Blanke, Kinnaert et al. 2003). In the MPC case of this thesis, reconfiguration refers to changing the model in reaction to faults.

Once the fault has been detected and identified, the controller needs to be reconfigured. This can be thought of as model matching. The desired performance is known, and can be used to determine the dynamical properties that should be produced by the new controller. Essentially this means that the new closed-loop system should still match the model of the non-faulty process. (Mahmoud, Xia 2013)

In this general example of controller reconfiguration, the closed-loop system consists of a linear plant and a state-feedback controller $u(k) = -\mathbf{K}x(k)$, and combined these give the model of the system. For a faulty system, the new state-feedback controller $u(k) - \mathbf{K}_f x(k)$ should be obtained so that the system behaves like the nominal loop. The new controller is applied to the system to minimize the difference between the dynamical properties of the non-faulty and faulty plant. (Mahmoud, Xia 2013)

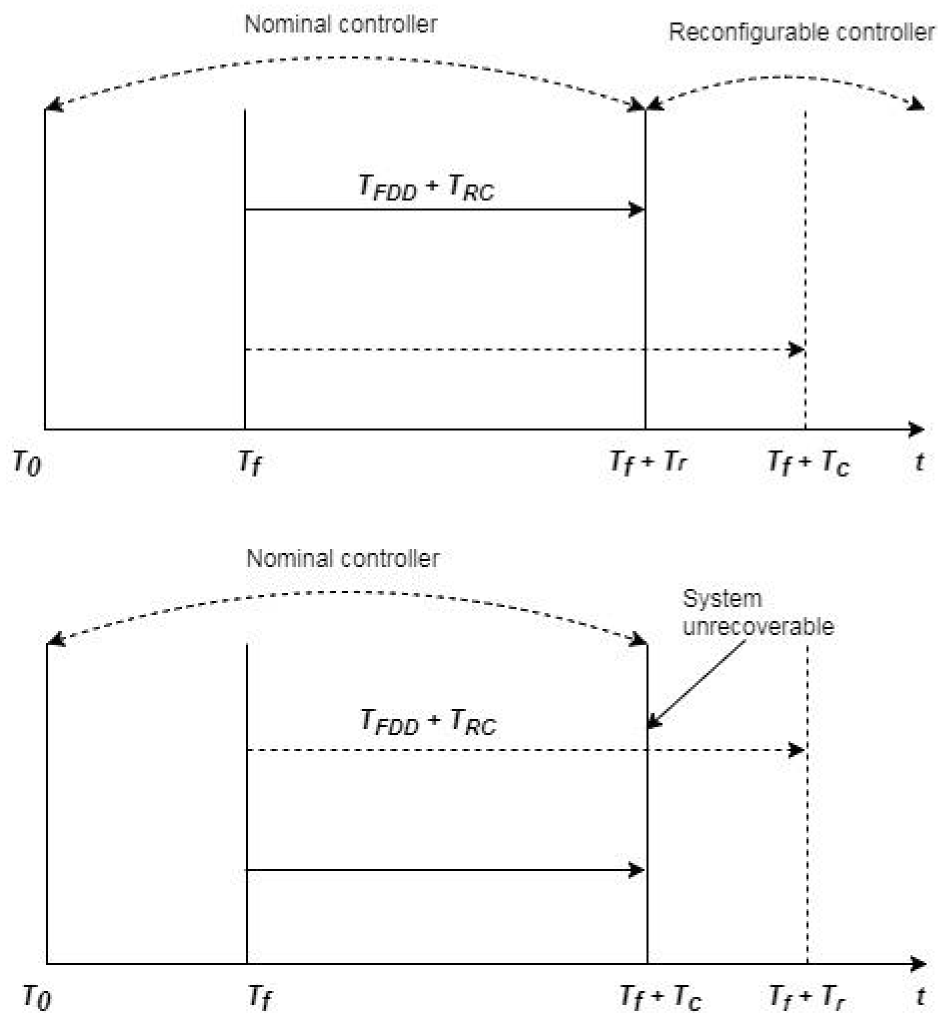

Fig. 5. Critical reaction time of an AFTCS; top: $T_r < T_c$, bottom: $T_r > T_c$. Adapted from (Jiang, Yu 2012)

4 Industrial and simulation examples of MPC and FTC

This chapter introduces three industrial or simulation examples. The first is a basic simulation example of a two CSTR system. The second introduces previous work from the Aalto University

Process Automation and Control research group, especially in the area of industrial dearomatization. The third section is an example of fault tolerant control using AI.

4.1 Basic CSTR example

This section introduces a two-tank example from (Mhaskar, Liu et al. 2013). Another popular example in fault tolerant control literature is the three-tank process, which the reader can familiarize themselves with from for example (Blanke, Kinnaert et al. 2003) or (Noura, Theilliol et al. 2009).

(Mhaskar, Liu et al. 2013) demonstrate the application of a fault detection and isolation, and reconfiguration method for two continuous stirred tank reactors (CSTRs) operating in series. Consider these CSTRs to be well mixed and non-isothermal reactors, where three irreversible exothermic reactions take place in parallel. The reactions are of form $A \overset{k_1}{\rightarrow} B,\ A \overset{k_2}{\rightarrow} U,\ A \overset{k_3}{\rightarrow} R$, and the schematic of the system can be seen from Figure 6. In the reactions, *A* is the reactant, *B* is the main product, and *U* and *R* are byproducts. The input to the first reactor is pure *A*, and the output is fed to the second reactor. The second reactor also has a feed of pure *A*. Using standard modelling assumptions, the model of the process is described by equations 2–5. (Mhaskar, Liu et al. 2013)

$$\frac{dT_1}{dt} = \frac{F_0}{V_1}(T_0 - T_1) + \sum_{i=1}^{3} \frac{-\Delta H_i}{\rho c_p} R_i(C_{A1}, T_1) + \frac{Q_1}{\rho c_p V_1} \quad (2)$$

$$\frac{dC_{A1}}{dt} = \frac{F_0}{V_1}(C_{A0} - C_{A1}) - \sum_{i=1}^{3} R_i(C_{A1}, T_1) \quad (3)$$

$$\frac{dT_2}{dt} = \frac{F_0}{V_2}(T_1 - T_2) + \frac{F_3}{V_2}(T_{03} - T_2) + \sum_{i=1}^{3} \frac{-\Delta H_i}{\rho c_p} R_i(C_{A2}, T_2) + \frac{Q_2}{\rho c_p V_2} \quad (4)$$

$$\frac{dC_{A2}}{dt} = \frac{F_0}{V_2}(C_{A1} - C_{A2}) + \frac{F_3}{V_2}(C_{A03} - C_{A2}) - \sum_{i=1}^{3} R_i(C_{A2}, T_2) \quad (5)$$

where $R_i(C_{Aj}, T_j) = k_{i0} \exp\left(-\frac{E_i}{RT_j}\right) C_{Aj}$, for $j = 1, 2$. T is the temperature of the reactor, C_A is the concentration of *A*, Q is the rate of heat exchange, and V is the volume of the reactor. The subscripts 1 and 2 refer to reactors 1 and 2. ΔH_i is the enthalpy, and E_i is the activation energy, where $i = 1, 2, 3$. c_p and ρ are the heat capacity and density of the fluid. (Mhaskar, Liu et al. 2013)

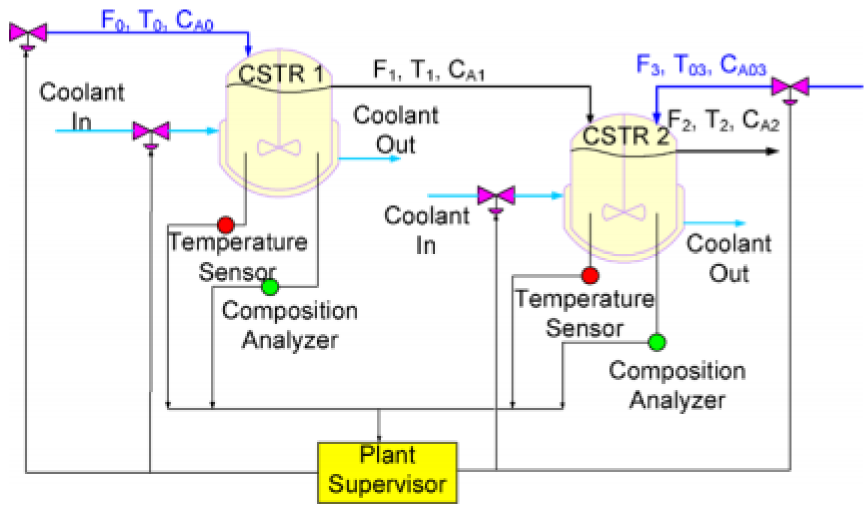

Fig. 6. A schematic of two CSTRs operating in series (Mhaskar, Liu et al. 2013)

When $Q_1 = 0$, CSTR 1 has three steady-states: two stable and one unstable. When $Q_2 = 0$, the unstable steady-state of CSTR 1 corresponds to two stable and one unstable steady-state for CSTR 2. The objective of the control is to stabilize the unstable steady-states. If the system contains actuator failures, the following manipulated inputs are considered:

- Q_1, the rate of heat into CSTR 1
- $T_0 - T_0^s$, the temperature of the feed to CSTR 1
- $C_{A0} - C_{A0}^s$, the reactant concentration of the feed to CSTR 1
- Q_2, the rate of heat into CSTR 2
- $T_{03} - T_{03}^s$, the temperature of the feed to CSTR 2
- $C_{A03} - C_{A03}^s$, the reactant concentration of the feed to CSTR 2.

The above inputs could be used in different combinations to stabilize the reactors by using temperature and concentration measurements from the reactor (full state-feedback). In the primary control configuration four inputs are used: Q_1, Q_2, C_{A0}, and C_{A03}. In the case of a partial failure, the fault needs to be detected and isolated, and a fall-back control configuration needs to be activated to maintain stability.

4.2 Active fault tolerant control for an industrial dearomatization process

The Aalto University Process Automation and Control research group has studied both fault tolerant control and model predictive control extensively in the past decade. While this thesis does not directly follow from any previous study, this section introduces some of them briefly.

(Kettunen, Jämsä-Jounela 2006) developed a fault tolerant MPC with embedded fault detection and isolation (FDI) for the heavy oil fractionator process of the Shell Control Problem (SCP). The SCP was introduced in (Prett, Morari 1987). The system uses different types of FDI methods to achieve fault tolerance with MPC: Principal Component Analysis (PCA), Partial Least Squares (PLS), and Subspace Model Identification (SMI). The FDI methods were tested by simulating drift and bias faults in a process measurement. Based on these methods, two FTC systems were successfully implemented. The simulation results show that the methods are effective in countering the faults. The authors note that the process was simulated, and tests with real process data may not be as neat. (Kettunen, Jämsä-Jounela 2006)

The complex industrial dearomatization process LARPO (Neste Oil, Naantali refinery) has gathered several studies. Worth a mention are at least (Sourander, Vermasvuori et al. 2009), (Kettunen, Jämsä-Jounela 2011) and the dissertation (Kettunen 2010). The process includes two trickle-bed reactors that are used to remove aromatic compounds, a distillation column for controlling end product specifications, heat exchangers, separation drums, a filling plate stripper, and some other process equipment for supplementary tasks. The control objective is to maintain the quality of the distillation column bottom product. (Kettunen, Jämsä-Jounela 2011)

The studies (Kettunen 2010) and (Kettunen, Jämsä-Jounela 2011) introduce three data-based FTC methods, and validate them on a simulation of the LARPO process. (Sourander, Vermasvuori et al. 2009) created a system with FDI and a logic for choosing predefined FTC actions. This system was tested and validated both on the simulation and online in the actual process in the refinery. The fault tolerance in the online validation was tested by manipulating the analyzer results to cause artificial faults similar to normally occurring ones. (Sourander, Vermasvuori et al. 2009) All presented FTC systems performed as expected and required.

(Zakharov, Yu et al. 2014) present a dynamic prognosis algorithm for use in choosing the most suitable controller reconfiguration without using a Lyapunov function. Dynamic prognosis means predicting process variable trajectories under distributed model predictive control (DMPC). It is performed when several configuration candidates are proposed after a fault has been diagnosed. Its task is to check whether the candidate configuration is able to achieve the new operating conditions while maintaining acceptable performance during the transition. The computation burden of the algorithm is reasonable with the assumption that the non-faulty subsystems remain as they are. The dynamic prognosis in DMPC aims to improve the applicability of existing FTC methods to large-scale systems.

4.3 Fault Tolerant Control using other methods

Simani et al. (2016) introduced a fault detection and compensation method for a hydroelectric system. They used Takagi-Sugeno (TS) fuzzy prototypes as nonlinear filters to acquire a prediction of the faults affecting the system. The FTC scheme used for the system was a MPC whose inputs were the predicted fault signals and the reference. The basic approach to obtain the control strategy was not dependent on the considered model. The first step was to use the fuzzy identification method to derive the FDD module. Next, the fault compensation strategy is formulated as an MPC that uses the reconstructed fault to obtain the optimized control law. In other words, the FDD module provides the fault estimation, which the MPC treats as a disturbance to be compensated. The overall strategy for fault accommodation is shown in Figure 7. (S. Simani, S. Alvisi et al. 2016)

In a fault-free situation, the MPC acts as a nominal controller, and handles the objectives and constraints of the system. When a fault occurs, the MPC uses the fault reconstruction by the FDD to compensate for the effect of the fault, and to essentially hide the fault from the overall system. In some fault cases, the nominal objectives cannot be achieved within the constraints, and the MPC can switch to degraded values for the objectives or update the constraints. (S. Simani, S. Alvisi et al. 2016)

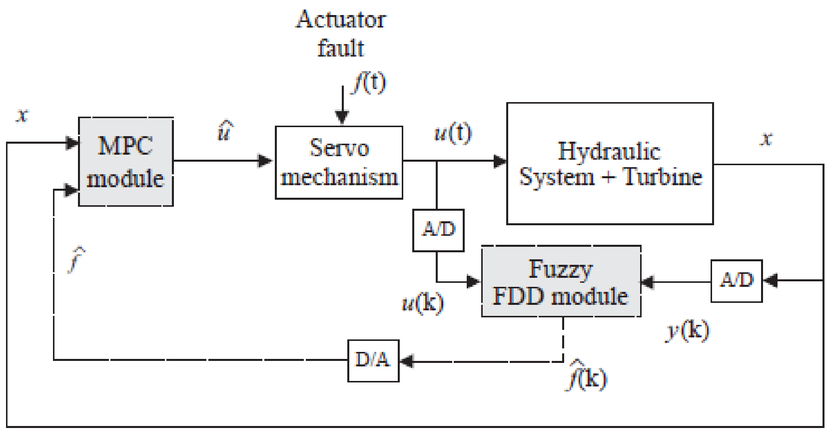

Fig. 7. Structure of the fault tolerant MPC (S. Simani, S. Alvisi et al. 2016)

Simani et al. (2016) used a state-space representation of the system and a cost function that minimizes the difference between the reference state and the potentially faulty real state of the system. They used the Simulink MPC Designer Toolbox and Control Design to implement the control strategy. Because there is a mismatch between the model and reality, a Kalman filter provides the state estimations for the MPC. The structure is shown in Figure 8. (S. Simani, S. Alvisi et al. 2016)

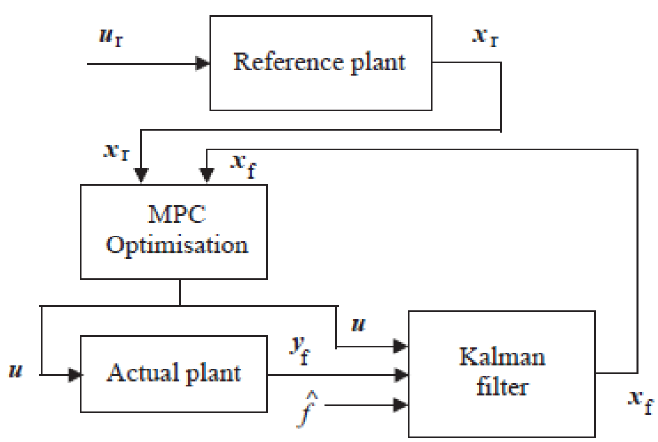

Fig. 8. Structure of the fault compensated MPC (S. Simani, S. Alvisi et al. 2016)

Experimental part

The aim of the experimental part of this thesis is to design and tune a supervisory MPC for the Tennessee Eastman process (Downs, Vogel 1993). The purpose is to achieve a controller that can later be used as a reconfigurable controller in a fault tolerant control system.

First, the Tennessee Eastman process, its basic PI-control strategy, and the MATLAB Simulink model used to simulate it are introduced. Next, the MPC is designed, implemented and tested. Last, the results of the testing are analyzed to ascertain the goal was reached.

5 Tennessee Eastman Process

5.1 Original process

The Tennessee Eastman (TE) process was first described by Downs and Vogel (1993) of the Eastman Chemical Company. The process is based on a real industrial process, though the properties such as components and kinetics were modified for the test problem. It is a testing benchmark created to enable study of a wide range of applications such as plant-wide control strategy, multivariable control, optimization, predictive control, estimation/adaptive control, nonlinear control, and process diagnostics.

The process consists of four reactions with four reactants (A, C, D, E) and an inert (B); these produce two products (G, H) and a byproduct (F). The reactions are:

$$\mathrm{A}(g) + \mathrm{C}(g) + \mathrm{D}(g) \rightarrow \mathrm{G}(liq), \text{Product 1} \tag{6}$$

$$\mathrm{A}(g) + \mathrm{C}(g) + \mathrm{E}(g) \rightarrow \mathrm{H}(liq), \text{Product 2} \tag{7}$$

$$\mathrm{A}(g) + \mathrm{E}(g) \rightarrow \mathrm{F}(liq), \text{Byproduct} \tag{8}$$

$$3\mathrm{D}(g) \rightarrow 2\mathrm{F}(liq), \text{Byproduct} \tag{9}$$

The reactions are exothermic and irreversible. Reaction eq. 6 has a higher activation energy and therefore the production of G is more temperature dependent. Also, in relation to reactant concentrations, the reactions are approximately first-order. The process consists of five unit operations: reactor, condenser, vapor-liquid separator, recycle compressor, and product stripper. (Downs, Vogel 1993) Figure 9 shows the process diagram. The process can be operated in six modes with three different product mass ratios (product stream from stripper). These modes are described in Table 1, and the setpoints of modes 1 and 3 in Table 2.

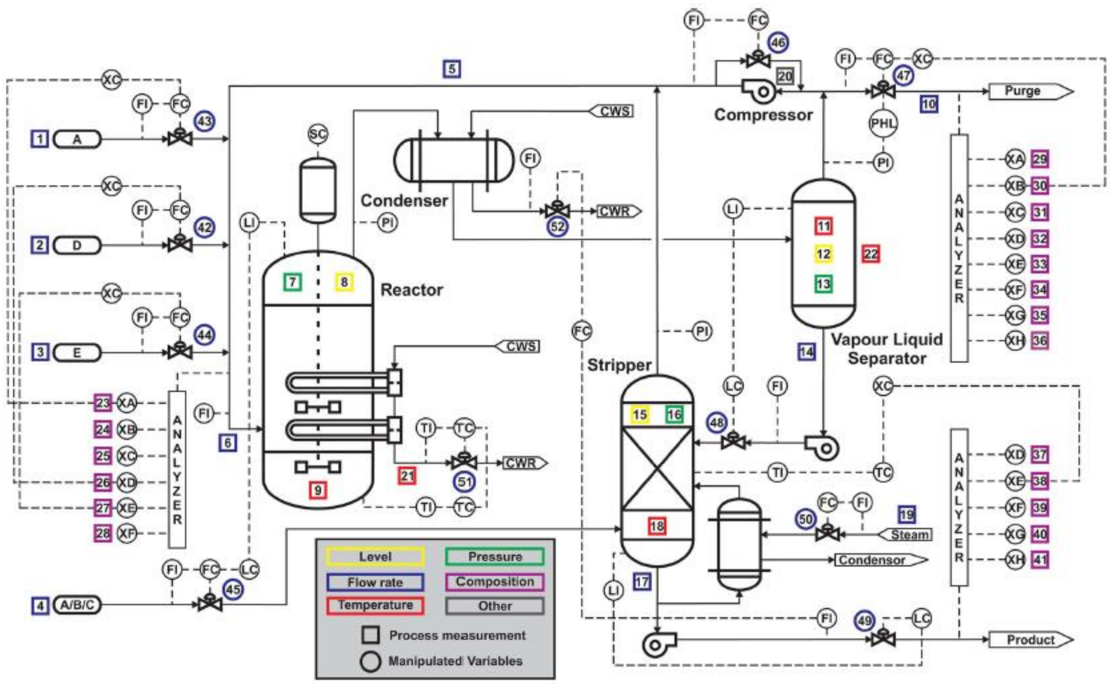

Fig. 9. Diagram of the Tennessee Eastman process (S. Yin, H. Luo et al. 2014)

Table 1. The process operation modes

Mode	G/H mass ratio	Production rate
1	50/50	7038 kg/h G and 7038 kg/h H (base case)
2	10/90	1408 kg/h G and 12669 kg/h H
3	90/10	10000 kg/h G and 1111 kg/h H
4	50/50	maximum production rate
5	10/90	maximum production rate
6	90/10	maximum production rate

Table 2. Setpoints of the operating modes 1 and 3

Setpoint	Mode 1	Mode 3
Production	22.89	18.04
Stripper level	50	50
Separator level	50	50
Reactor level	65	65
Reactor pressure	2800	2800
Mole % G in product	53.8	90.09
yA	63.1373	62.11
yAC	51.0	47.43
Reactor temperature	122.9	121.9
Recycle valve	0	77.62
Steam valve	0	1

The reactant feeds are gaseous, and the liquid products leave the reactor as vapors. The reactions are catalyzed by a catalyst dissolved in the reactor's liquid phase. Due to this, the catalyst doesn't leave the reactor. The reactions are exothermic so the reactor has a cooling bundle to remove the heat. The reactor output is cooled to condense the products and moved to a vapor-liquid separator. Any remaining reactants and non-condensed components are recycled through a compressor back to the feed of the reactor. Condensed products go to a stripping column where any remaining reactants are removed. The products G and H are separated in a downstream unit process which is not included in this study. The byproduct and inert are purged primarily as a vapor from the separator.

The feeds are products from other processes in the plant. Therefore, there is variation in the holdup available for them. Stream 3 (component E) has significant holdup available, streams 1 and 2 (A and D) have some holdup available, and stream 4 (A and C) has little holdup available. Due to this, the variation in the feed streams 1, 2, and 4 should be minimized.

Variability in the product stream should be minimized. This is because the distillation system used to refine the products can't handle fast changes. Changes of more than ±5% in flowrate of the product flow (8-16 h^{-1}) or ±5 mol-% G in composition (6-10 h^{-1}) are particularly harmful.

The TE process has 12 manipulated variables and 41 measurements. These are listed in Tables 3, 4, and 5. Some of the measured values have constraints, these are described in Table 6. Table 7 lists disturbances that might occur in the process.

Table 3. Process manipulated variables

Variable name	Variable number	Base case value (%)	Low limit	High limit	Units
D feed flow (stream 2)	XMV (1)	63.053	0	5811	kg/h
E feed flow (stream 3)	XMV (2)	53.980	0	8354	kg/h
A feed flow (stream 1)	XMV (2)	24.644	0	1.017	kscmh
A and C feed flow (stream 4)	XMV (4)	61.302	0	15.25	kscmh
Compressor recycle valve	XMV (5)	2.210	0	100	%
Purge valve (stream 9)	XMV (6)	40.064	0	100	%
Separator pot liq. flow (stream 10)	XMV (7)	39.100	0	65.71	m3/h
Stripper liq. prod. flow (stream 11)	XMV (8)	46.534	0	49.10	m3/h
Stripper steam valve	XMV (9)	47.466	0	100	%
Reactor cw. flow	XMV (10)	41.106	0	227.1	m3/h
Condenser cw. flow	XMV (11)	18.114	0	227.6	m3/h
Agitator speed	XMV (12)	50.000	150	250	rpm

Table 4. Continuous process measurements

Variable name	Variable number	Base case value	Units
A feed (stream 1)	XMEAS(1)	0.25052	kscmh
D feed (stream 2)	XMEAS(2)	3664.0	kg/h
E feed (stream 3)	XMEAS(3)	4509.3	kg/h
A and C feed (stream 4)	XMEAS(4)	9.3477	kscmh
Recycle flow (stream 6)	XMEAS(5)	26.902	kscmh
Reactor feed rate (stream 6)	XMEAS(6)	42.339	kscmh
Reactor pressure	XMEAS(7)	2705.0	kPa gauge
Reactor level	XMEAS(8)	75.000	%
Reactor temperature	XMEAS(9)	120.40	°C
Purge rate (stream 9)	XMEAS(10)	0.33712	kscmh
Prod. separator temperature	XMEAS(11)	80.109	°C
Prod. separator level	XMEAS(12)	50.000	%
Prod. separator pressure	XMEAS(13)	2633.7	kPa gauge
Prod. separator underflow (stream 10)	XMEAS(14)	25.160	m3/h
Stripper level	XMEAS(15)	50.000	%
Stripper pressure	XMEAS(16)	3102.2	kPa gauge
Stripper underflow (stream 11)	XMEAS(17)	22.949	m3/h
Stripper temperature	XMEAS(18)	65.731	°C
Stripper steam flow	XMEAS(19)	230.31	kg/h
Compressor work	XMEAS(20)	341.43	kW
Reactor cw. outlet temperature	XMEAS(21)	94.599	°C
Separator cw. outlet temperature	XMEAS(22)	77.297	°C

Table 5. Sampled process measurements

Reactor feed analysis (stream 6)

Sampling Frequency [0.1h] Dead time [0.1h]

Component	Variable number	Base case value	Units
A	XMEAS(23)	32.188	mol%
B	XMEAS(24)	8.8933	mol%
C	XMEAS(25)	26.383	mol%
D	XMEAS(26)	6.8820	mol%
E	XMEAS(27)	18.776	mol%
F	XMEAS(28)	1.6567	mol%

Purge gas analysis (stream 9)

Sampling Frequency [0.1h] Dead time [0.1h]

Component	Variable number	Base case value	Units
A	XMEAS(29)	32.958	mol%
B	XMEAS(30)	13.823	mol%
C	XMEAS(31)	23.978	mol%
D	XMEAS(32)	1.2656	mol%
E	XMEAS(33)	18.576	mol%
F	XMEAS(34)	2.2633	mol%
G	XMEAS(35)	4.8436	mol%
H	XMEAS(36)	2.2986	mol%

Product analysis (stream 11)
Sampling Frequency [0.25h] Dead time [0.25h]

Component	Variable number	Base case value	Units
D	XMEAS(37)	0.01787	mol%
E	XMEAS(38)	0.83570	mol%
F	XMEAS(39)	0.09858	mol%
G	XMEAS(40)	53.724	mol%
H	XMEAS(41)	43	mol%

Table 6. Process operating constraints

	Normal operating limits		Shutdown limits	
Process variable	Low limit	High limit	Low limit	High limit
Reactor pressure	none	2895 kPa	none	3000 kPa
Reactor level	50% (11.8 m3)	100% (21.3 m3)	2.0 m3	24.0 m3
Reactor temperature	none	150 °C	none	175 °C
Product separator level	30% (3.3 m3)	100% (9.0 m3)	1.0 m3	12.0 m3
Stripper base level	30% (3.5 m3)	100% (6.6 m3)	1.0 m3	8.0 m3

Table 7. Process disturbances

Variable number	Process variable	Type
IDV (1)	A/C feed ratio, B composition constant (stream 4)	Step
IDV (2)	B composition, A/C ratio constant (stream 4)	Step
IDV (3)	D feed temperature (stream 2)	Step
IDV (4)	Reactor cooling water inlet temperature	Step
IDV (5)	Condenser cooling water inlet temperature	Step
IDV (6)	A feed loss (stream 1)	Step
IDV (7)	C header pressure loss – reduced availability (stream 4)	Step
IDV (8)	A, B, C feed composition (stream 4)	Random variation
IDV (9)	D feed temperature (stream 2)	Random variation
IDV (10)	C feed temperature (Stream 4)	Random variation
IDV (11)	Reactor cooling water inlet temperature	Random variation
IDV (12)	Condenser cooling water inlet temperature	Random variation
IDV (13)	Reaction kinetics	Slow drift
IDV (14)	Reactor cooling water valve	Sticking
IDV (15)	Condenser cooling water valve	Sticking
IDV (16)	Unknown	Unknown
IDV (17)	Unknown	Unknown
IDV (18)	Unknown	Unknown
IDV (19)	Unknown	Unknown
IDV (20)	Unknown	Unknown

5.2 Existing control strategy

Ricker (1996) designed a decentralized control strategy for the TE process. Downs and Vogel (1993) described six operating modes. In addition to these, Ricker considered the following points:

- *Product composition* must stay within ±5 mol-% of its setpoint for amount of product G.
- *Production rate* must stay within ±5 % of its setpoint for volumetric flow. Some modes require maximum production rate, and the system must be able to push the process to at least one constraint without violating other specifications or shutdown limits.
- *Liquid inventories* have specified bounds. Optimal operation of the process minimizes the amount of liquid in the reactor. Separator and stripper inventories minimize variations in production rate, and have no effect on the economics of the process.
- *Reactor pressure* has a high limit of 3 MPa, above which the process shuts down. However, optimal operation requires operation near the high limit, and the system must be able to control the pressure closely.
- Some feed streams have limited availability, which causes *feed variability*.
- *Chemical inventories* must be controlled to avoid the depletion or accumulation of any materials.
- *Analyzers* might be temporarily out of service, but the system must still be able to operate.
- *Disturbance rejection.*
- The system should be able to maintain *optimal operation.* Either minimizing the costs or maximizing the production rate depending on the operating mode.

(Ricker 1996)

The process has twelve degrees of freedom. Based on the list of control goals, at least six must be used to control the following measured variables:

1. production rate,
2. mol-% of product G in product stream,
3. reactor pressure,
4. reactor liquid level,

5. separator liquid level, and
6. stripper liquid level.

Additionally, agitation affects heat transfer only in the reactor, and is therefore fixed at 100% to maximize cooling potential. As a result, there are five degrees of freedom that must be assigned appropriately. The recommended loops are described in Table 8. (Ricker 1996)

Table 8. Loop characteristics for the Ricker (1996) control strategy; manipulated variables described in Table 3.

Loop	Controlled variable	Manipulated variable
1	A feed rate (stream 1)	XMV (3)
2	D feed rate (stream 2)	XMV (1)
3	E feed arte (stream 3)	XMV (2)
4	C feed rate (stream 4)	XMV (4)
5	Purge rate (stream 9)	XMV (6)
6	Separator liquid rate (stream 10)	XMV (7)
7	Stripper liquid rate (stream 11)	XMV (8)
8	Production rate	F_{p}
9	Stripper liquid level	Ratio in loop 7
10	Separator liquid level	Ratio in loop 6
11	Reactor liquid level	Setpoint of loop 17
12	Reactor pressure	Ratio in loop 5
13	Mol-% G in stream 11	E_{adj} [see thingy]
14	y_A [see eq]	Ratio in loop 1, r_1
15	y_{AC} [see eq]	Sum of $r_1 + r_4$
16	Reactor temperature	Reactor cooling valve
17	Separator temperature	Condenser cooling valve
18	Maximum reactor pressure	Production index, F_{p}
19	Reactor level override	Recycle valve, XMV (5)

5.3 Revised simulation model

Ricker (2005) created an archive of MATLAB and SIMULINK compatible code for the simulation of the Tennessee Eastman process. Later, Bathelt, Ricker et al. (2015) noticed that simulation of the TE process gave inconsistent results depending on the solver used. This was an undesirable effect since it would require providing information about simulation settings with any applications. Thus, they analyzed the existing code to find the cause and presented a revised model.

Bathelt, Ricker et al. (2015) considered two major aspects during the revision. The structure and algorithms of the code had to be revised to adapt to the structure of the simulation loop. The model was also extended with additional outputs and new process disturbances. They accomplished three objectives with regard to the code. These were revision of random number generation and updating the disturbance process mechanism, revision of the execution of the function calculating current process values, and revision of the data structure of the model. (Bathelt, Ricker et al. 2015)

The revised model has added measurements and new output groups which are introduced in Appendix 1. Figures 10–12 show the Simulink model.

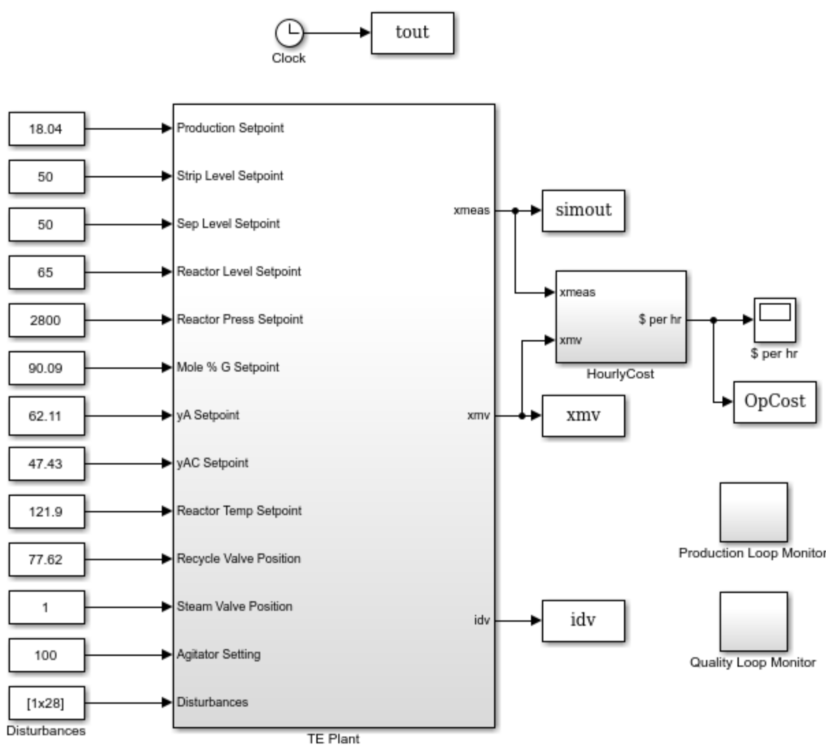

Fig. 10. Part of the Simulink model for Tennessee Eastman process (Mask)

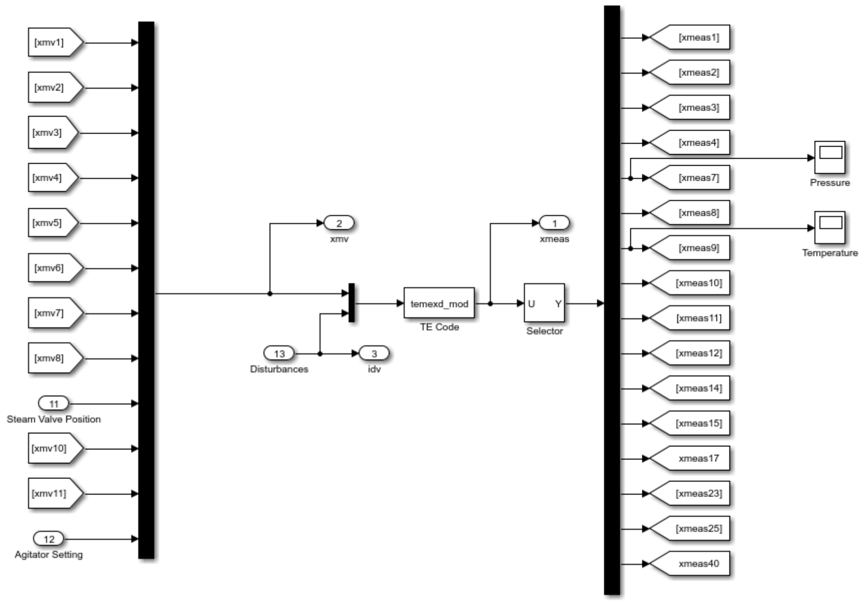

Fig. 11. Part of the Simulink model for Tennessee Eastman process (control inputs and process outputs)

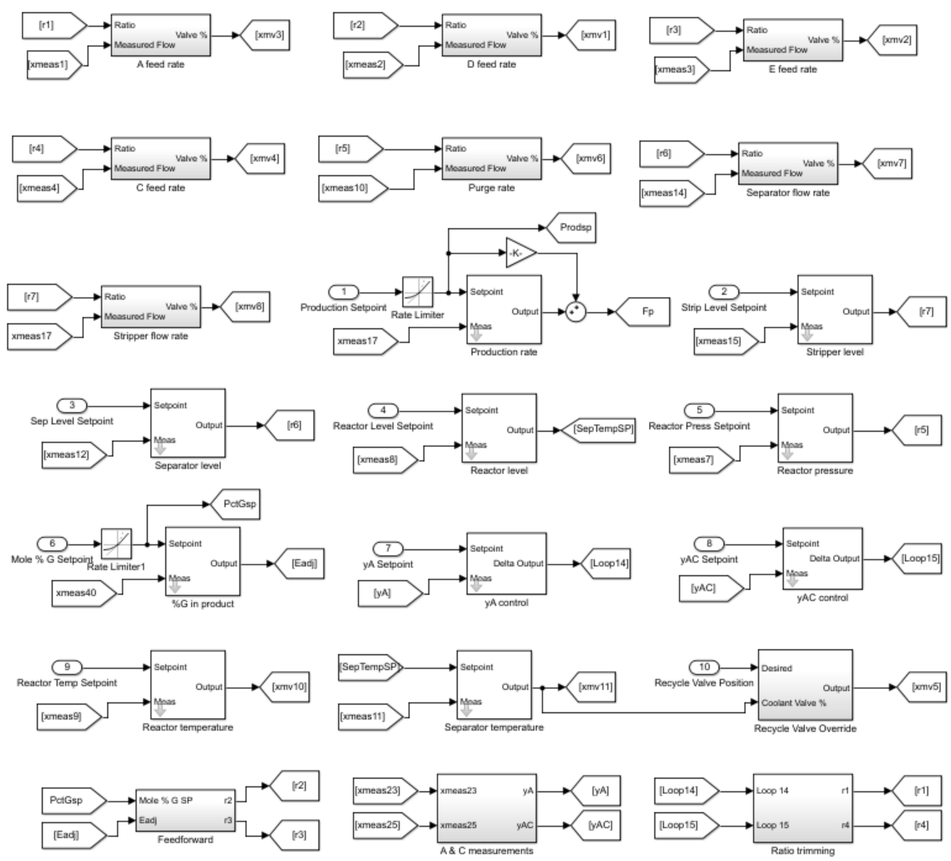

Fig. 12. Part of the Simulink model for Tennessee Eastman (PI controls)

5.4 Previous applications

The Tennessee Eastman Process has been previously used to study various control methods. Nonlinear MPCs were studied by (Ricker, Lee 1995), (Zheng 1998), (Magni et al. 2001), and (Vallerio et al. 2014). (Sriniwas, ARkun 1997) designed a control strategy using input-output models, and (Yeh et al. 2003) used TE to study the use of neural networks in estimating process compositions. (Tian, Hoo 2005) used multiple model-based control, and (Karra et al. 2008) developed adaptive control for multivariable time-varying systems. (Assali, McAvoy 2010) and (Kuhl et al. 2011) studied the selection and estimation of parameters. The TE can also be controlled by distributed control, this was studied by (Shao, Cinar 2015) and (Li et al. 2015).

Fault tolerant control is not implemented in this thesis, but previous research has been done by (Lennox 2004), (Yin et al. 2012), (Yin et al. 2013), and (Luppi et al. 2015).

6 MPC implementation

6.1 General outline

This thesis focuses on the implementation and testing of an MPC that can be used as a reconfigurable controller to achieve fault tolerance. (Sriniwas, Arkun 1997) presented an MPC based on input-output models, which was used in a supervisory role to adjust the setpoints of the lower level PI controls. As the PI structure is used to stabilize the process, turning off the MPC will not destabilize the system, and it is not necessary for the MPC to manipulate all loops. (Sriniwas, Arkun 1997) Thus, it was decided that the MPC implemented here should supervise only 3–4 control loops, and that these loops should be chosen with the intention of maintaining performance even in the case of faults. The control loops are described in Table 8 (Chapter 5).

For the MPC in this thesis, three loops were chosen to be supervised. The loops are reactor level (loop 11), reactor temperature (loop 16), and stripper level (loop 9). The reactor level and temperature loops were chosen because the reactor has the most significant effect on the product. The temperature and pressure loops are naturally connected, the temperature loop was chosen over the pressure loop, because the behavior of the reactor pressure is considerably nonlinear, and the temperature loop and its faults haven't been studied extensively.

The Figure 13 shows the overall control scheme.

6.2 MPC implementation

The Simulink model used to simulate the TE process was introduced earlier in this thesis. Simulink also has a ready-made block for MPC controller, and Figures 14 and 15 show the structural changes made to the simulation model. The MPC was implemented so that its inputs are the constant setpoints (reference) and the process measurements, and its outputs are setpoints given to the PI-controllers on the lower level.

The MPC was designed using MATLAB's MPC Designer tool. Using the configuration shown in Figure 15, the MPC Designer was launched and the model linearized. The resulting linear model had 81 states. This was deemed excessive, and therefore, MATLAB's Model Reducer tool was used reduce the model to 6 states. The number of states was chosen because less than 5 states made the system quite unstable and there was no marked improvement from more than 6 states.

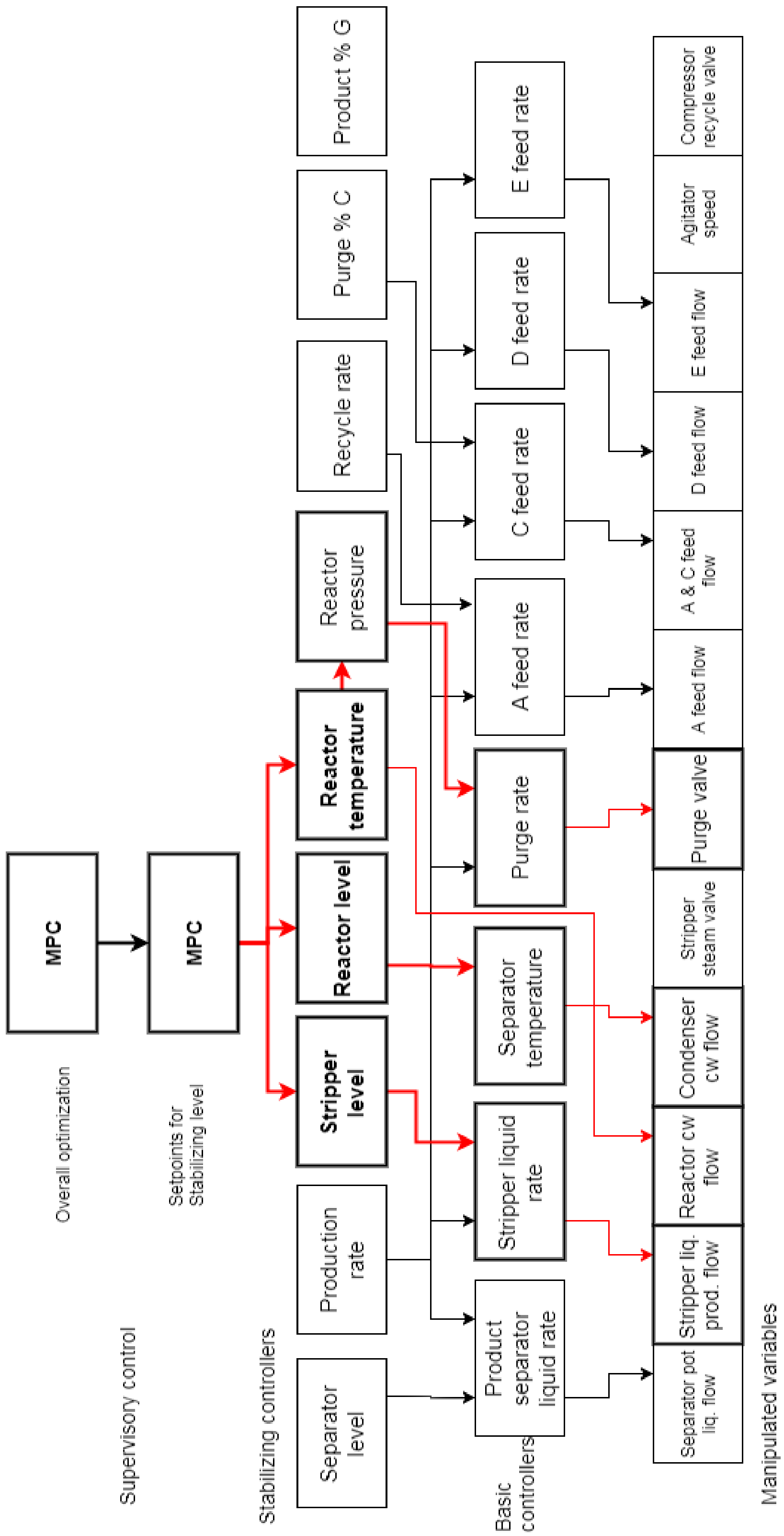

Fig. 13. The overall control scheme

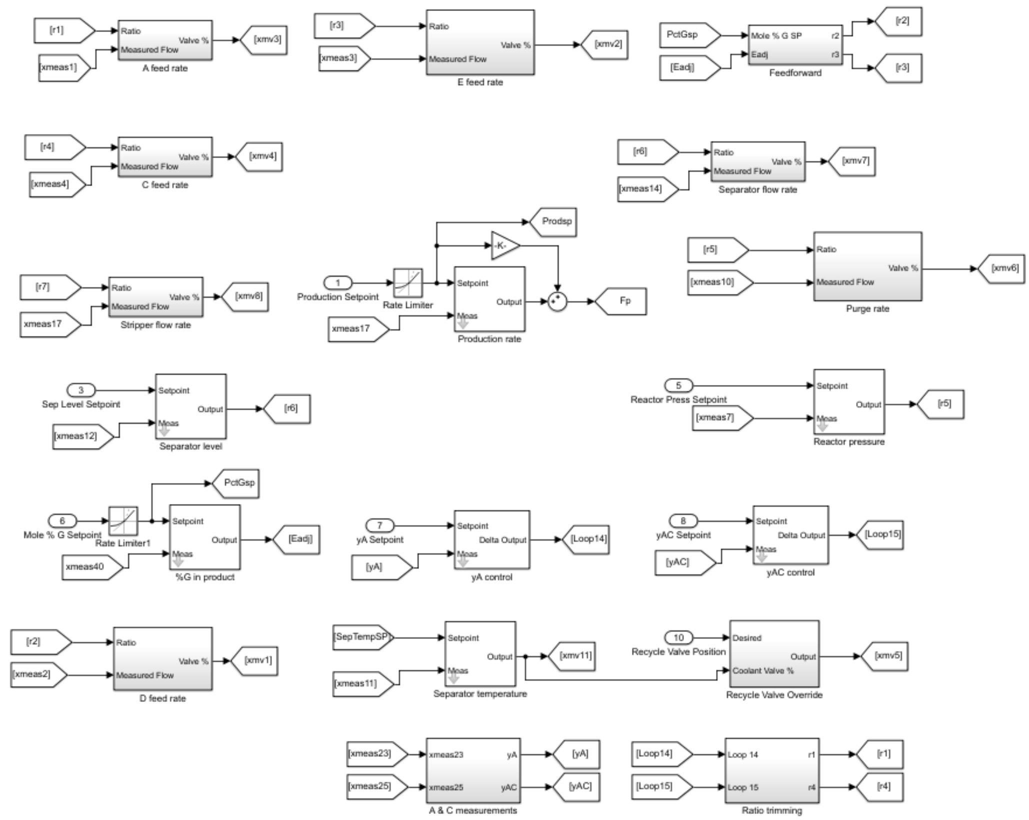

Fig. 14. Simulink MPC: loops not controlled by MPC

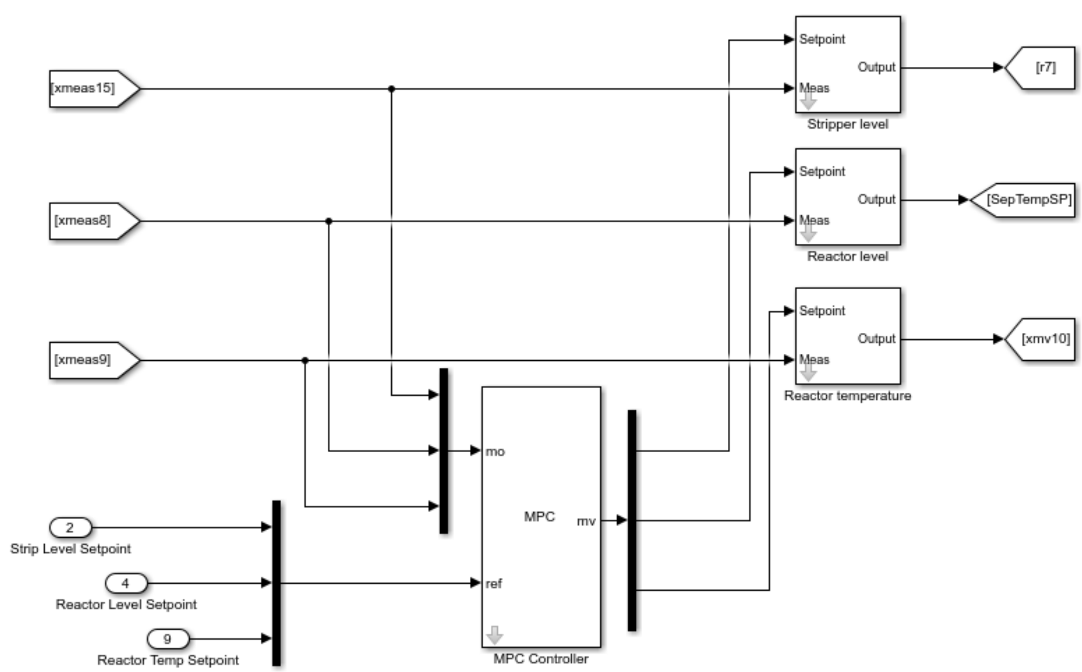

Fig. 15. Simulink MPC: loops controlled by MPC

MATLAB’s Model Predictive Control Toolbox includes an app, functions, and Simulink blocks for MPC design and simulation. It allows for specification of plant and disturbance model, constraints, horizons, and weights. The performance of the controller can be evaluated by running closed-loop simulations. (Mathworks 2017a)

The MPC toolbox recognizes both numeric linear-time-invariant (LTI) models and identified models (System Identification Toolbox). LTI models that can be used are transfer function, state space, and zero-pole-gain. The controller uses a discrete-time state-space system to perform all calculations. Therefore, when a plant model is specified the software performs the following steps as needed.

1. Conversion to state-space
2. Discretization or resampling
    - A continuous time model is converted to discrete-time
    - A discrete time model with differing sample time is resampled
3. Delay removal
4. Conversion to dimensionless variables
    - Scale factors should be specified

(Mathworks 2017b)

The MPC solves a quadratic program (QP) as an optimization problem at each control interval. The QP problem includes a cost function, constraints, and a decision. The cost function is a scalar measure of controller performance that is minimized. Constraints are conditions the solution must satisfy due to physical bounds. The decision is the adjustments to manipulated variables that minimize the cost function. (Mathworks 2017c)

The MPC QP solver converts the optimization problem to a general form QP problem.

$$\min_{x}\left(\frac{1}{2}x^T H x + f^T x\right) \tag{10}$$

which is subject to the linear inequality constraints $Ax \geq b$ where x is the solution vector, H is the Hessian matrix, A is a matrix of linear constraint coefficients, and b and f are vectors. These are calculated at each control interval. (Mathworks 2017d)

MATLAB QP solver uses the KWIK algorithm (Schmid, Biegler 1994). The KWIK algorithm is robust, but certain points should be considered:

- Linear constraints might be violated due to numerical rounding off. Violations of magnitude 10^{-6} are allowed.
- When testing for optimal solution the toolbox uses a nonadjustable tolerance.
- The search is an iterative process, with a preset maximum for number of iterations. With some configurations the default maximum might be so large the solver appears to stop responding.
- Hard constraints can be infeasible, which will cause the algorithm to terminate immediately.

(Mathworks 2017d)

The simulation model can be run in two modes, mode 1 and mode 3 (see chapter 5). The MPC was tuned while running the process in mode 3, and tested in both modes. The tuning was done in stages.

First, the effect of sample time, and prediction and control horizons was studied. The minimum prediction horizon $N_1 = 1$ in all cases. Tables 9–13 show the mean values and variations of production cost, quality, reactor level and temperature, and stripper level with three different horizons and three different sample times. The sample time 0.2 was chosen, because it has the smallest variation in the process measurements. The horizons were chosen to be control horizon $N_u = 5$ with prediction horizon $N = 8$, because they showed the best response.

Second, the effect of weights on the control inputs was studied. The weights were chosen to be 0.01 for the levels and the 0.03 for the temperature. Other studied weights are not shown, because their results were either obviously worse or had no significant difference from the case with no weights.

Last, the performance tuning option in the MPC Designer tool was studied. However, this had either no effect or a detrimental one, so the values were left untouched. The nominal values and constraints were directly the values from the process. The final controller values are collected in Table 14.

Table 9. Cost mean and variation with different sample times and horizons

	3 / 6		5 / 8		9 / 12	
st	Mean	Var	Mean	Var	Mean	Var
0.2	44.09	38.70	**43.98**	**42.55**	44.06	40.07
0.3	43.95	46.45	43.00	43.39	44.24	43.20
0.4	44.03	44.72	44.12	47.00	43.97	46.97

Table 10. Quality mean and variation with different sample times and horizons

	3 / 6		5 / 8		9 / 12	
st	Mean	Var	Mean	Var	Mean	Var
0.2	90.09	2.51	**90.09**	**2.78**	90.08	2.85
0.3	90.08	3.24	90.09	2.69	90.09	2.94
0.4	90.08	2.91	90.07	2.56	90.07	2.95

Table 11. Reactor level mean and variation with different sample times and horizons

	3 / 6		5 / 8		9 / 12	
st	Mean	Var	Mean	Var	Mean	Var
0.2	65.02	4.57	**65.01**	**3.90**	65.02	4.33
0.3	64.97	4.54	65.01	4.05	64.99	4.30
0.4	64.99	4.29	65.08	5.05	65.03	4.32

Table 12. Reactor temperature mean and variation with different sample times and horizons

	3 / 6		5 / 8		9 / 12	
st	Mean	Var	Mean	Var	Mean	Var
0.2	121.90	0.31	**121.90**	**0.27**	121.90	0.32
0.3	121.90	0.38	121.90	0.30	121.90	0.29
0.4	121.90	0.28	121.90	0.30	121.90	0.36

Table 13. Stripper level mean and variation with different sample times and horizons

	3 / 6		5 / 8		9 / 12	
st	Mean	Var	Mean	Var	Mean	Var
0.2	50.00	8.30	**50.07**	**9.04**	50.09	8.74
0.3	49.94	9.64	50.04	10.04	50.02	9.18
0.4	49.91	9.46	49.94	9.21	50.02	9.90

Table 14. Tuned values for the MPC

Variable	Nominal value	Constraints		Weights
		Low	High	
Stripper level	49 %	30 %	100 %	0.01
Reactor level	65 %	50 %	100 %	0.01
Reactor temperature	122°C	0°C	175°C	0.03
Sample time	0.2 h			
Prediction horizon	8			
Control horizon	5			

7 Dynamic behavior of the process under MPC

The dynamic behavior of the process under MPC was studied in two different operating modes, six (twelve) setpoint changes, and four process disturbances. The modes were mode 1 and mode 3. The disturbance cases were

1. No disturbances,
2. step change in A/C feed ratio, B composition constant (IDV 1),
3. step change in B composition, A/C ratio constant (IDV 2),
4. random variation in A, B, C feed composition (IDV 8)
5. slow drift in reacton kinetics (IDV 13).

The setpoint changes were step and ramp (30 hours) changes in

1. reactor level ($65\% \rightarrow 68\%$),
2. reactor temperature ($121.9℃ \rightarrow 124.9℃$),
3. reactor pressure ($2800kPa \rightarrow 2830kPa$),
4. stripper level ($50\% \rightarrow 53\%$),
5. separator level ($50\% \rightarrow 53\%$),
6. G mol-% in product ($90.09\% \rightarrow 93.09\%$).

The MPC was also tested with all disturbances introduced in Table 7 to ensure that only total loss of feed A would cause the system to fail.

This chapter presents and analyses the most important simulation results, the plotted values of the three controlled variables in the studied cases. Quality and cost graphs, and the effect of the process disturbances on other measurements can be found in Appendices 2 and 3. All cases were simulated for 72 hours, but the figures only show 30-60 hours depending on relevance.

7.1 Behavior of the process with process disturbances

Figures 16–20 and 21–25 show the disturbance plots (with MPC) for mode 3 and mode 1, respectively. The black vertical line in the figures indicates the start of the disturbance (10 hours in all shown cases).

Figure 16 shows the behavior of the process in mode 3 under the MPC with no disturbances. The process is steady and all variations from setpoint are within acceptable bounds.

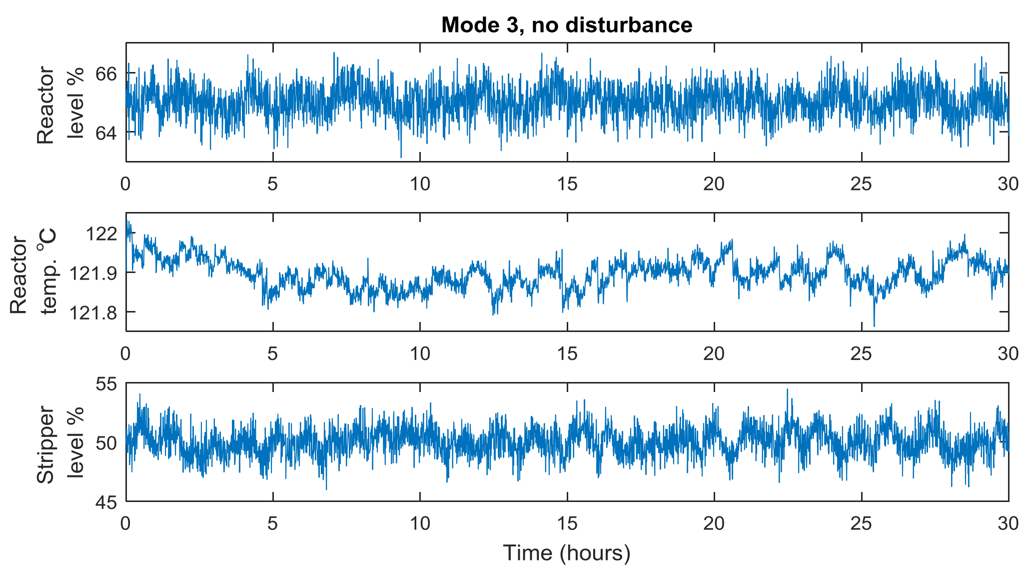

Fig. 16. Process behavior in mode 3 with no disturbances

Figure 17 shows the behavior of the process when a step-shaped disturbance in the A/C feed ratio (IDV 1) occurs at 10 hours of simulation. All three controlled variables show clear disturbances between 15-25 hours and 30-35 hours. Variation settles back to normal levels after 40 hours. The variation in temperature is less than 1 degree throughout and essentially negligible. The variation in stripper level is not significantly larger than in the basic case. However, the variation in the reactor level could benefit from further study into the controller.

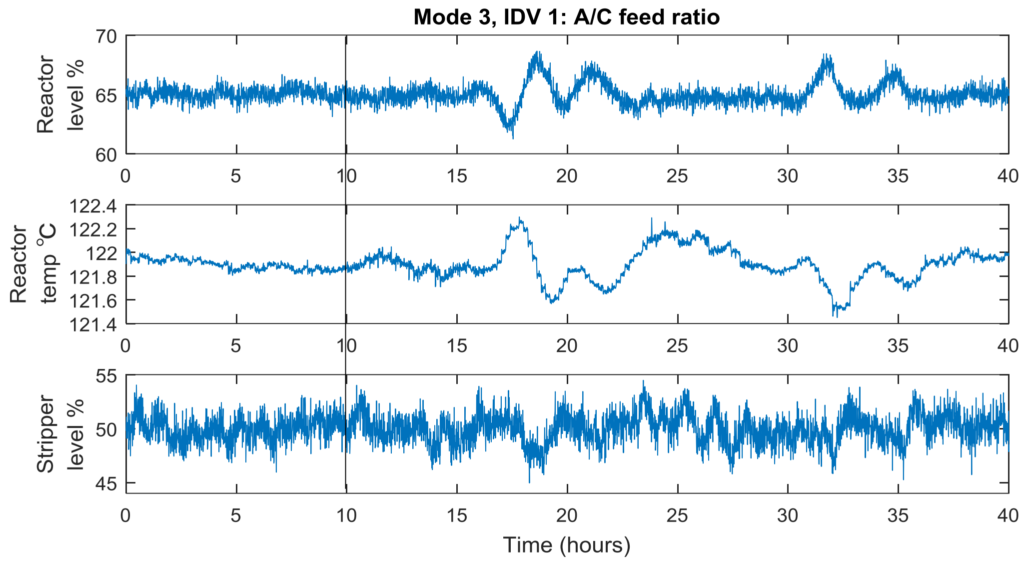

Fig. 17. Process behavior in mode 3 with step disturbance in A/C feed ratio. The vertical line shows start of disturbance

Figure 18 shows the behavior of the process in mode 3 when a step-shaped disturbance in the composition of B feed (IDV 2) occurs at 10 hours of simulation. In all three variables the disturbance doesn't become apparent until 20 hours of simulation. However, when it does, the controller cannot settle the process back down and the slow oscillation in the variables persists. In the case of the temperature, the variation is still under 1 degree.

Figure 19 shows the behavior of the process in mode 3 when a random variation disturbance in the A, B, and C compositions (IDV 8) occurs at 10 hours of simulation. Because the disturbance is random variation, the variations in the variables occur at random intervals, but the controller is able to settle the process between the disturbances.

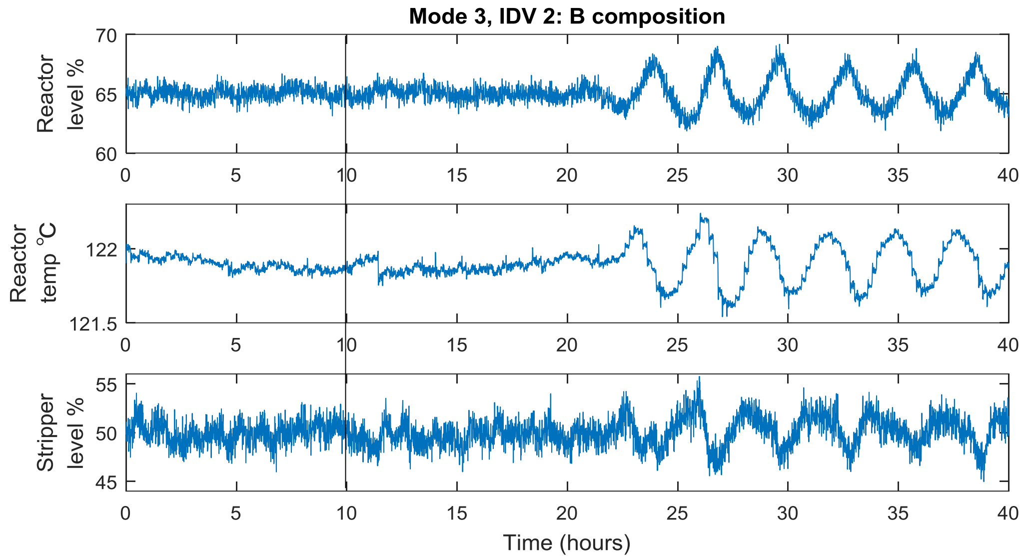

Fig. 18. Process behavior in mode 3 with step disturbance in B feed composition. The vertical line shows start of disturbance

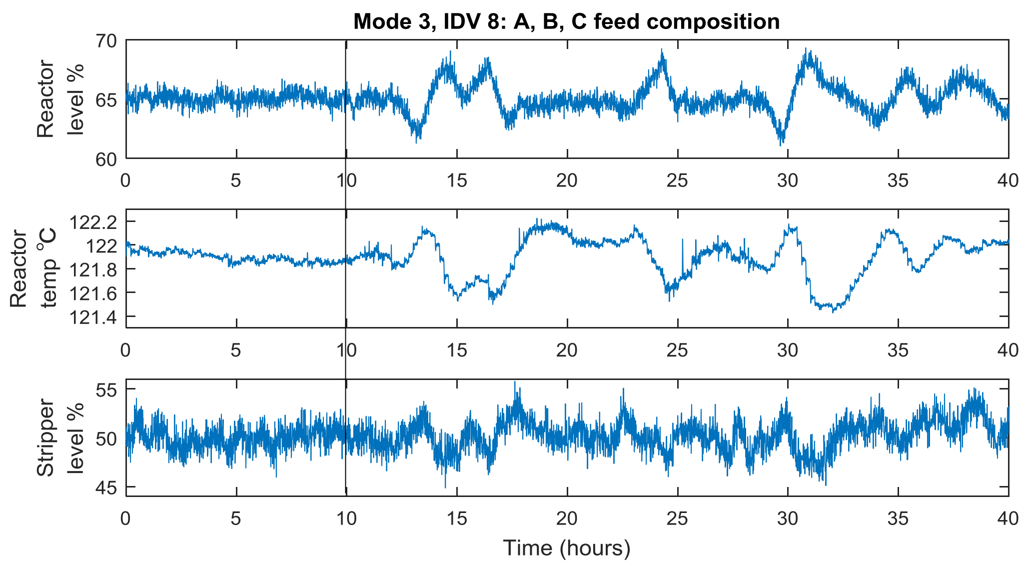

Fig. 19. Process behavior in mode 3 with random variation disturbance in A, B, C feed composition. The vertical line shows start of disturbance

Figure 20 shows the behavior of the process in mode 3 when a drift-shaped disturbance in reaction kinetics (IDV 13) starts at 10 hours of simulation. Level controls behave similarly to the IDV 8 case with the process settling between the disturbances. The temperature doesn't appear to settle, but the variation remains under 1 degree.

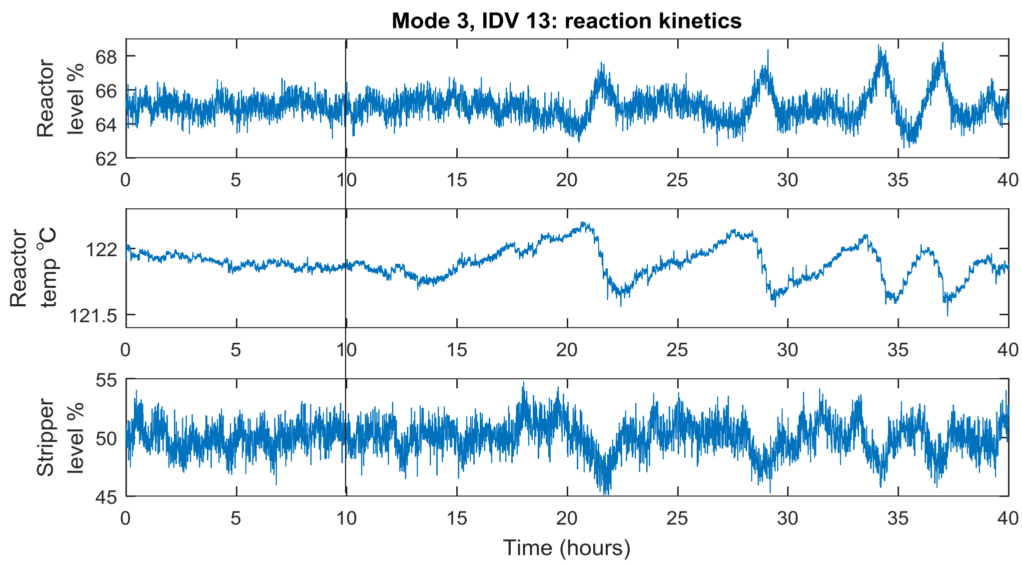

Fig. 20. Process behavior in mode 3 with drift disturbance in reaction kinetics. The vertical line shows start of disturbance

The controller performs sufficiently well in mode 3 with process disturbances. The case with change in B composition could benefit from further tuning, but the other cases either perform well or would require an adaptive model. The performance in mode 1 is studied next.

Figure 21 shows the behavior of the process in mode 1 under the MPC with no disturbances. As with mode 3, the process is steady and all variations from setpoint are within acceptable bounds.

Figure 22 shows the behavior of the process in mode 1 when a step-shaped disturbance in the A/C feed ratio (IDV 1) occurs at 10 hours of simulation. Reactor level shows a slightly larger than normal variation between 10-25 hours. Reactor temperature and stripper level show larger variations between 10-35 hours. The disturbance in temperature appears large, but remains around 1 degree. However, the stripper level changes 10 percentage points in less than 10 hours which causes the production flow to remain only barely within limits. This case could benefit from further study.

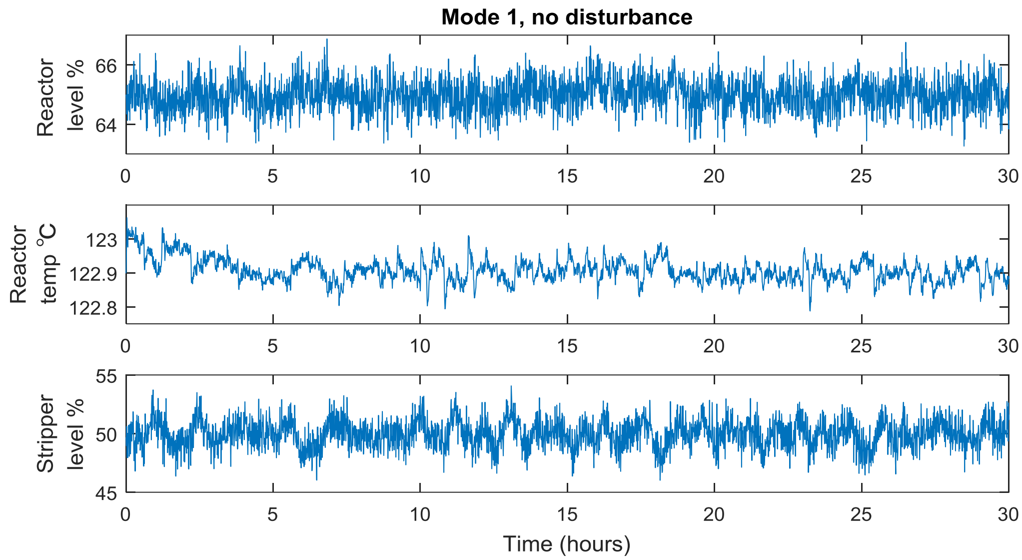

Fig. 21. Process behavior in mode 1 with no disturbances

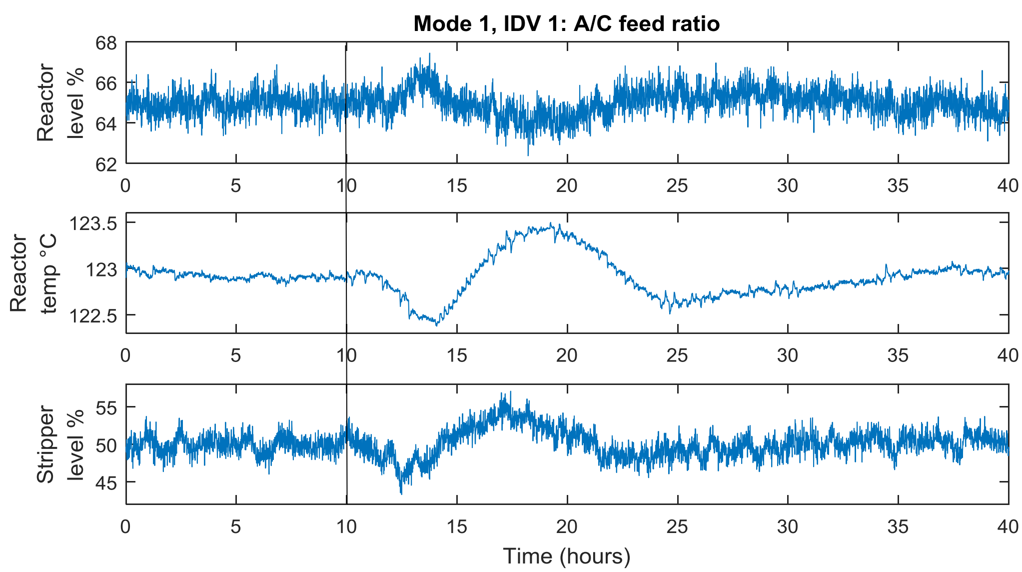

Fig. 22. Process behavior in mode 1 with step disturbance in A/C feed ratio. The vertical line shows start of disturbance

Figure 23 shows the behavior of the process in mode 1 when a step-shaped disturbance in the composition of B feed (IDV 2) occurs at 10 hours of simulation. Unlike the situation in mode 3, in mode 1 the variation is barely more significant than in the basic case.

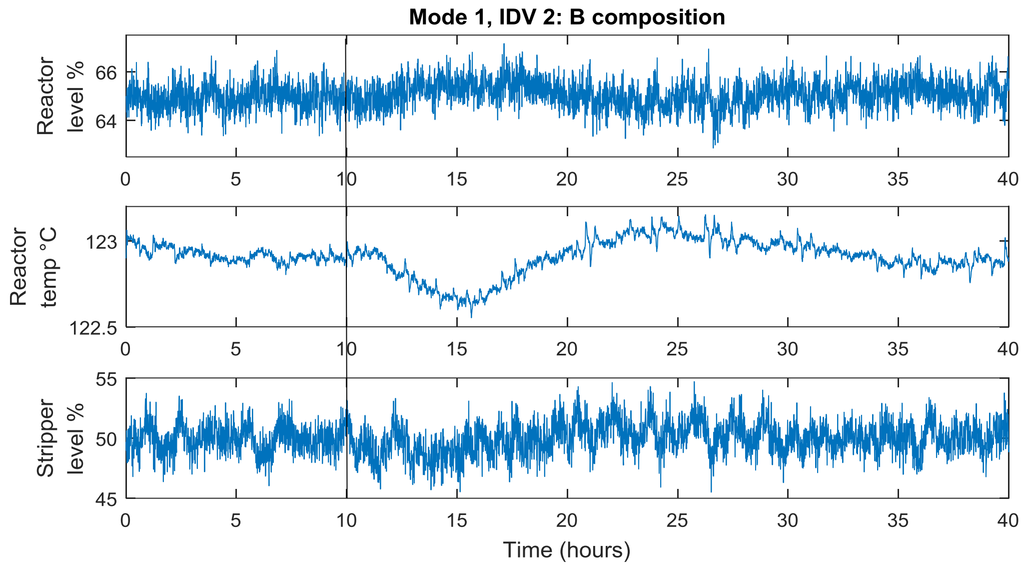

Fig. 23. Process behavior in mode 1 with step disturbance in B feed composition. The vertical line shows start of disturbance

Figure 24 shows the behavior of the process in mode 1 when a random variation disturbance in the A, B, and C compositions (IDV 8) occurs at 10 hours of simulation. This disturbance causes large variation in all three variables. The case was simulated additionally for 200 hours to ascertain the process remains stable. However, this situation should be studied further.

Figure 25 shows the behavior of the process in mode 1 when a drift-shaped disturbance in reaction kinetics (IDV 13) starts at 10 hours of simulation. Similarly to the case with IDV 8 the variations caused by this disturbance are large, and the process was simulated for additional time. The variations are less severe than in the previous case, but the situation could benefit from further study.

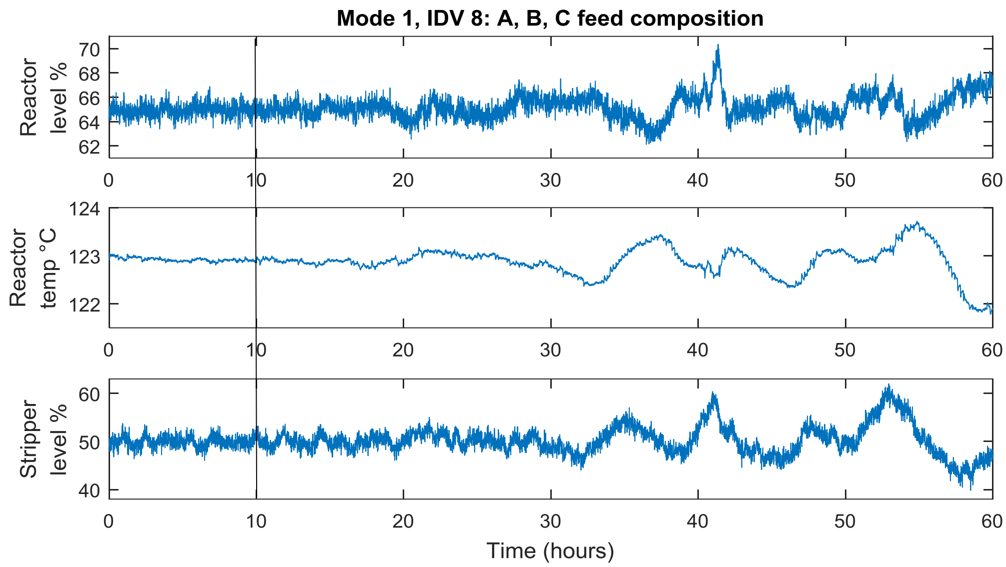

Fig. 24. Process behavior in mode 1 with random variation disturbance in A, B, C feed composition. The vertical line shows start of disturbance

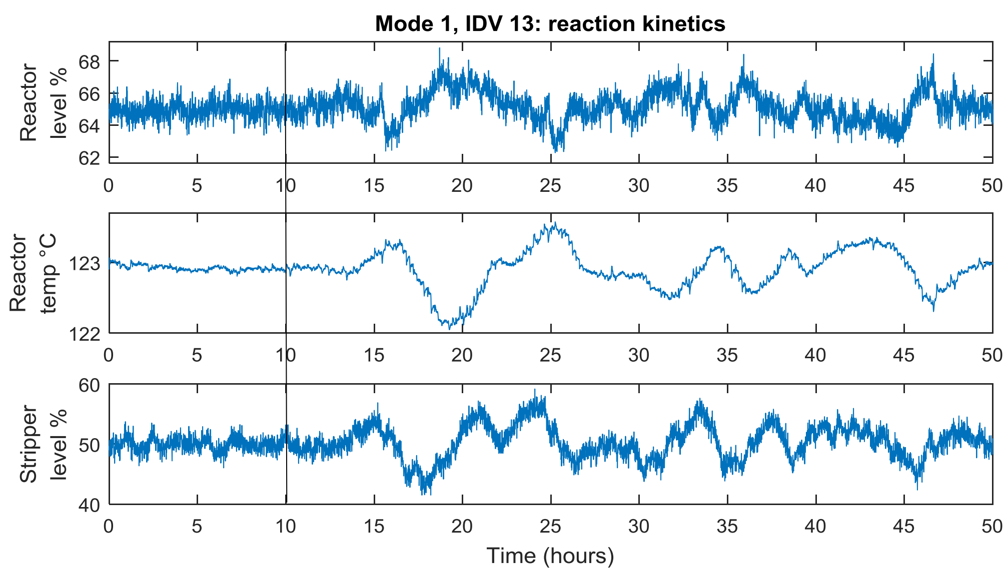

Fig. 25. Process behavior in mode 1 with drift disturbance in reaction kinetics. The vertical line shows start of disturbance

Several disturbance cases in mode 1 require or could benefit from further study. One cause of this is probably the fact that the model was identified in mode 3 and the process is in parts highly nonlinear.

7.2 Behavior of the process with setpoint changes

Figures 26–31 show the behavior of the process when step-changes are made to setpoints. Figures 32–37 show the behavior of the process with ramp-changes to setpoints. The results shown here are for ramps of 30 hours. Other lengths were studied but had no significant enough difference to be described here. All figures show the three variables (reactor level, reactor temperature, stripper level) in both modes 1 and 3, and a mode 3 comparison of PI and MPC.

Figure 26 shows the process behavior when a step change of +3 is introduced to the reactor level setpoint. Mode 1 reactor level follows the setpoint change closely. Mode 3 reactor level rises initially further than the setpoint, but settles within two hours. Both MPCs react faster than the PI. Reactor temperature has a slight spike at the time of the step for both MPCs, but the variation stays under 0.5 degrees. The PI control causes the stripper level to go almost out of constraints, both MPCs perform comparatively almost perfectly.

Figure 27 shows the process behavior when a step change of +3 is introduced to the reactor temperature setpoint. Mode 3 reactor level has significant variation (in the setpoint) for 20 hours after the step change; the mean remains close to the setpoint. Mode 1 reactor level remains steady. PI control has a large drop almost to the lower limit at the time of step, but otherwise settles faster than the mode 3 MPC. Reactor temperature has a brief overshoot in all cases, and slight oscillation (less than 1 degree change per hour) in mode 3, but follows the setpoint very well. Stripper level has some variation in both MPCs, mode 3 causes slow oscillation in setpoint. The PI control causes the stripper level to go close to both limits in the span of two hours.

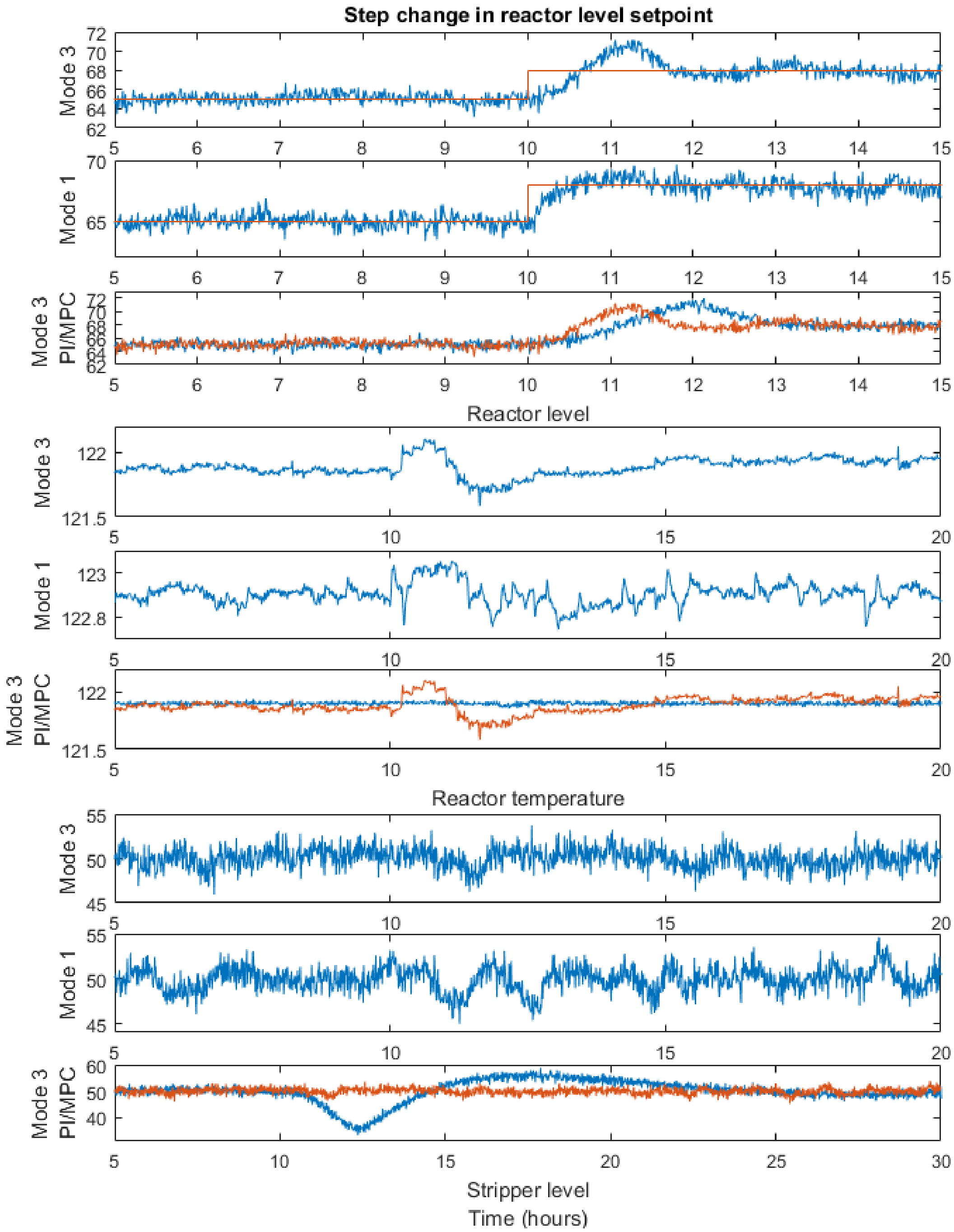

Fig. 26. Step change in reactor level setpoint

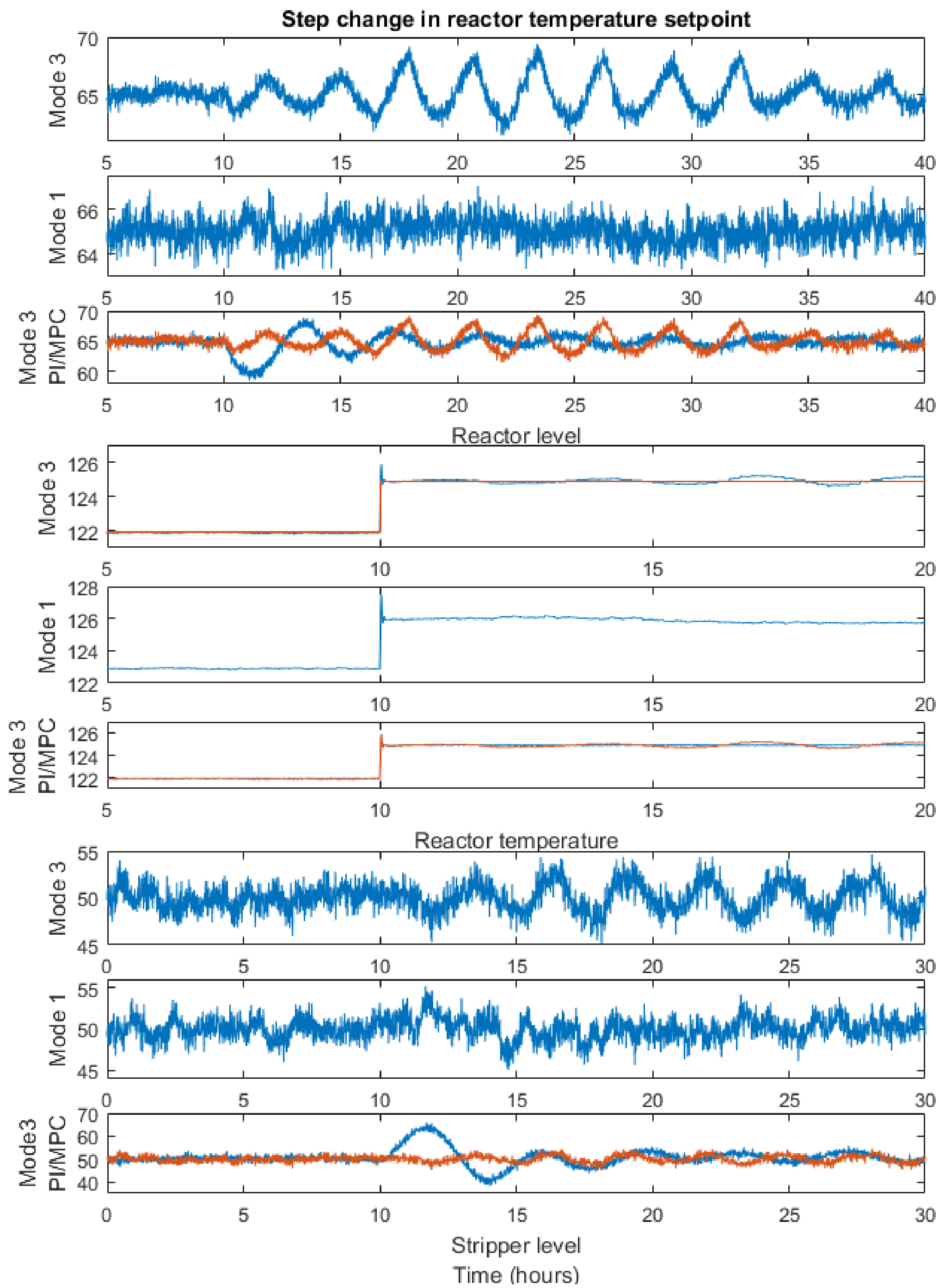

Fig. 27. Step change in reactor temperature setpoint

Figure 28 shows the process behavior when a step change of +30 is introduced to the reactor pressure setpoint. Reactor level in mode 3 has slow oscillation in setpoint (5 percentage points). Variation in reactor temperature with both MPC appears worrying, but a study of the scale shows it is actually insignificant (less than 0.5 degrees). The stripper level shows no significant change.

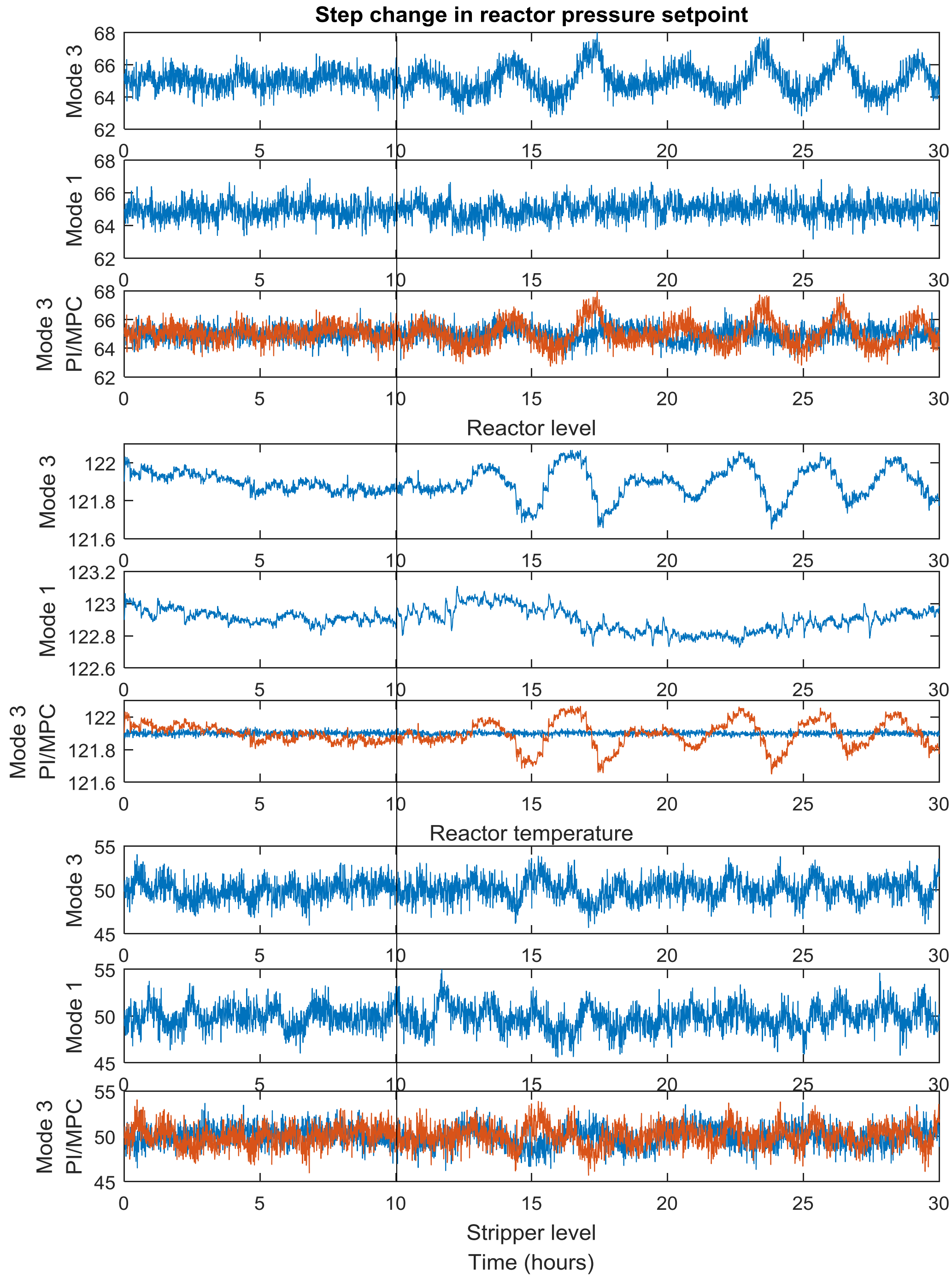

Fig. 28. Step change in reactor pressure setpoint; line indicates time of step

Figure 29 shows the process behavior when a step change of +3 is introduced to the stripper level setpoint. The stripper level transitions to the new setpoint smoothly. The MPCs react faster than the PI control. The reactor is upstream of the stripper, so a change there has no effect.

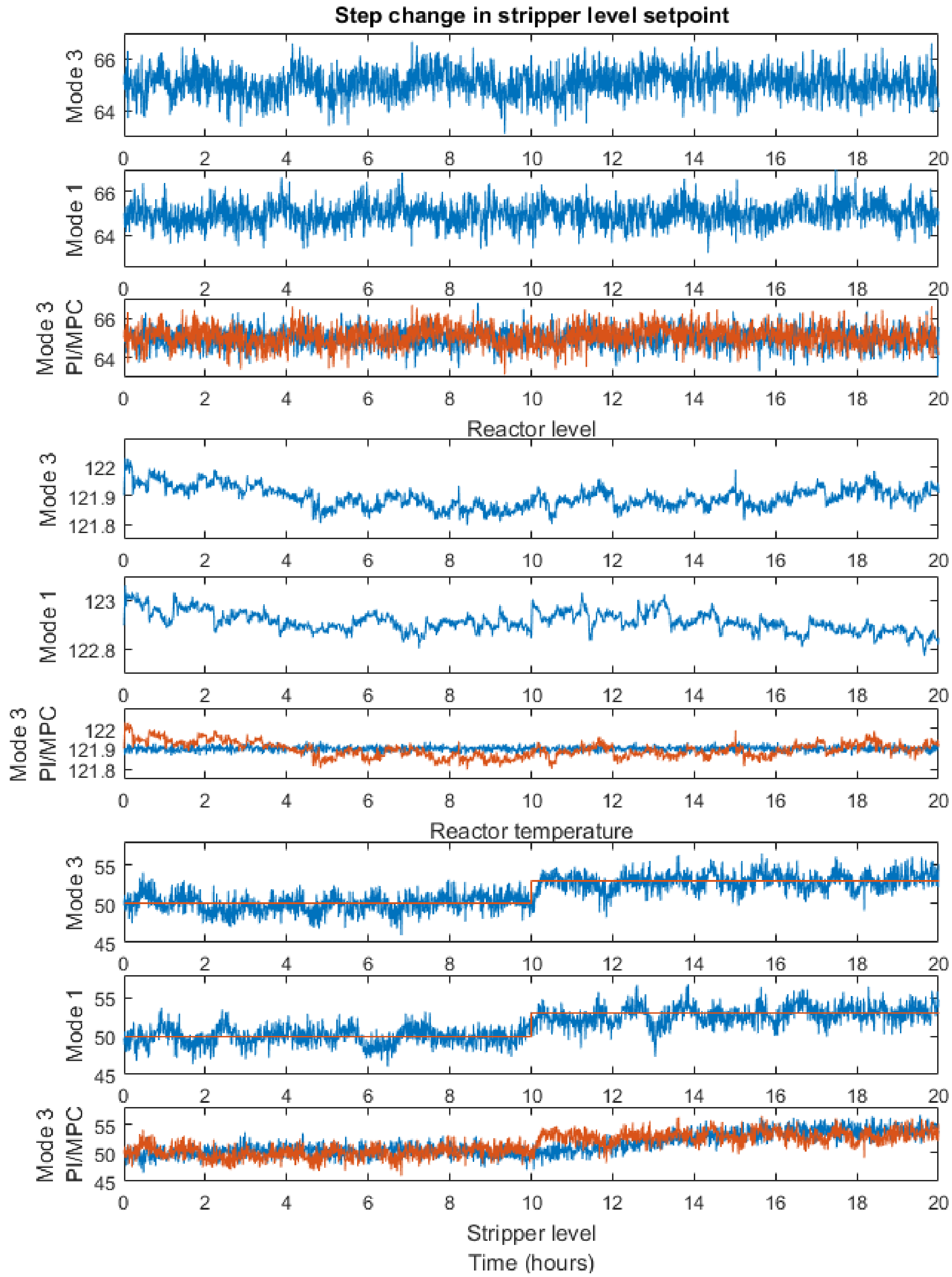

Fig. 29. Step change in stripper level setpoint

Figure 30 shows the process behavior when a step change of +3 is introduced to the separator level setpoint. A change in the separator level causes a disturbance in the stripper with PI control, other cases show no significant difference.

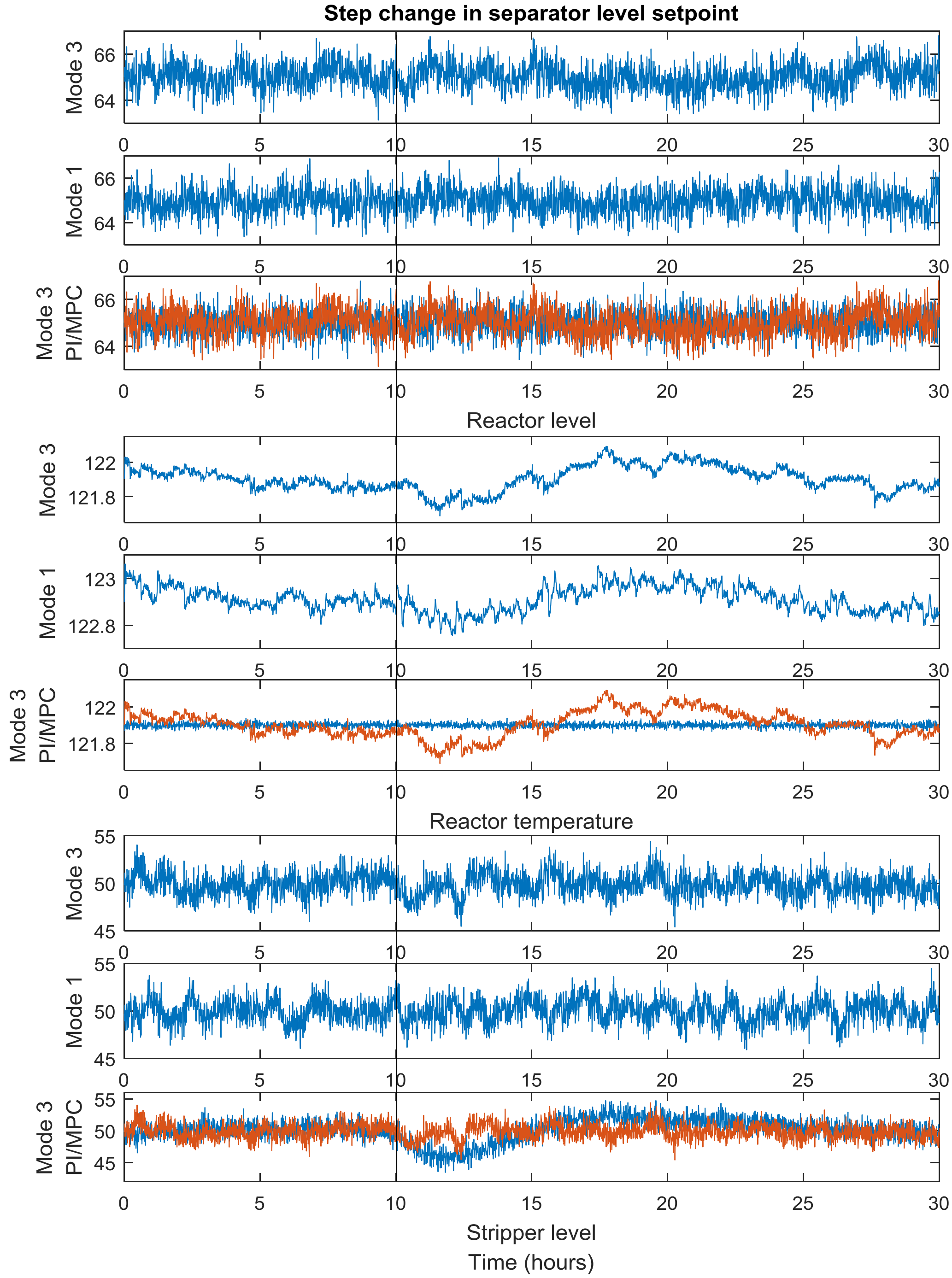

Fig. 30. Step change in separator level setpoint

Figure 31 shows the process behavior when a step change of +3 is introduced to the G mol-% setpoint. Mode 3 MPC causes fairly significant oscillation in the setpoint for all three variables starting 10 hours after step change. Mode 1 MPC shows no disturbance. Stripper level with PI control has some larger disturbances, but overall remains steady.

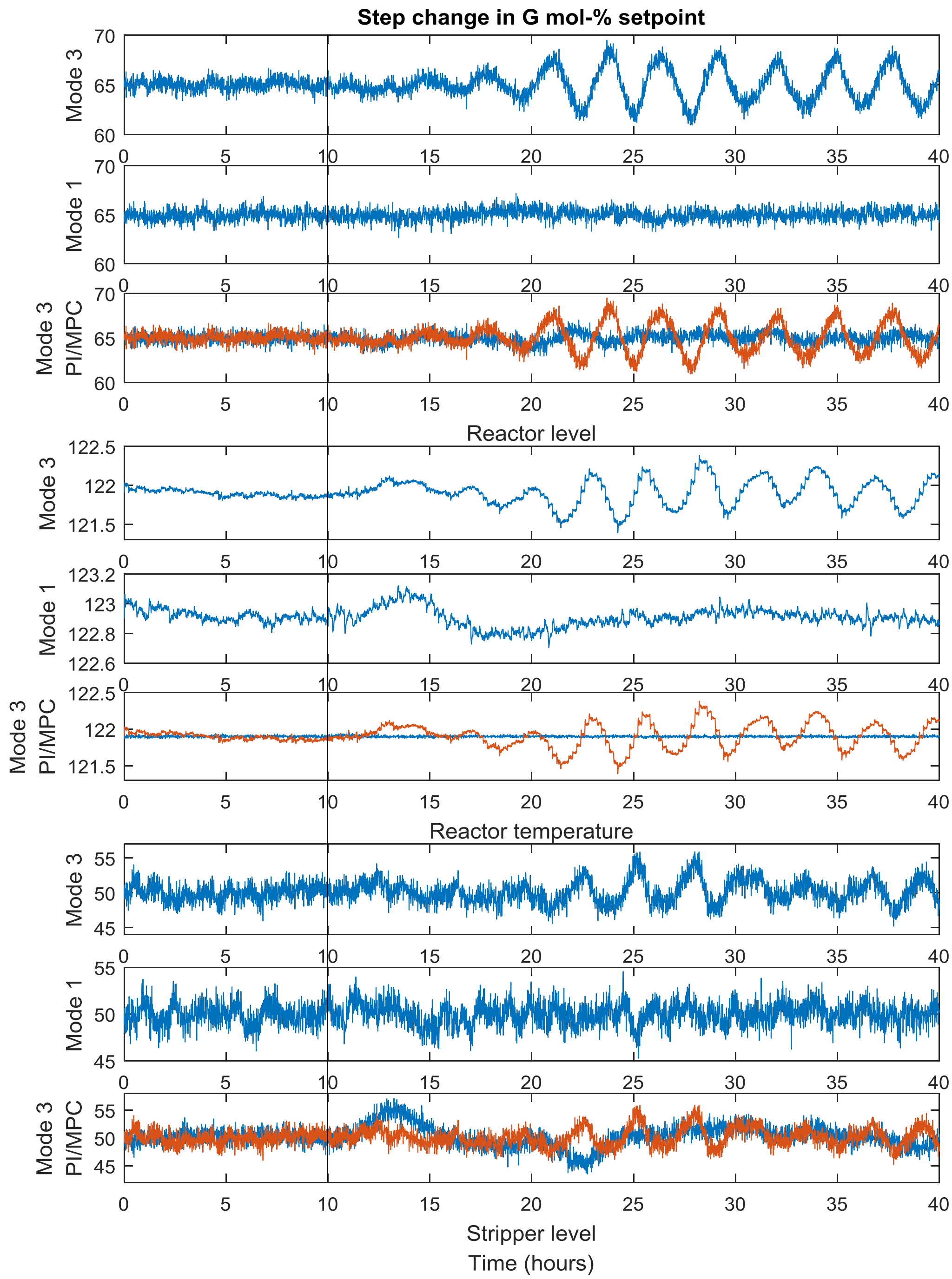

Fig. 31. Step change in G mol-% in product setpoint

Figure 32 shows the process behavior when a ramp change of +3 is introduced to the reactor level setpoint. Reactor level smoothly follows the setpoint change in all cases. Stripper level has a slight downward disturbance at the beginning of the ramp, otherwise no significant effects.

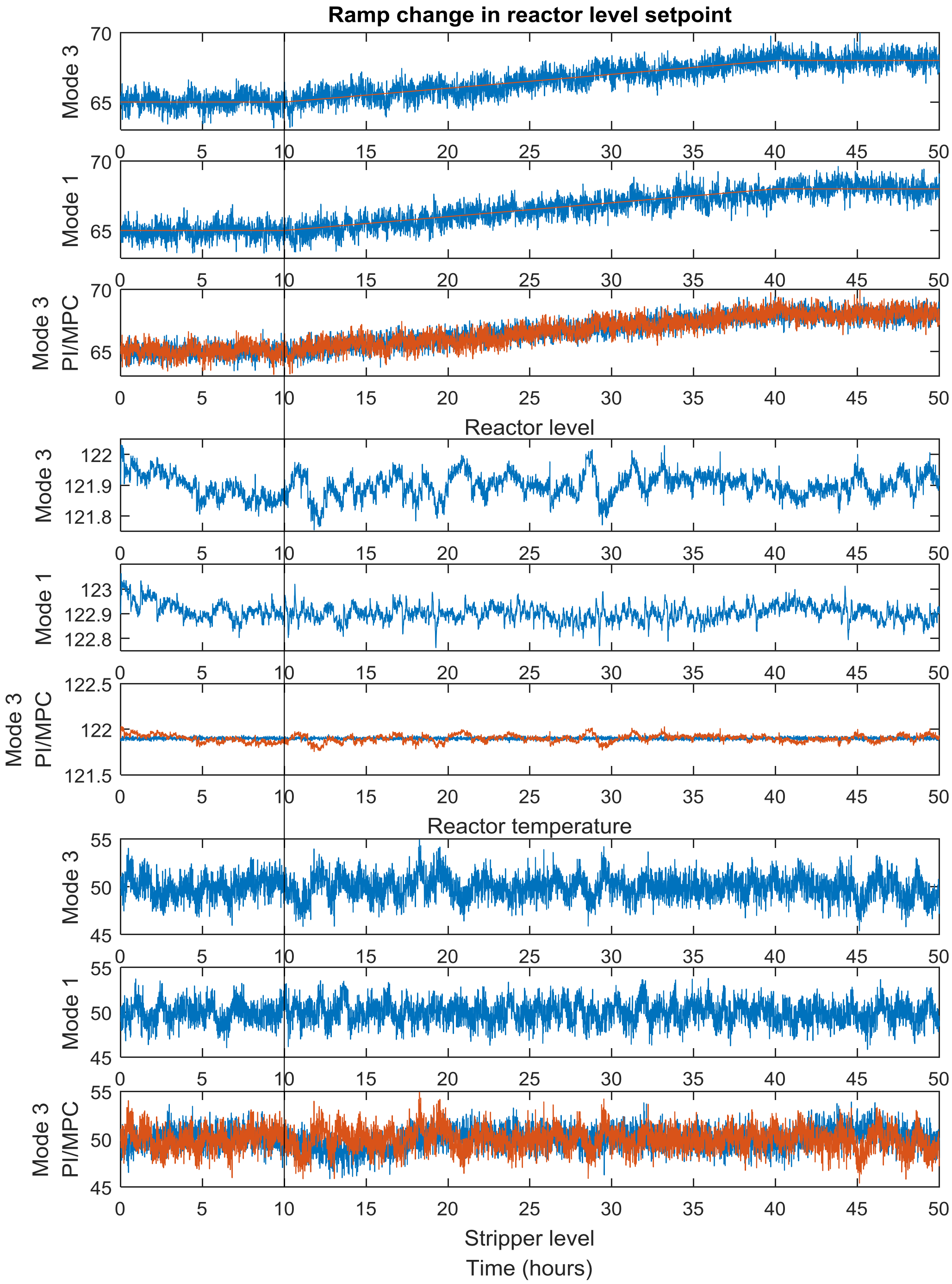

Fig. 32. Ramp change in reactor level setpoint

Figure 33 shows the process behavior when a ramp change of +3 is introduced to the reactor temperature setpoint. Mode 3 MPC causes the reactor level to oscillate after 20 hours of the ramp. Mode 1 MPC and PI control show no significant difference. Reactor temperatures follow the setpoint change smoothly, mode 3 MPC causes slight oscillation in setpoint after 15 hours of the ramp change. Stripper level shows no disturbances in any case.

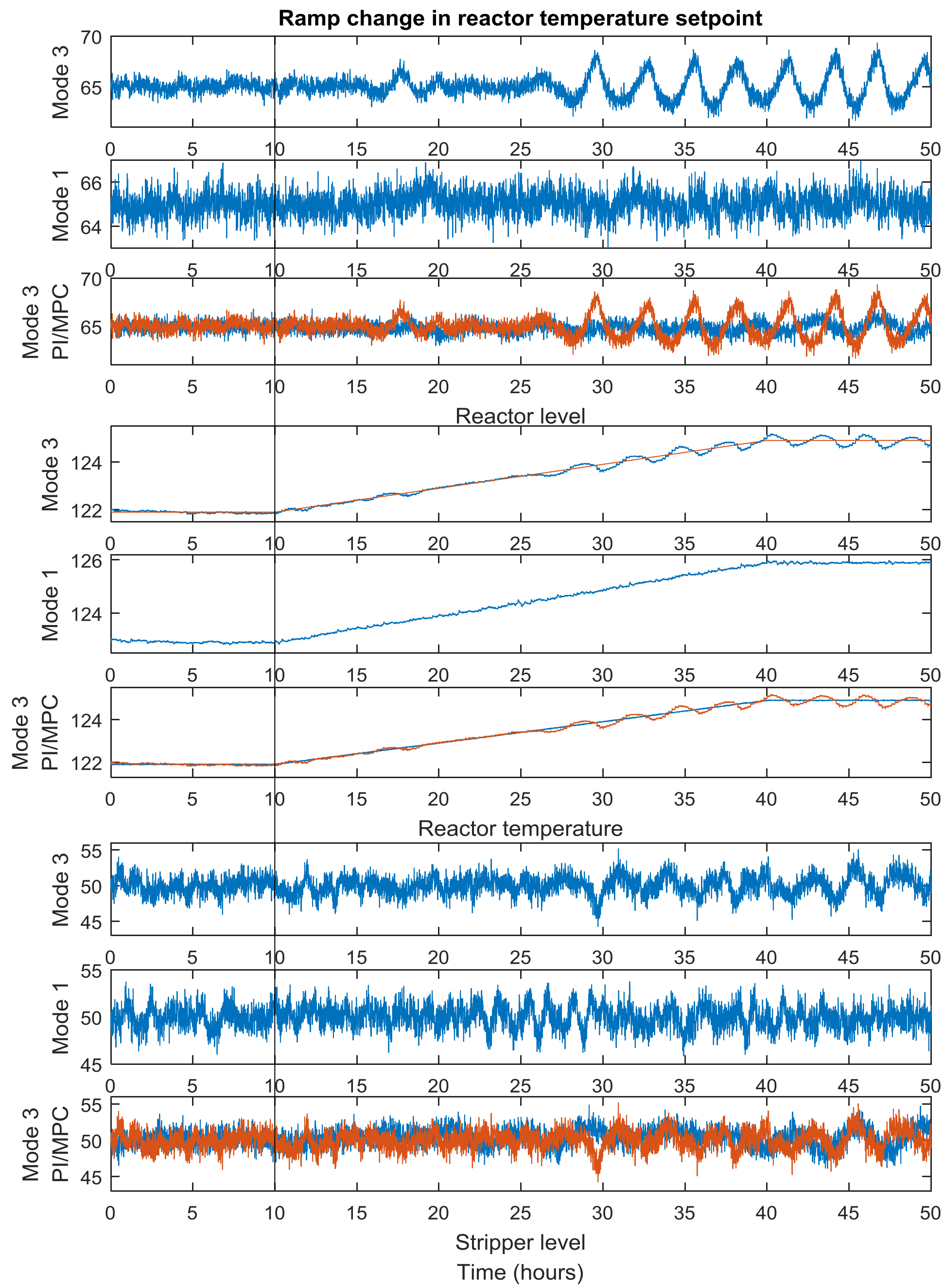

Fig. 33. Ramp change in reactor temperature setpoint

Figure 34 shows the process behavior when a ramp change of +30 is introduced to the reactor pressure setpoint. A slow change in the reactor pressure setpoint has no observable effect on the three variables in any of the cases.

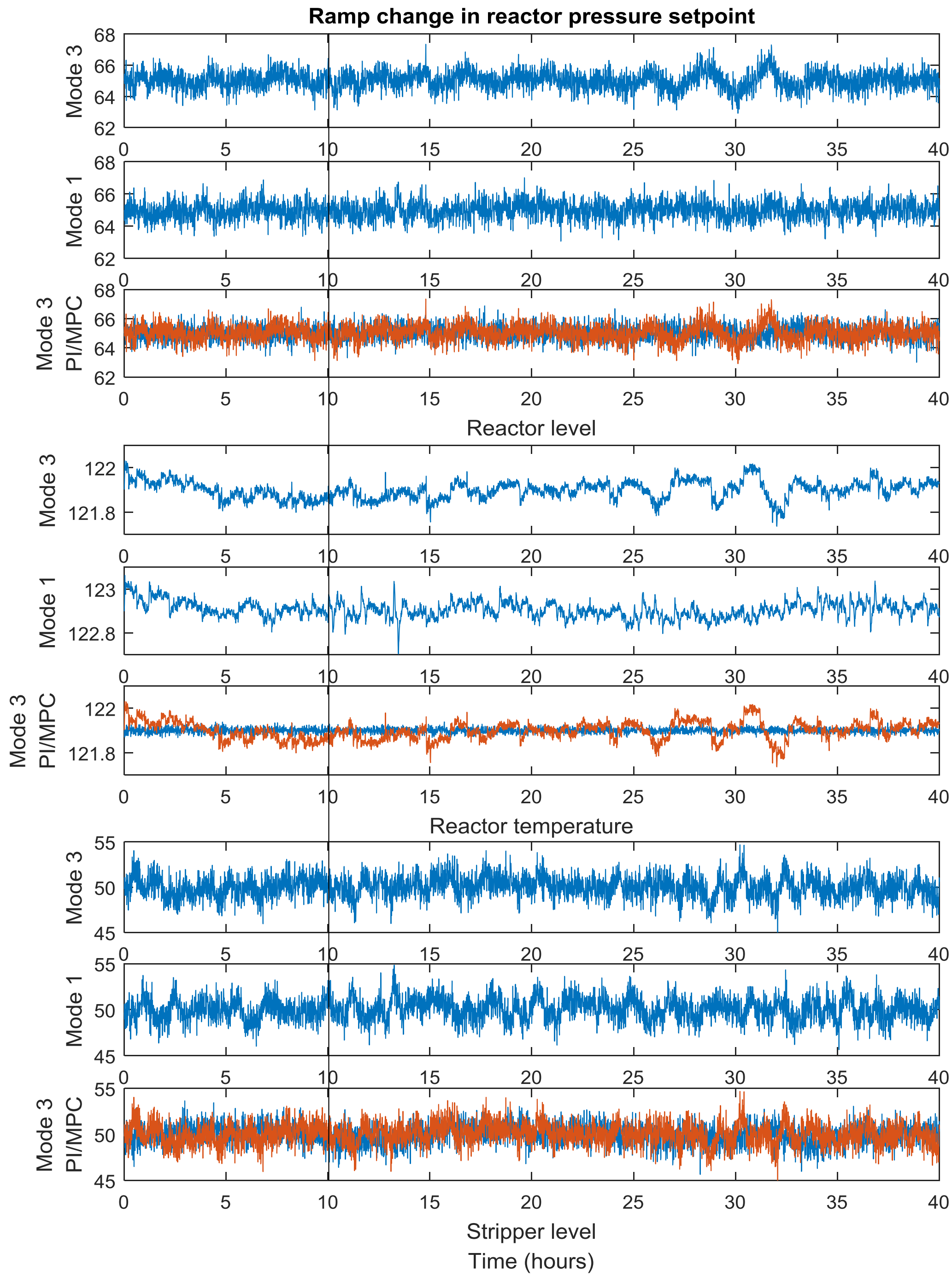

Fig. 34. Ramp change in reactor pressure setpoint

Figure 35 shows the process behavior when a ramp change of +3 is introduced to the stripper level setpoint. The stripper follows the ramp change well. As with the step change, the reactor is upstream of the stripper, and not affected by this change.

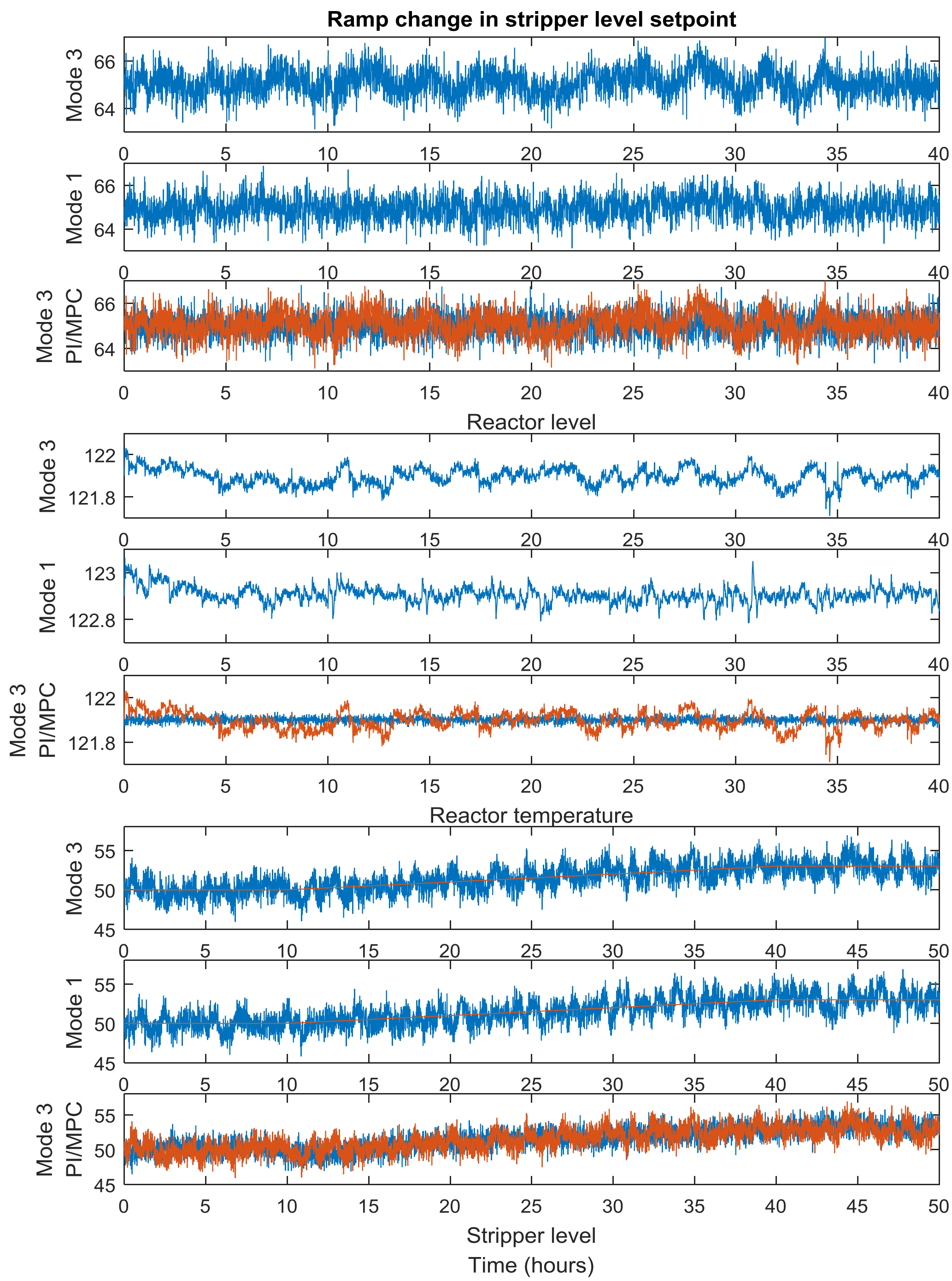

Fig. 35. Ramp change in stripper level setpoint

Figure 36 shows the process behavior when a ramp change of +3 is introduced to the separator level setpoint. A slow change in the separator level setpoint has no observable effect on the three variables in any of the cases.

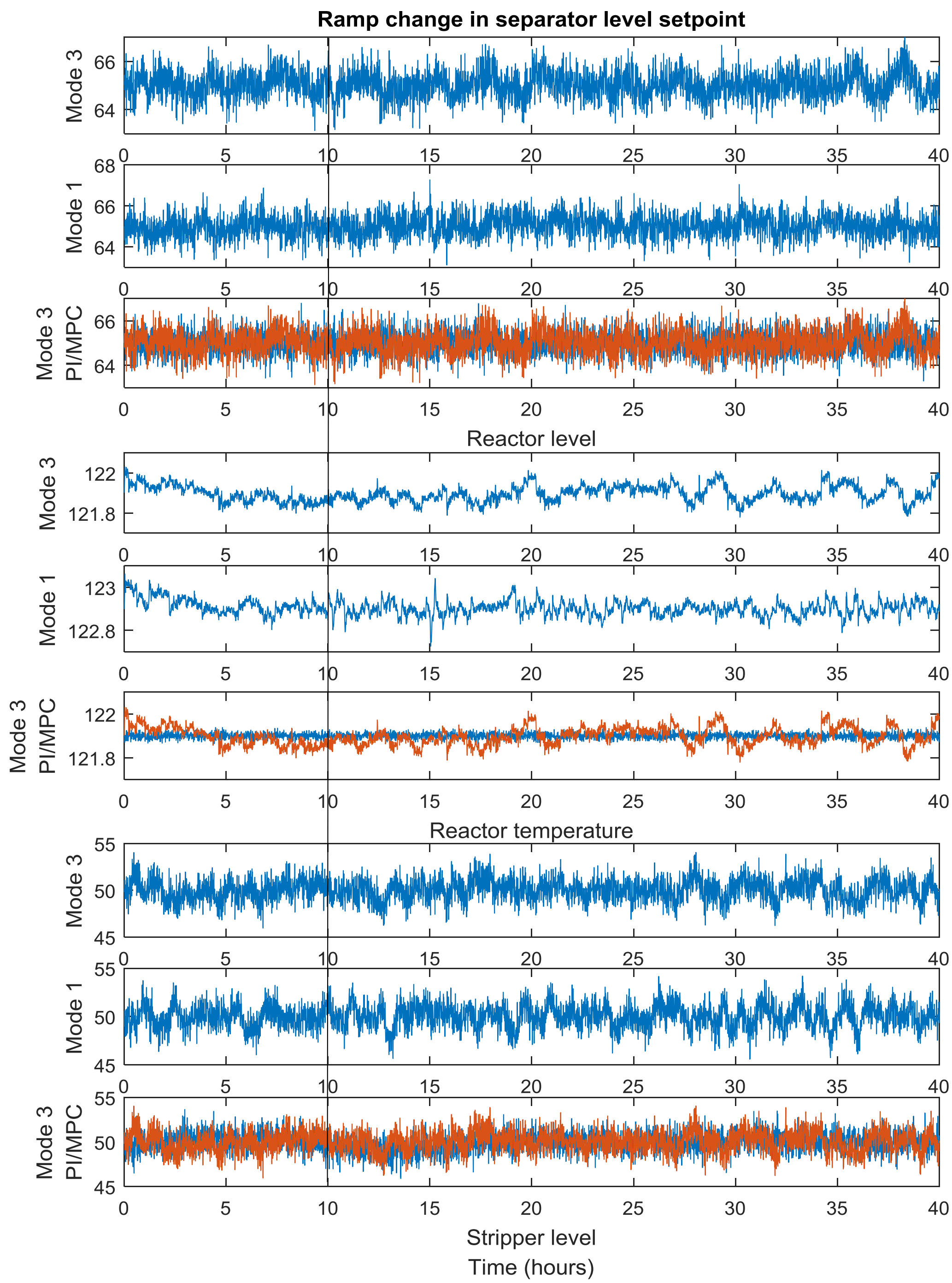

Fig. 36. Ramp change in separator level setpoint

Figure 37 shows the process behavior when a ramp change of +3 is introduced to the G mol-% setpoint. In mode 3 both the reactor level and temperature show significant oscillation in setpoint after 15 hours of the ramp change. The stripper level also shows some oscillation after 20 hours of the ramp change. All three variables are reasonably steady in mode 1 and with PI control.

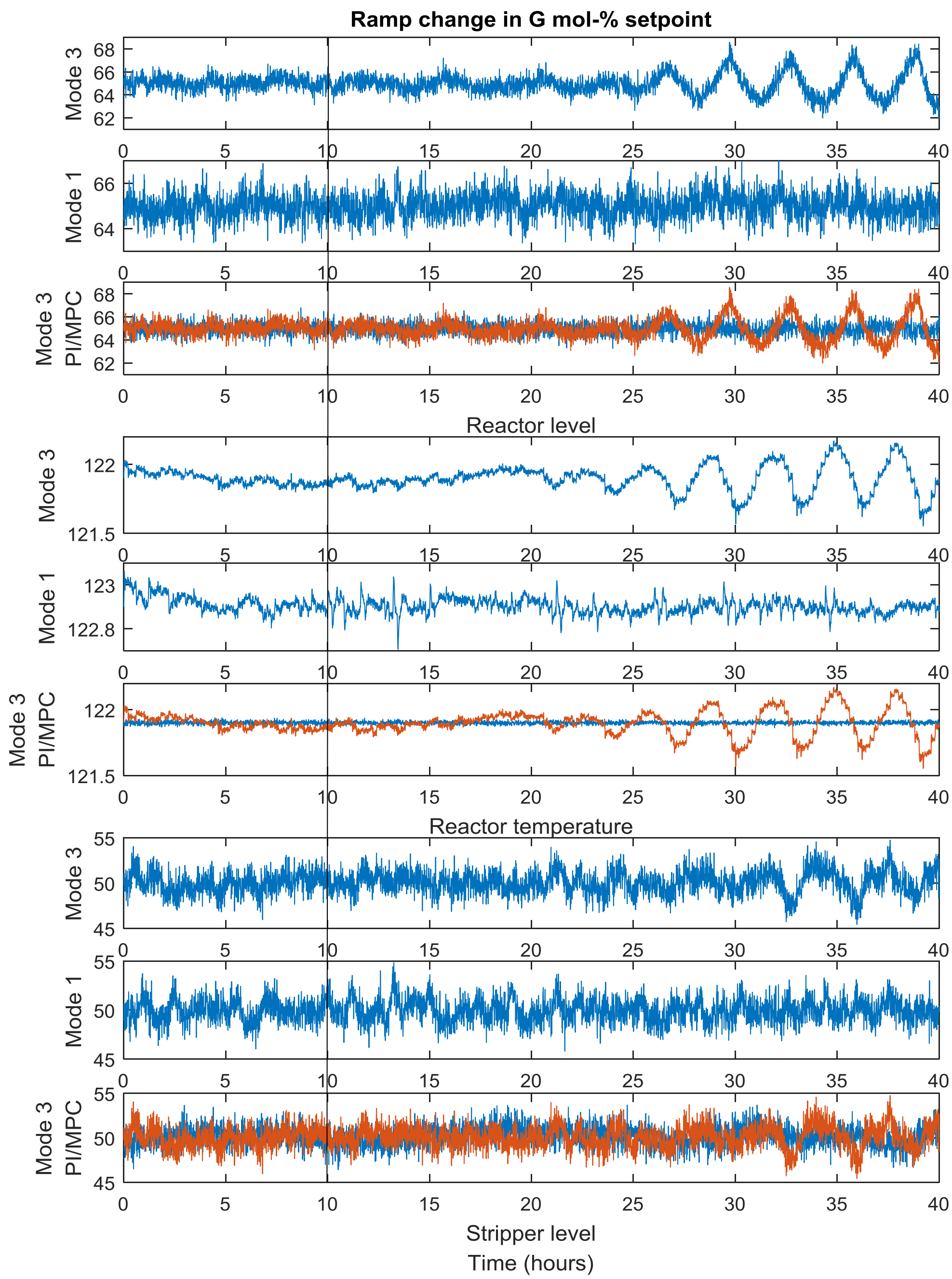

Fig. 37. Ramp change in G mol-% in product setpoint

The ramp changes to setpoints behave better than the step changes in the majority of the situations. The only exceptions are with mode 3 MPC, where setpoint changes to both reactor temperature and G mol-% cause some oscillation. The cause of this oscillation should be studied further.

8 Effect of faults under MPC

The behavior of the MPC was also studied in the case of mechanical faults. The purpose of fault tolerance is mainly to negate the effect of these on the process. The faults studied were

1. variation in reactor cooling water inlet temperature (IDV 11),
2. valve stiction in the temperature loop (IDV 14),
3. both (IDV 11 + IDV 14) at the same time, and
4. drift in the level sensor in the stripper.

Figures 38–41 are the plots from mode 3. Figure 38 shows the process behavior when the disturbance 11 (random variation in reactor cooling water inlet temperature) starts at 10 hours of simulation. Figure 39 shows the process behavior when the disturbance 14 (stiction in the cooling water valve) starts at 10 hours of simulation. Figure 40 shows the process behavior when the disturbances 11 and 14 both start at 10 hours of simulation. Figure 41 shows the process behavior when a sensor drift fault starts at 10 hours of simulation.

Figures 42–45 are the plots from mode 1. Figure 42 shows the process behavior when the disturbance 11 starts at 10 hours of simulation. Figure 43 shows the process behavior when the disturbance 14 starts at 10 hours of simulation. Figure 44 shows the process behavior when the disturbances 11 and 14 both start at 10 hours of simulation. Figure 45 shows the process behavior when a sensor drift fault starts at 10 hours of simulation.

A comparison of the basic PI control and MPC can be found in Appendix 4.

Figure 38 shows the behavior of the process in mode 3 when a random variation disturbance in the cooling water inlet temperature (IDV 11) starts at 10 hours of simulation. The disturbance is in the cooling system of the reactor and has no significant effect on the levels. On the reactor temperature the effect of the fault is immediate. The variation remains within a degree on both sides of the setpoint, and the fastest change is a degree in 10 minutes.

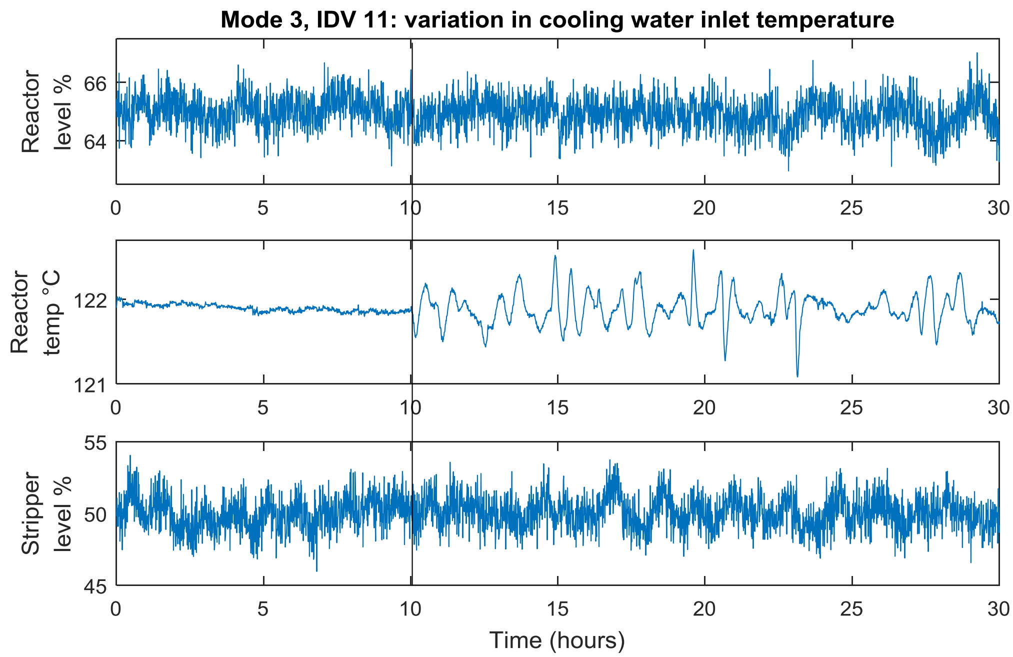

Fig. 38. Process behavior in mode 3 with random variation disturbance in reactor cooling water inlet temperature (IDV 11). The vertical line shows start of disturbance

Figure 39 shows the behavior of the process in mode 3 when a stiction fault in the cooling valve (IDV 14) starts at 10 hours of simulation. The disturbance is in the cooling system of the reactor and has no significant effect on the levels. For the reactor temperature the simulation shows high frequency oscillation (a change of 0.8 degrees up and down within 5 minutes). The MPC causes some oscillation also in the setpoint, but the mean of the temperature remains steady.

Figure 40 shows the behavior of the process in mode 3 when both variation in cooling water temperature and stiction in the valve (IDV 11 and IDV 14) start at 10 hours of simulation. The disturbances are in the cooling system of the reactor and have no significant effect on the levels. A combination of the two previous faults behaves as would be expected. The variation remains within a degree on both sides of the setpoint, and there are periods of high frequency oscillation.

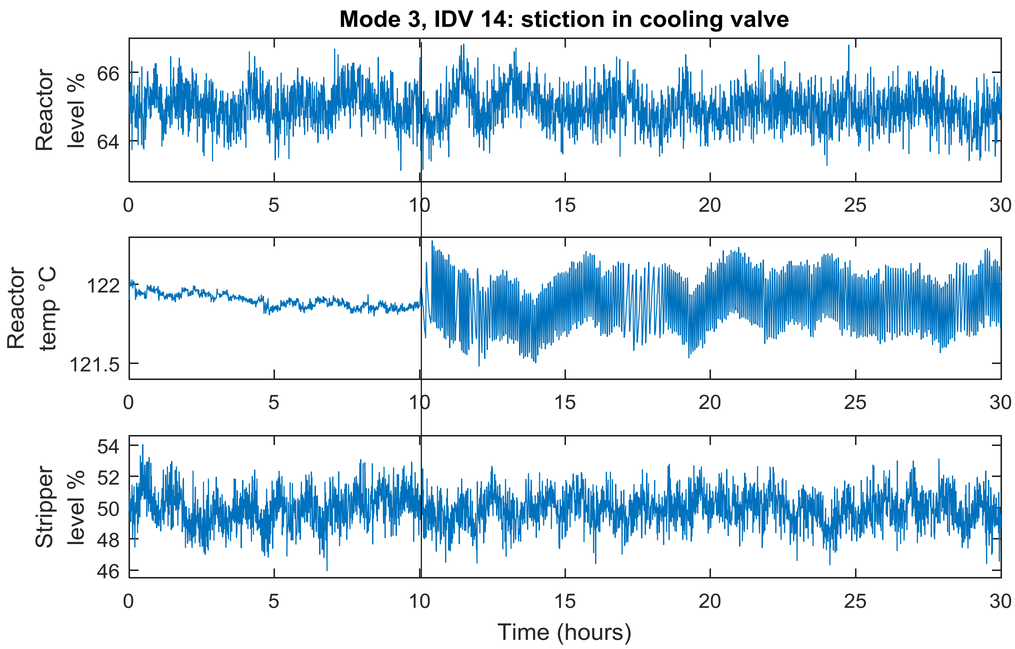

Fig. 39. Process behavior in mode 3 with a stiction fault in reactor cooling valve (IDV 14). The vertical line shows the start of disturbance

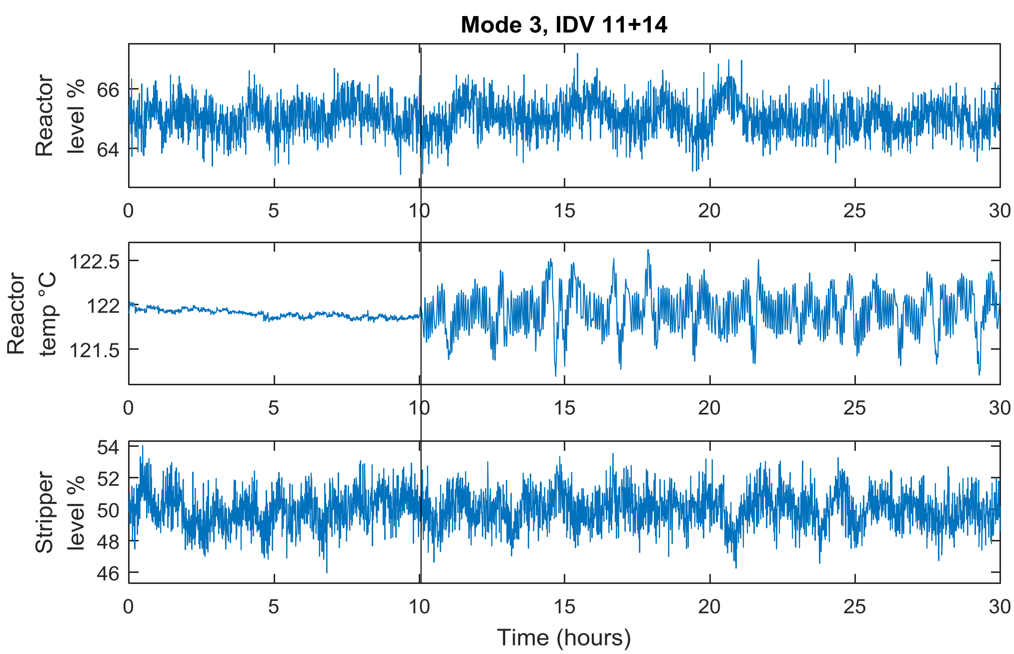

Fig. 40. Process behavior in mode 3 with variation in cooling water temperature and stiction in cooling valve (IDV 11 + IDV 14). The vertical line shows the start of disturbance

Figure 41 shows the behavior of the process in mode 3 when a drift shaped fault in the stripper level sensor starts at 10 hours of simulation. The reactor is upstream of the stripper in the process, so faults in the stripper have no effect on reactor level or temperature. A positive drift in the sensor causes the controller to think the stripper level is higher than it actually is, which results in the real level being proportionally lower than the setpoint.

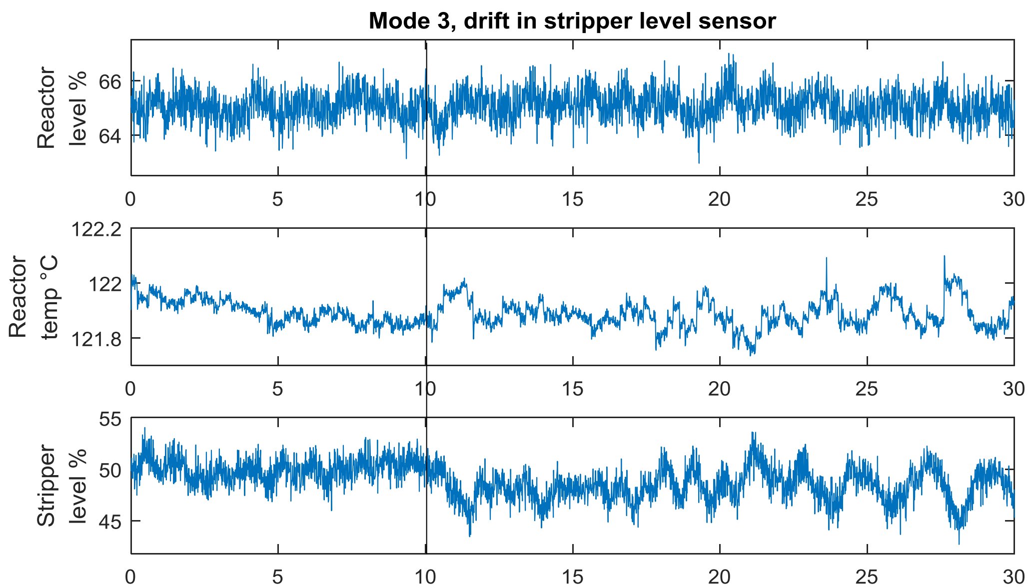

Fig. 41. Process behavior in mode 3 with a drift fault in stripper level sensor. The vertical line shows the start of disturbance

Figure 42 shows the behavior of the process in mode 1 when a random variation disturbance in the cooling water inlet temperature (IDV 11) starts at 10 hours of simulation. Mode 1 behaves similarly to mode 3. The disturbance is in the cooling system of the reactor and has no significant effect on the levels. On the reactor temperature the effect of the fault is immediate. The variation remains within a degree on both sides of the setpoint, and the fastest change is a degree in 10 minutes.

Figure 43 shows the behavior of the process in mode 1 when a stiction fault in the cooling valve (IDV 14) starts at 10 hours of simulation. Mode 1 behaves similarly to mode 3. The disturbance is in the cooling system of the reactor and has no significant effect on the levels. For the reactor temperature the simulation shows high frequency oscillation (a change of 0.8 degrees up and down within 5 minutes). The mean of the temperature follows the setpoint.

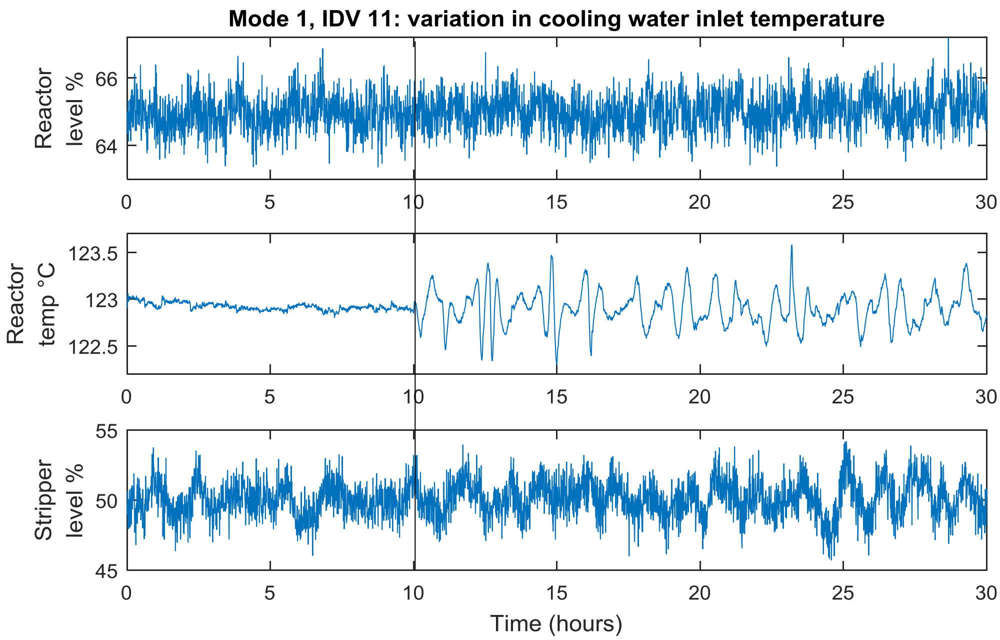

Fig. 42. Process behavior in mode 1 with random variation disturbance in reactor cooling water inlet temperature (IDV 11). The vertical line shows start of disturbance

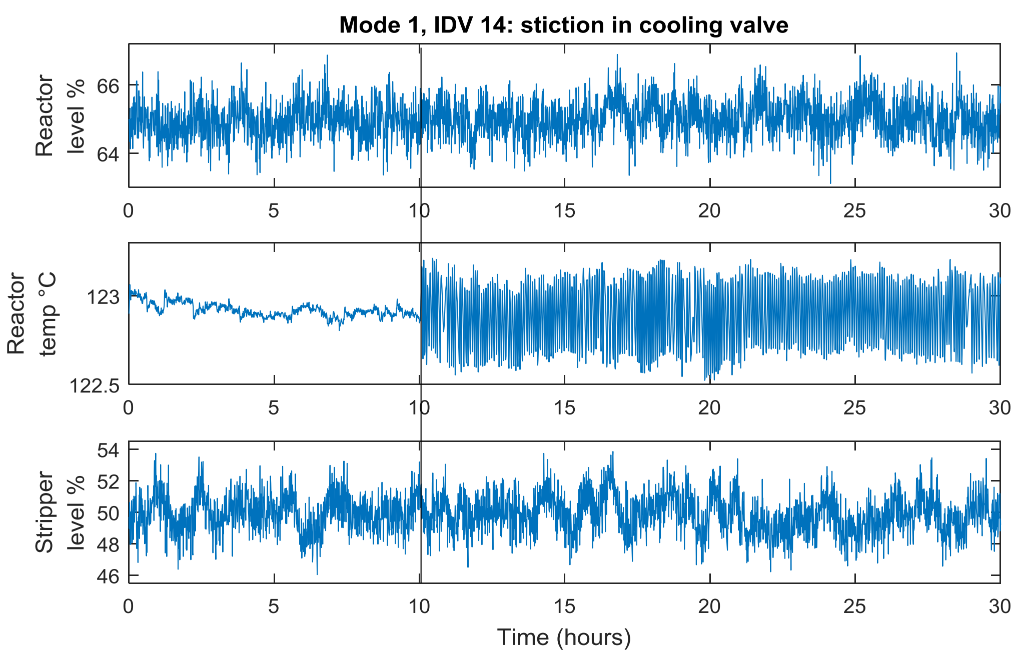

Fig. 43. Process behavior in mode 1 with a stiction fault in reactor cooling valve (IDV 14). The vertical line shows the start of disturbance

Figure 44 shows the behavior of the process in mode 1 when both variation in cooling water temperature and stiction in the valve (IDV 11 and IDV 14) start at 10 hours of simulation. Mode 1 behaves similarly to mode 3. A combination of the two previous faults behaves as would be expected. The variation remains within a degree on both sides of the setpoint, and there are periods of high frequency oscillation.

Figure 45 shows the behavior of the process in mode 1 when a drift shaped fault in the stripper level sensor starts at 10 hours of simulation. Mode 1 behaves similarly to mode 3. The reactor is upstream of the stripper in the process, so faults in the stripper have no effect on reactor level or temperature. A positive drift in the sensor causes the controller to act like the stripper level is higher than it actually is, which results in the real level being proportionally lower than the setpoint.

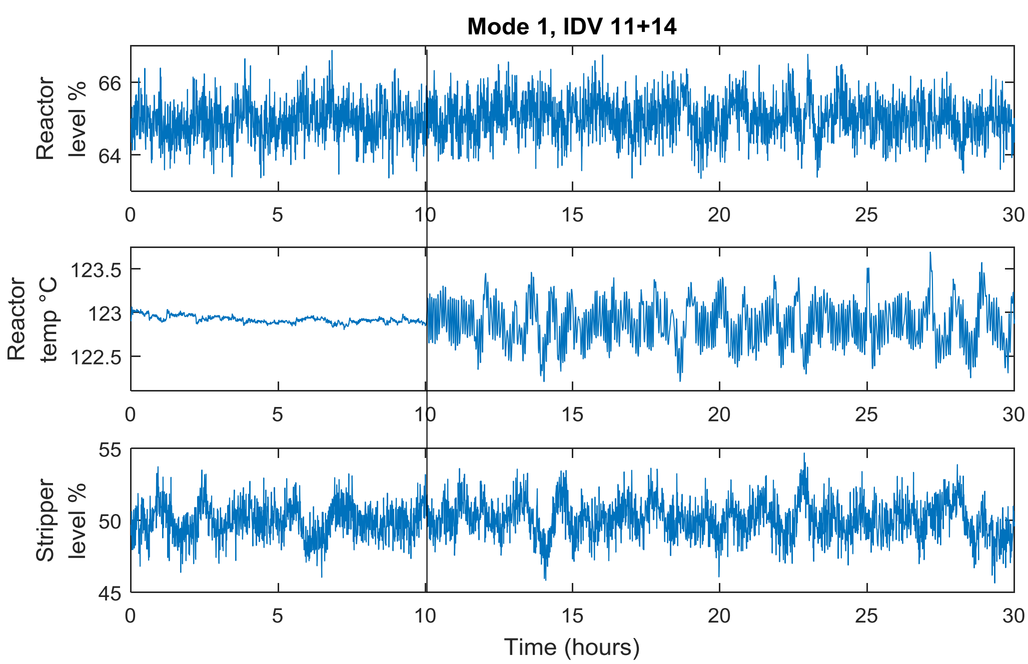

Fig. 44. Process behavior in mode 1 with variation in cooling water temperature and stiction in cooling valve (IDV 11 + IDV 14). The vertical line shows the start of disturbance

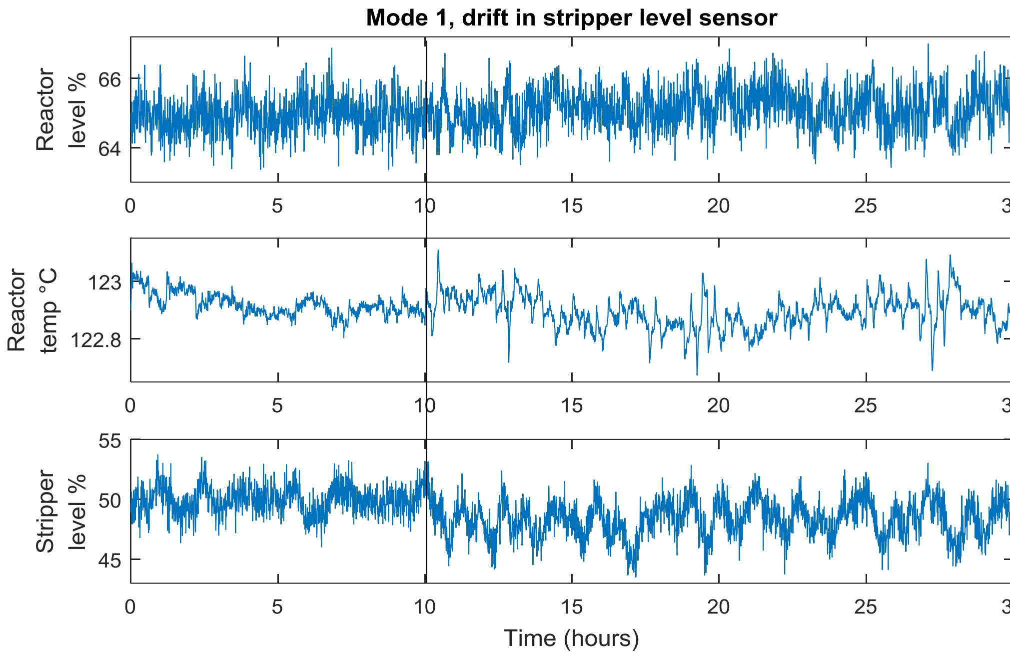

Fig. 45. Process behavior in mode 1 with a drift fault in stripper level sensor. The vertical line shows the start of disturbance

9 Summary and discussion of the results

In the previous chapters the design and testing of a MPC strategy was presented. The implemented control methodology is a supervisory one that provides optimized setpoints to three control loops on the stabilizing lower PI control level. Currently, the MPC itself has unchanging setpoints, but in a real process it would have either a higher level optimizing controller or an operator giving it setpoints.

The aim of the control is to maintain the product quality and production rate even in the case of disturbances and faults. The product composition must stay within 5 mol-% of its setpoint and the production rate must stay within 5 % of its setpoint.

The MPC supervises three loops, and a linear state space model was identified to capture the dynamics of these loops. The MPC parameters; horizons and weights, have been tuned following the general principles about the process dynamics.

From the studied set point changes within the three loops it was found that the MPC performs well, compared to the base PI control, as it able to provide faster response by manipulating the set points for the down level.

The studied mechanical faults affect the expected measurements. IDV 11 and 14 are faults in the cooling system and therefore affect mainly the temperature by producing high frequency oscillations. A drift in a stripper level sensor naturally affects mainly the level measurement as it deviates from its natural value. The obtained results with the proposed MPC strategy show that the controller is able to some extent reduce the produced oscillations in the cases of IDV 11 and IDV 14 by providing optimized set points, thus reducing the end product variability. However, it cannot fully suppress the effects of the faults which will require the implementation of a FDI mechanism. The same effects are observed in the case of a level sensor drift fault, where the MPC is unable to handle the fault, but the system behavior is slightly better compared to the case of base PI control.

The MPC was designed in mode 3 and only the nominal values were changed when testing in mode 1. In real processes, the move from one operating mode to another requires retuning of the controller, as the operation point of the process is changed. In the conducted study, no retuning was made, in order to assess the potential of the designed control strategy to react on regime changes. The obtained results show that the proposed MPC performed reasonably well regardless of the tuning, which proved its flexibility in relation to regime changes.

10 Conclusions

In this thesis the theoretical background of receding horizon (model predictive) control and fault tolerant control were presented. The aim was to design and study the potential of a multivariable MPC, that can later be extended into supervisory fault tolerant control.

In the experimental part a linear MPC was implemented using MATLAB's Model Predictive Control Toolbox. The MPC was tested with various process disturbances and faults in two operating modes.

From the conducted experiments, it was found that the system remained stable in all cases, even though disturbances and faults caused oscillation in the process variables, including the cases when the operational regime was changed. Additionally, the proposed MPC strategy was able to some extent reduce the effects of occurring faults and disturbances, while keeping the end product variability within the admissible margins of 5%. In order to improve the performance of the system a suitable FDI mechanism should be implemented, in order to allow the system to respond to the effects caused by the faults.

From the preformed research, it can be concluded that the designed MPC strategy is operational and able to respond to major system dynamical changes, as it drives the system back to desired operational regions by maintaining lower product variability. Supplying an additional FDI feature will increase the efficiency of the control system, as it will be able to suppress the effects caused by the faults as well.

References

ASSALI, W.A. and MCAVOY, T., 2010. *Optimal Selection of Dominant Measurements and Manipulated Variables for Production Control*. Industrial & Engineering Chemistry Research, **49**(17), pp. 7832-7842.

BATHELT, A., RICKER, N.L. and JELALI, M., 2015. *Revision of the Tennessee Eastman Process Model.* IFAC-PapersOnline, **48**(8), pp. 309-314

BELLMAN, R., 1957. *Dynamic programming.* Princeton: Princeton University Press.

BLANKE, M., KINNAERT, M., LUNZE, J. and STAROSWIECKI, M., 2003. *Diagnosis and fault-tolerant control.* Berlin: Springer.

CAMACHO, E.F. and BORDONS, C., 2007. *Model Predictive Control.* 2nd edn. London: Springer-Verlag London.

CHARITOPOULOS, V.M. and DUA, V., 2016. Explicit model predictive control of hybrid systems and multiparametric mixed integer polynomial programming. *AIChE Journal,* **62**(9), pp. 3441-3460.

CLARKE, D.W., MOHTADI, C. and TUFFS, P.S., 1987. *Generalized predictive control—Part I. The basic algorithm.* Automatica, **23**(2), pp. 137-148.

DENN, M.M., 1986. *Process modeling.* Harlow: Longman.

DOWNS, J.J. and VOGEL, E.F., 1993. A plant-wide industrial process control problem. *Computers and Chemical Engineering,* **17**(3), pp. 245-255.

GANI, A., MHASKAR, P. and CHRISTOFIDES, P.D., 2007. Fault-tolerant control of a polyethylene reactor. *Journal of Process Control,* **17**(5), pp. 439-451.

JIANG, J. and YU, X., 2012. Fault-tolerant control systems: A comparative study between active and passive approaches. *Annual Reviews in Control,* **36**(1), pp. 60-72.

KARRA, S., SHAW, R., PATWARDHAN, S.C. and NORONHA, S., 2008. *Adaptive Model Predictive Control of Multivariable Time-Varying Systems*. Industrial & Engineering Chemistry Research, **47**(8), pp. 2708-2720.

KETTUNEN, M. and JÄMSÄ-JOUNELA, S.-., 2011. Data-based, fault-tolerant model predictive control of a complex industrial dearomatization process. *Industrial and Engineering Chemistry Research,* **50**(11), pp. 6755-6768.

KETTUNEN, M. and JÄMSÄ-JOUNELA, S.-., 2006. Fault tolerant MPC with an embedded FDI system, *IFAC Proceedings Volumes (IFAC-PapersOnline)* 2006, pp. 143-148.

KETTUNEN, M., 2010. *Data-based fault-tolerant model predictive controller an application to a complex dearomatization process*, Aalto-yliopiston teknillinen korkeakoulu.

KÜHL, P., DIEHL, M., KRAUS, T., SCHLÖDER, J.P. and BOCK, H.G., 2010. *A real-time algorithm for moving horizon state and parameter estimation*. Computers & Chemical Engineering, 35(1), pp. 71-83.

LEE, E.B. and MARKUS, L., 1967. *Foundations of optimal control theory.* New York: Wiley.

LENNOX, B., 2005. *Integrating fault detection and isolation with model predictive control*. Int. J. Adapt. Control Signal Process., **19**, pp. 199–212.

LI, L., XIONG, L., XU, O., HU, S. and SU, H., 2015. *Decomposition-based modeling algorithm by CCA-PLS for large scale processes.* American Control Conference (ACC), Chicago, IL, 2015, pp. 1321-1326.

LUPPI, P.A., OUTBIB, R. and BASUALDO, M.S., 2015. *Nominal Controller Design Based on Decentralized Integral Controllability in the Framework of Reconfigurable Fault-Tolerant Structures.* Industrial & Engineering Chemistry Research, **54**(4), pp. 1301-1312.

MACIEJOWSKI, J.M., 2002. *Predictive control : with constraints.* Harlow: Pearson Education.

MAHMOUD, M. and XIA, Y., 2013. *Analysis and Synthesis of Fault-Tolerant Control Systems.* Oxford: Wiley.

MAGNI, L., OPIZZI, S. AND SCATTOLINI, R., 2001. *Tracking of non-square nonlinear systems via model predictive control.* European Control Conference (ECC), Porto, 2001, pp. 951-956.

MATWORKS, 2017a. Model Predictive Control Toolbox. Available: https://se.mathworks.com/help/mpc/index.html

MATHWORKS, 2017b. MPC Modeling. Available: https://se.mathworks.com/help/mpc/gs/mpc-modeling.html

MATHWORKS, 2017c. Optimization Problem. Available: https://se.mathworks.com/help/mpc/ug/optimization-problem.html

MATHWORKS, 2017d. QP Solver. Available: https://se.mathworks.com/help/mpc/ug/qp-solver.html

MAYNE, D.Q., 2014. Model predictive control: Recent developments and future promise. *Automatica,* **50**(12), pp. 2967-2986.

MHASKAR, P., LIU, J. and CHRISTOFIDES, P.D., 2013. *Fault-tolerant process control : methods and applications.* London ; New York: Springer.

NOURA, H., THEILLIOL, D., PONSART, J.-. and CHAMSEDDINE, A., 2009. *Fault-tolerant Control Systems.* Springer London.

OGUNNAIKE, B.A. and RAY, W.H., 1994. *Process dynamics, modelling, and control.* 1st edn. New York: Oxford University Press.

PARK, B.-., LEE, J.-. and KWON, W.H., 1999. Robust one-step receding horizon control for constrained systems. *International Journal of Robust and Nonlinear Control,* **9**(7), pp. 381-395.

PRETT, D.M. and MORARI, M., 1987. *Shell Process Control Workshop.* Stoneham: Butterworth Publishers.

RICHALET, J., RAULT, A., TESTUD, J.L. and PAPON, J., 1976. Algorithmic control of industrial processes. *Proceedings of the Fourth IFAC symposium on identification and system parameter estimation,* , pp. 1119-1167.

RICKER, N.L., 23.01.2015, 2015-last update, Tennessee Eastman Challenge Archive. Available: http://depts.washington.edu/control/LARRY/TE/download.html2017].

RICKER, N.L., 1996. *Decentralized control of the Tennessee Eastman Challenge Process.*

RICKER, N.L. and LEE, J.H., 1995. *Nonlinear model predictive control of the Tennessee Eastman challenge process.* Computer & Chemical Engineering, **19**(9), pp. 961-981.

SCHMID, C. AND BIEGLER, L.T., 1994. *Quadratic programming methods for reduced Hessian SQP.* Computer & Chemical Engineering, **18**(9), pp. 817-832.

SHAO, Q.M. and CINAR, A., 2015.*Coordination scheme and target tracking for distributed model predictive control.* Chemical Engineering Science, **136**, pp. 20-26.

SIMANI, S., ALVISI, S. and VENTURINI, M., 2016. *Fault tolerant model predictive control applied to a simulated hydroelectric system,* 2016 3rd Conference on Control and Fault-Tolerant Systems (SysTol) 2016, pp. 251-256.

SERON, M.M., GOODWIN, G.C. and DE DONA, J.A., 2003. *Characterization of receding horizon control for constrained linear systems.* Asian Journal of Control*,* **5**(2), pp. 271-286.

SJÖBERG, J., ZHANG, Q., LJUNG, L., BENVENISTE, A., DELYON, B., GLORENNEC, P., HJALMARSSON, H. and JUDITSKY, A., 1995. *Nonlinear black-box modeling in system identification: a unified overview.*

SOURANDER, M., VERMASVUORI, M., SAUTER, D., LIIKALA, T. and JÄMSÄ-JOUNELA, S.-., 2009. *Fault tolerant control for a dearomatisation process.* Journal of Process Control*,* **19**(7), pp. 1091-1102.

SRINIWAS, G.R. and ARKUN, Y., 1997. *Control of the Tennessee Eastman process using input-output models.* Journal of Process Control, **7**(5), pp. 387-400.

TIAN, Z. and HOO, K.A., 2005. *Multiple Model-Based Control of the Tennessee-Eastman Process.* Industrial & Engineering Chemistry Research, **44**(9), pp. 3187-3202.

VALLERIO, M., IMPE, J.V. and LOGIST, F., 2014. *Tuning of NMPC controllers via multi-objective optimisation.* Computers & Chemical Engineering, **61**, pp. 38-50.

YEH, T.-M., HUANG, M.-C. and HUANG, C.-T., 2003. *Estimate of process compositions and plantwide control from multiple secondary measurements using artificial neural networks.* Computers & Chemical Engineering, **27**(1), pp. 55-72.

YIN, S., DING, S.X., HAGHANI, A., HAO, H. and ZHANG, P., 2012. *A comparison study of basic data-driven fault diagnosis and process monitoring methods on the benchmark Tennessee Eastman process.* Journal of Process Control, **22**(9), pp. 1567-1581.

YIN, S., LUO, H. and DING, S.X., 2014. *Real-Time Implementation of Fault-Tolerant Control Systems With Performance Optimization.* IEEE Transactions on Industrial Electronics, **61**(5), pp. 2402-2411.

ZAKHAROV, A., YU, M. and JAMSA-JOUNELA, S.-., 2014. A dynamic prognosis algorithm in distributed fault tolerant model predictive control, *2014 IEEE Conference on Control Applications, CCA 2014* 2014, pp. 1238-1243.

ZHENG, A., 1998. *Nonlinear model predictive control of the Tennessee Eastman process.* PRoceedings of the 1998 American Control Conference (ACC), Philadelphia, PA, 1998, pp. 1700-1704.

Appendix 1. Revised model tables

Added measurements: Table A1

Process disturbances: Table A2

Monitoring outputs (internal values of reactor and process): Table A3

Table A1. Outputs of the revised model

Number	Description	Base value	Unit
1 – 41	see tables C and D	-	-
42	Temperature A feed (stream 1)	45	°C
43	Temperature D feed (stream 2)	45	°C
44	Temperature E feed (stream 3)	45	°C
45	Temperature A and C feed (stream 4)	45	°C
46	Reactor cooling water inlet temperature	35	°C
47	Reactor cooling water flow	93.37	m3/h
48	Condenser cooling water inlet temperature	40	°C
49	Condenser cooling water flow	49.37	m3/h
50 – 55	Composition of A feed (stream 1); components A through F	base values of outputs 52 – 75 are given in table 1 of [Downs and Vogel]	mol%
56 – 61	Composition of D feed (stream 2); components A through F		mol%
62 – 67	Composition of E feed (stream 3); components A through F		mol%
68 – 73	Composition of A and C feed (stream 4); components A through F		mol%

Table A2. Monitoring output of random-variation-disturbances

Number	IDV	Description	Unit
1	8	A composition in stream 4	mol%
2	8	B composition in stream 4	mol%
3	8	C composition in stream 4	mol%
4	9	D feed temperature (stream 2)	°C
5	10	A and C feed temperature (stream 4)	°C
6	11	Reactor cooling water inlet temperature	°C
7	12	Condenser cooling water inlet temperature	°C
8	13	Deviation in reaction kinetics	1
9	13	Deviation in reaction kinetics	1
10	16	Deviation in the heat transfer of the heat exchanger (originally specified as unknown)	1
11	17	Deviation in heat transfer in reactor (originally specified as unknown)	1
12	18	Deviation in heat transfer in condenser (originally specified as unknown)	1

13	20	unknown	1
14	21	A feed temperature (stream 1)	°C
15	22	E feed temperature (stream 3)	°C
16	23	A feed flow (stream 1)	kmol/h
17	24	D feed flow (stream 2)	kmol/h
18	25	E feed flow (stream 3)	kmol/h
19	26	A and C feed flow (stream 4)	kmol/h
20	27	Reactor cooling water flow	m3/h
21	28	Condenser cooling water flow	m3/h

Table A3. Monitoring output of reaction and process; values 1 - 15 are related to the reactor

Number	Description	Unit
1	Substance conversion rate component A	kmol/h
2	Substance conversion rate component C	kmol/h
3	Substance conversion rate component D	kmol/h
4	Substance conversion rate component E	kmol/h
5	Substance conversion (production) rate component F	kmol/h
6	Substance conversion (production) rate component G	kmol/h
7	Substance conversion (production) rate component H	kmol/h
8	Partial pressure of component A	kPa abs
9	Partial pressure of component B	kPa abs
10	Partial pressure of component C	kPa abs
11	Partial pressure of component D	kPa abs
12	Partial pressure of component E	kPa abs
13	Partial pressure of component F	kPa abs
14	Partial pressure of component G	kPa abs
15	Partial pressure of component H	kPa abs
16 - 21	Delay-free and disturbance-free measurements of reactor feed analysis	mol%
22 - 29	Delay-free and disturbance-free measurements of purge gas analysis	mol%
30 - 34	Delay-free and disturbance-free measurements of product analysis	mol%
35 - 40	Delay-free and disturbance-free measurements of feed A analysis	mol%
41 - 46	Delay-free and disturbance-free measurements of feed D analysis	mol%
47 - 52	Delay-free and disturbance-free measurements of feed E analysis	mol%
53 - 58	Delay-free and disturbance-free measurements of feed C analysis	mol%
59	Production costs related to product amount based on measurements	ct/(kmol product)
60	Production costs related to product amount based on disturbance free process values	ct/(kmol product)
61	Production costs related to time based on measurements	$/h
62	Production costs related to time based on dist. free process values	$/h

Appendix 2. Quality and Cost graphs

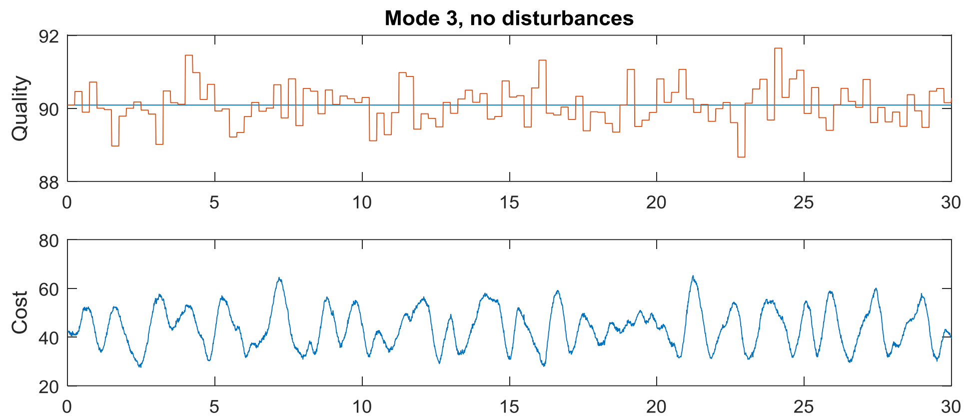

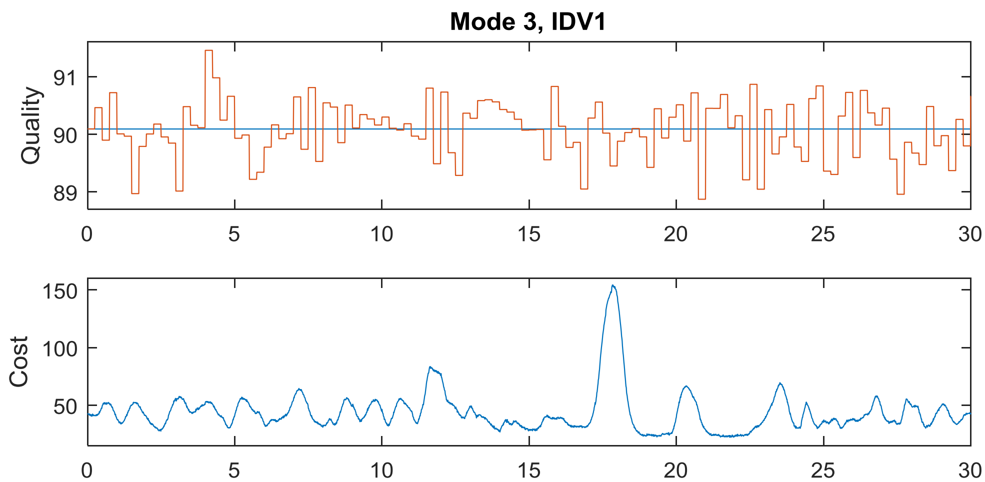

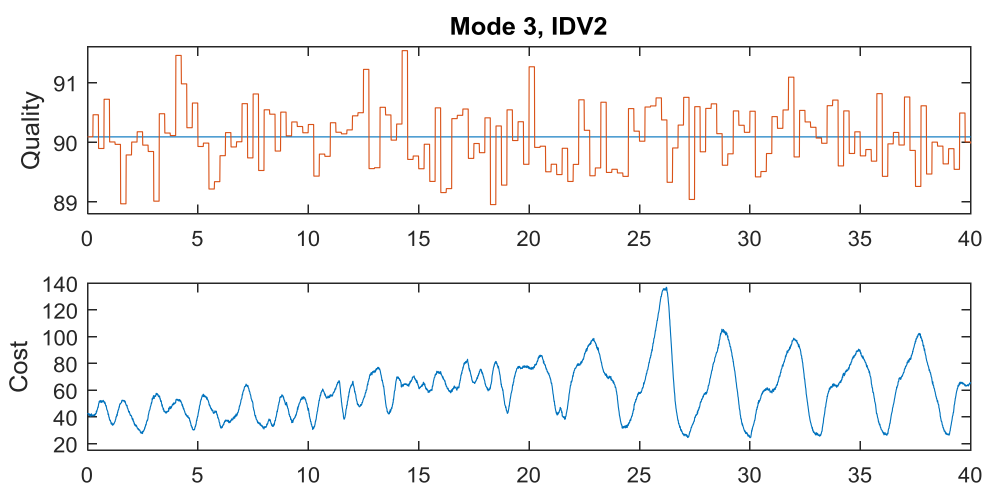

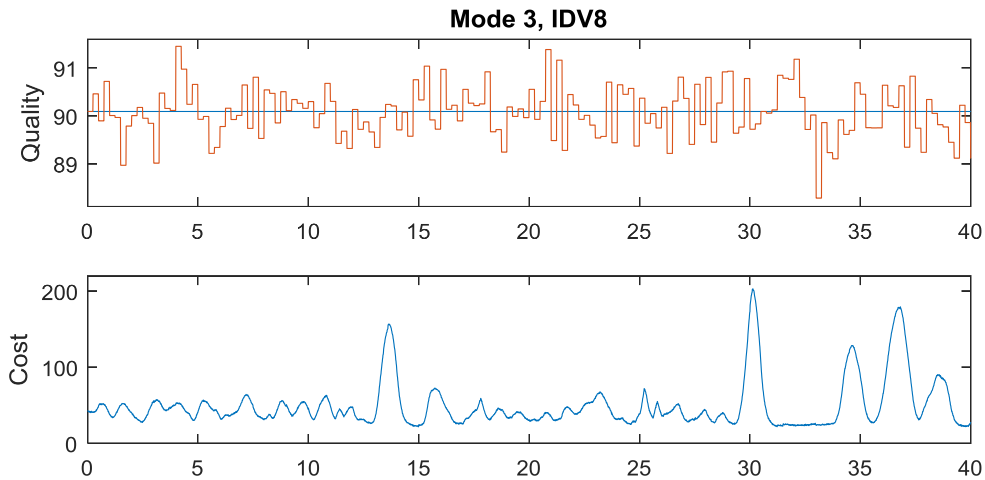
Mode 3, IDV8
Quality
91
90
89
0
5
10
15
20
25
30
35
40
Cost
200
100
0
0
5
10
15
20
25
30
35
40

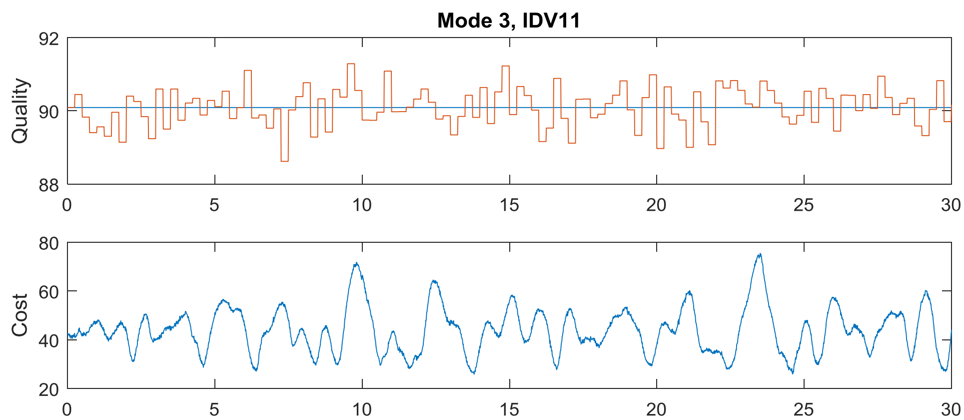
Mode 3, IDV11
Quality
92
90
88
0
5
10
15
20
25
30
Cost
80
60
40
20
0
5
10
15
20
25
30

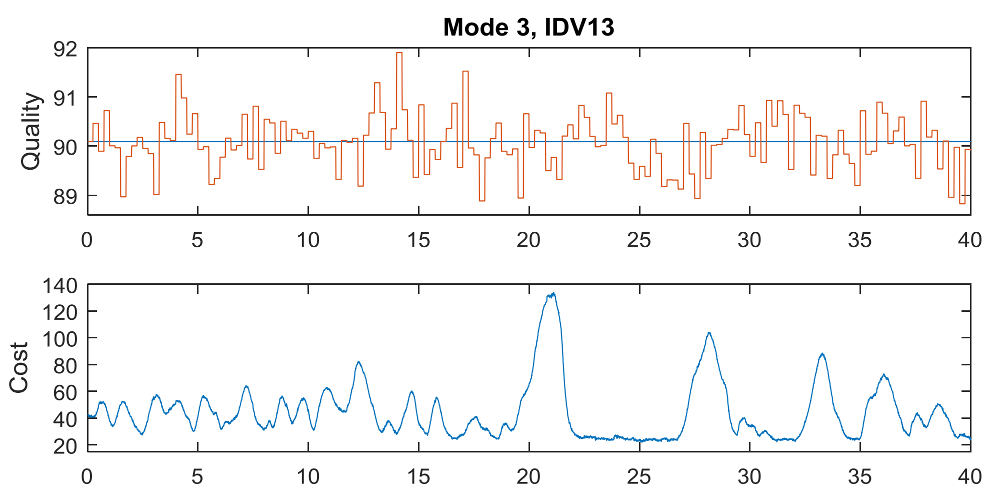
Mode 3, IDV13
Quality
92
91
90
89
0
5
10
15
20
25
30
35
40
Cost
140
120
100
80
60
40
20
0
5
10
15
20
25
30
35
40

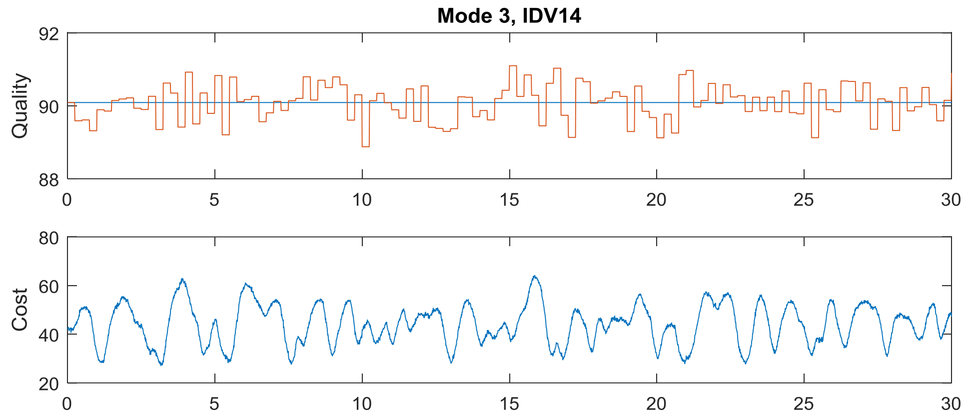
Mode 3, IDV14
Quality
Cost

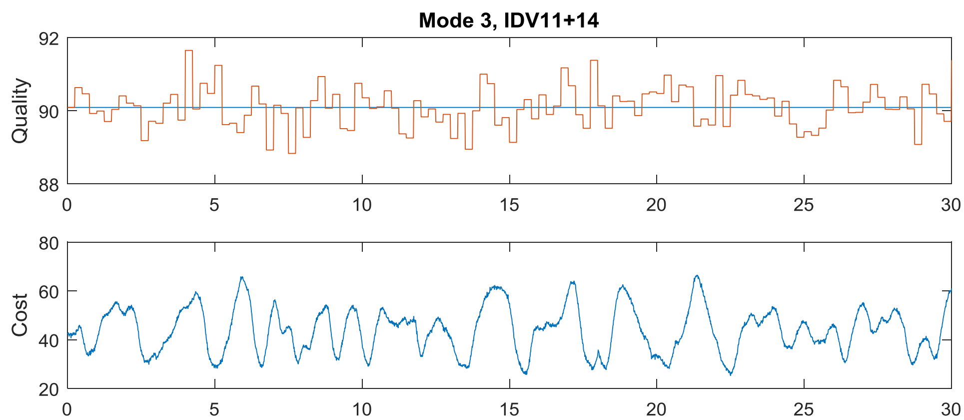
Mode 3, IDV11+14
Quality
Cost

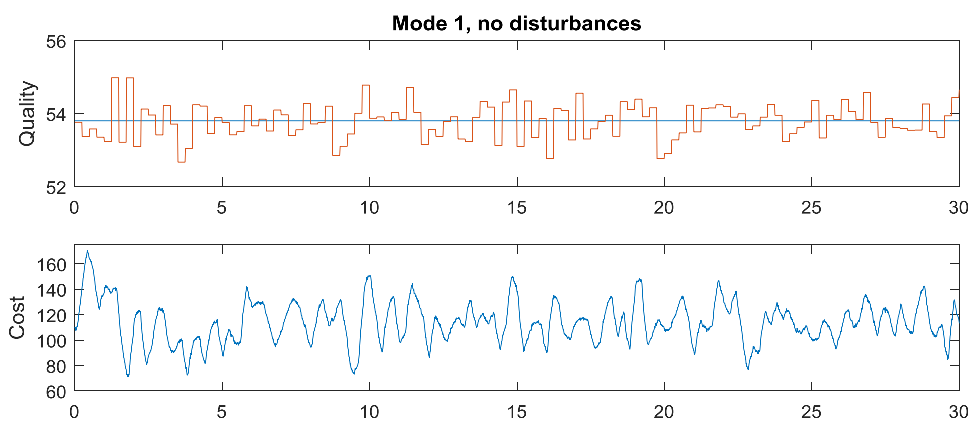
Mode 1, no disturbances
Quality
Cost

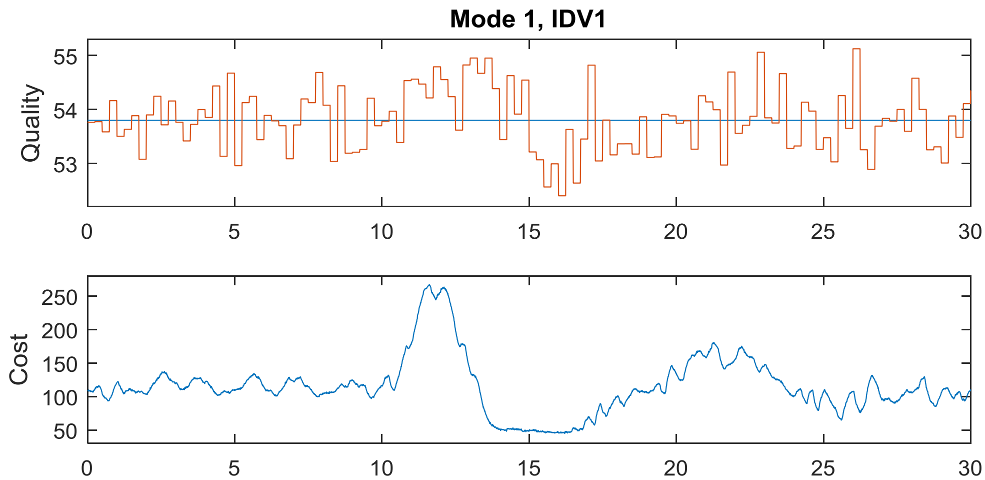
Mode 1, IDV1
Quality
Cost

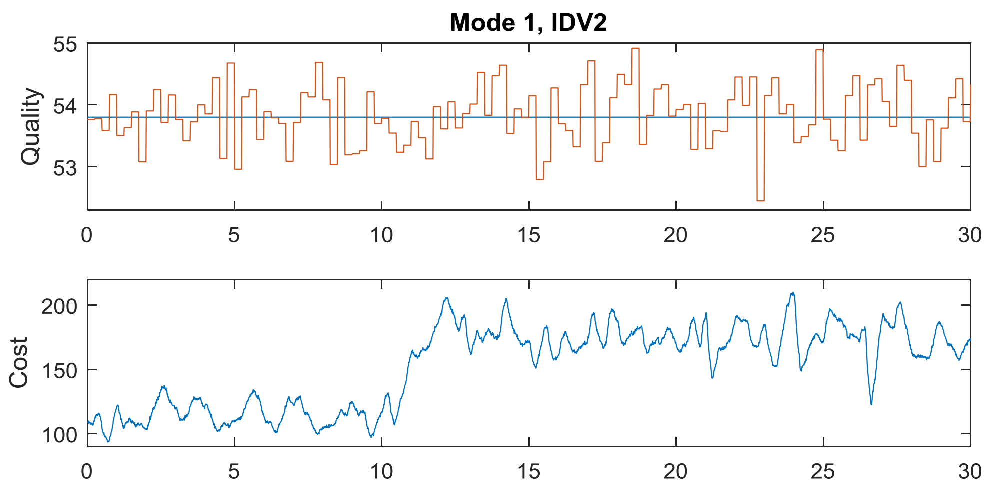
Mode 1, IDV2
Quality
Cost

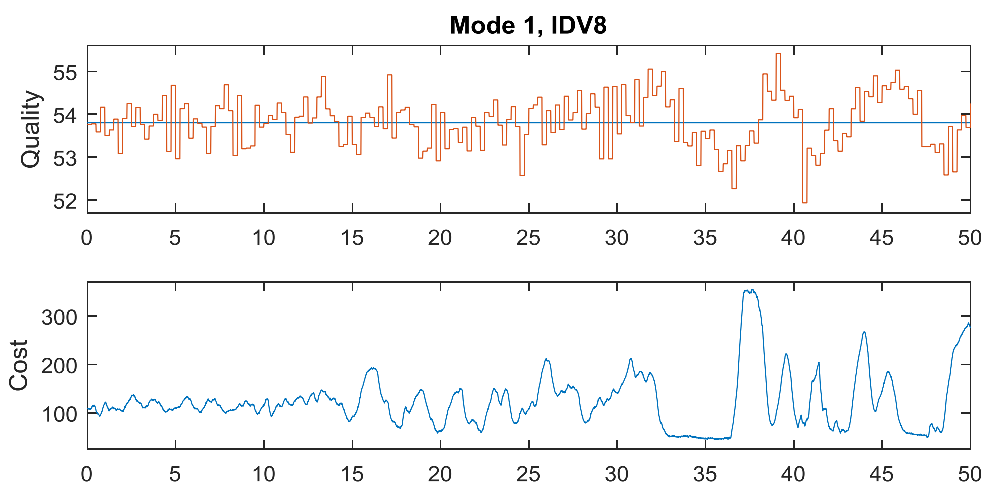
Mode 1, IDV8
Quality
Cost

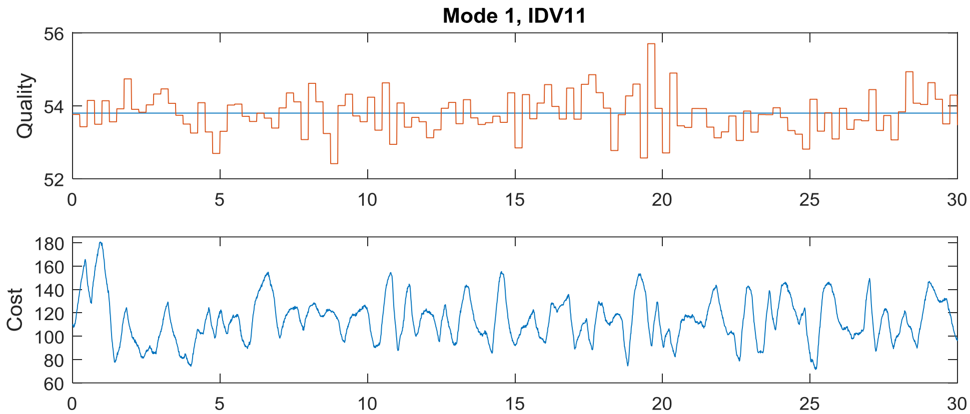
Mode 1, IDV11
Quality
Cost

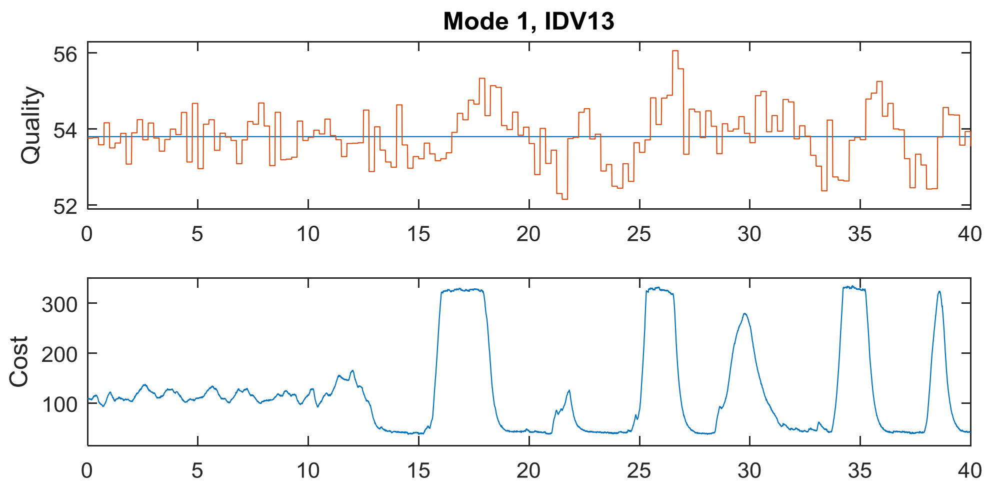
Mode 1, IDV13
Quality
Cost

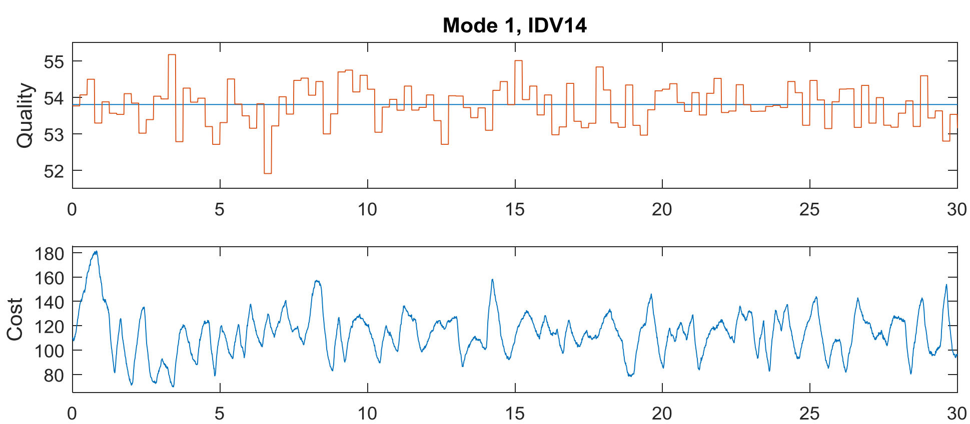
Mode 1, IDV14
Quality
Cost

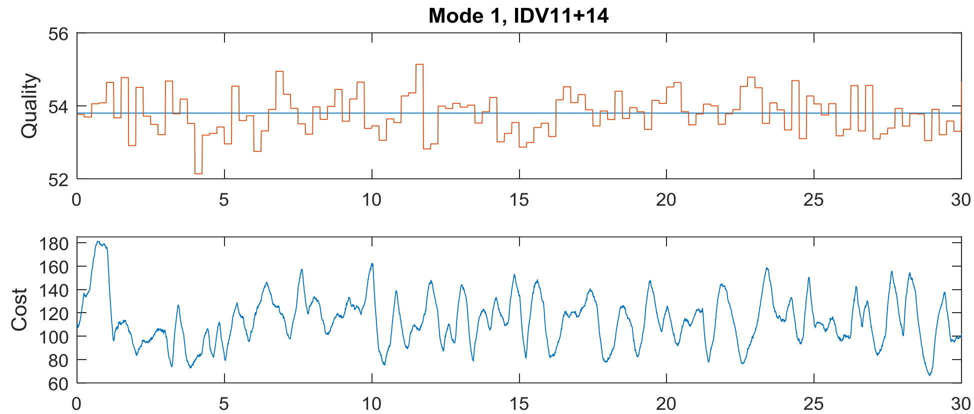

Mode 1, IDV11+14
Quality
56
54
52
0
5
10
15
20
25
30
Cost
180
160
140
120
100
80
60
0
5
10
15
20
25
30

Appendix 3 Dynamic behavior

1: A feed , 2: D feed, 3: E feed, 4: A and C feed, 5: recycle flow, 6: reactor feed rate, 7: reactor pressure, 11: separator temperature, 12: separator level, 13: separator pressure, 16: stripper pressure, 18: stripper temperature, 23: feed analysis A, 24: feed analysis B, 25: feed analysis C, 26: feed analysis D, 27: feed analysis E, 37: product analysis D, 38: product analysis E, 39: product analysis F

Mode 3

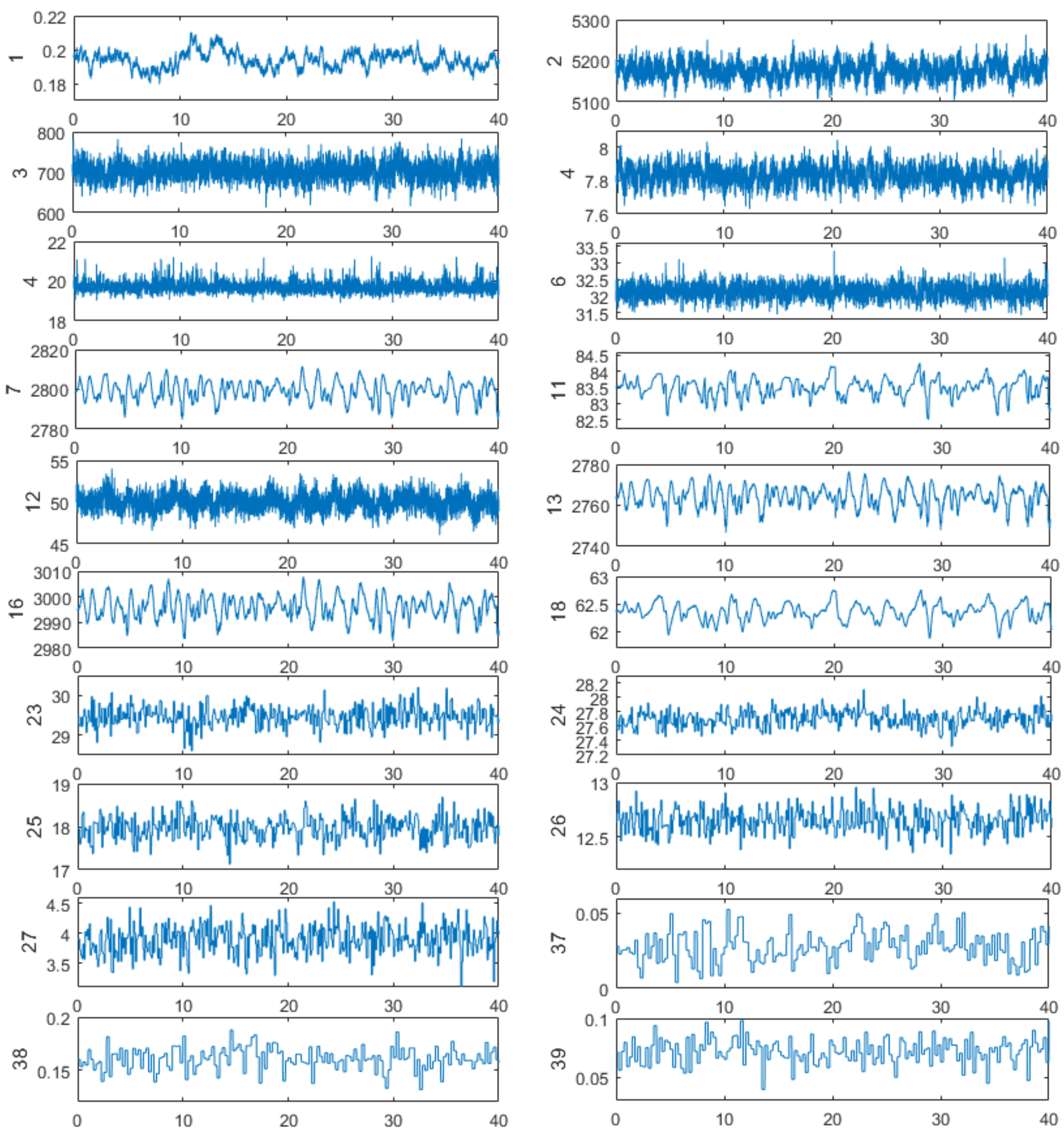

No disturbances

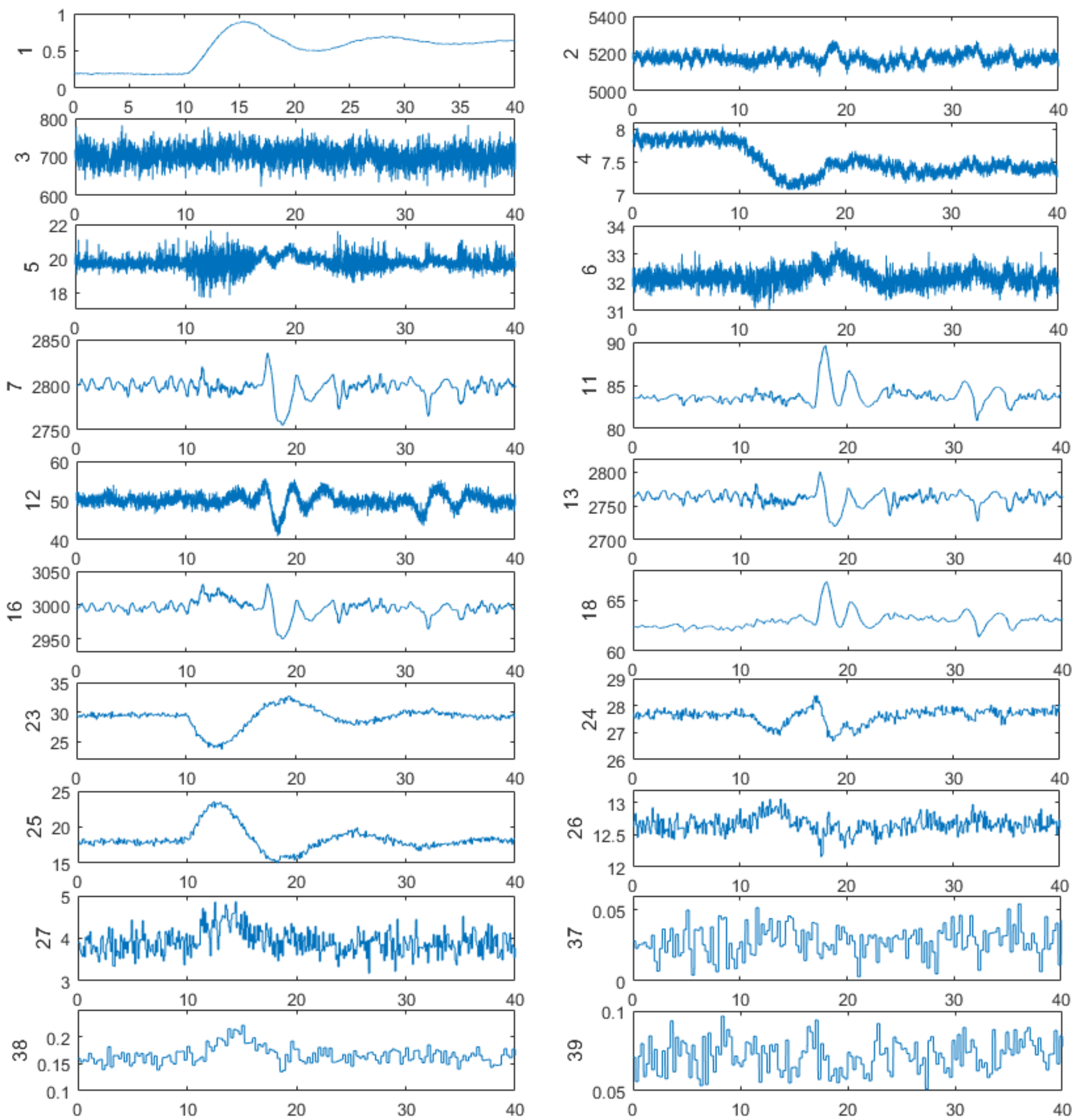

IDV1

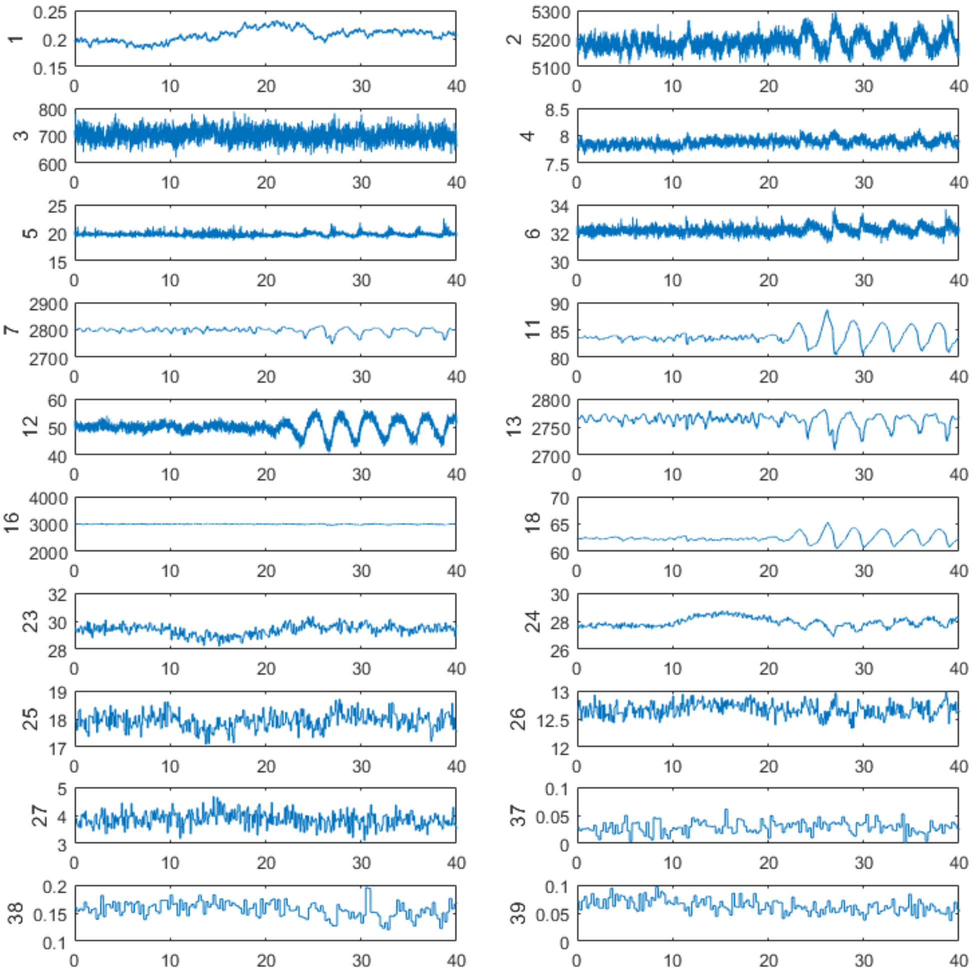
1
0.25
0.2
0.15
2
5300
5200
5100
3
800
700
600
4
8.5
8
7.5
5
25
20
15
6
34
32
30
7
2900
2800
2700
11
90
85
80
12
60
50
40
13
2800
2750
2700
16
4000
3000
2000
18
70
65
60
23
32
30
28
24
30
28
26
25
19
18
17
26
13
12.5
12
27
5
4
3
37
0.1
0.05
0
38
0.2
0.15
0.1
39
0.1
0.05
0
0
10
20
30
40

IDV2

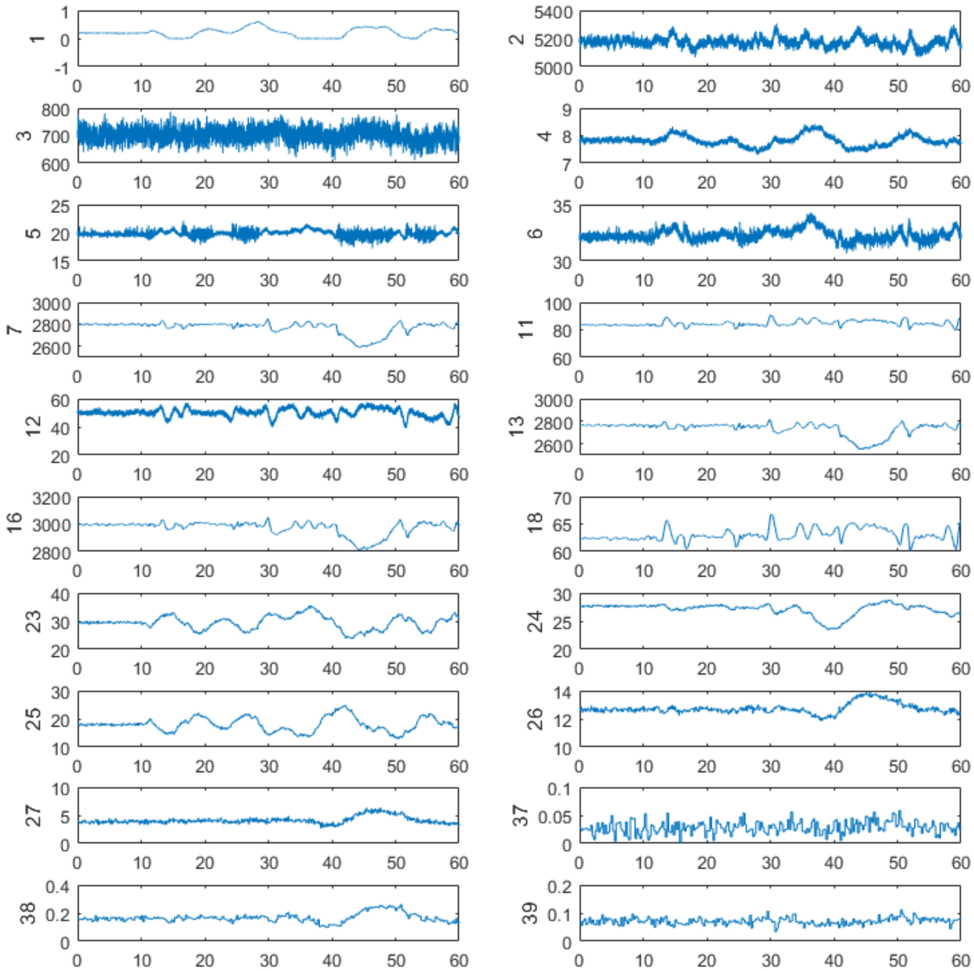

IDV8

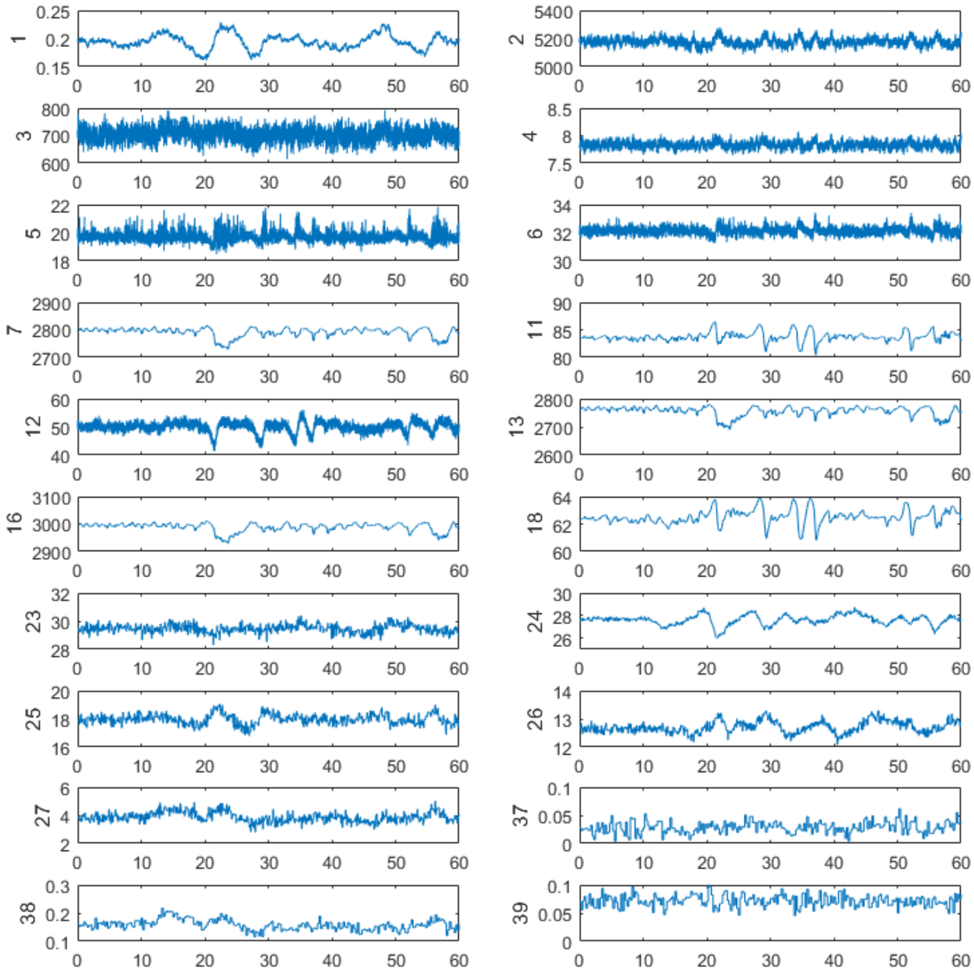

IDV13

Mode 1

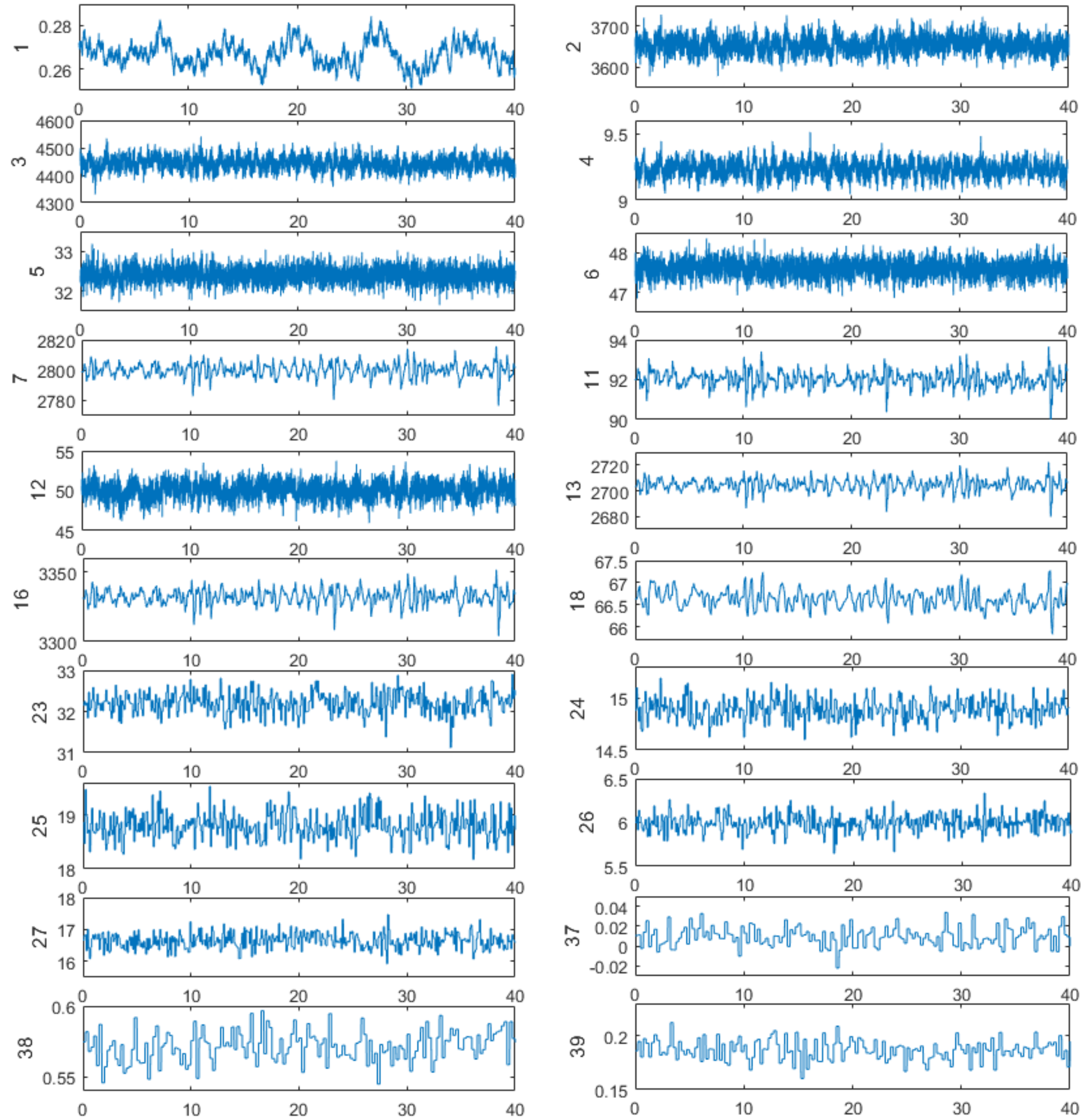

No disturbances

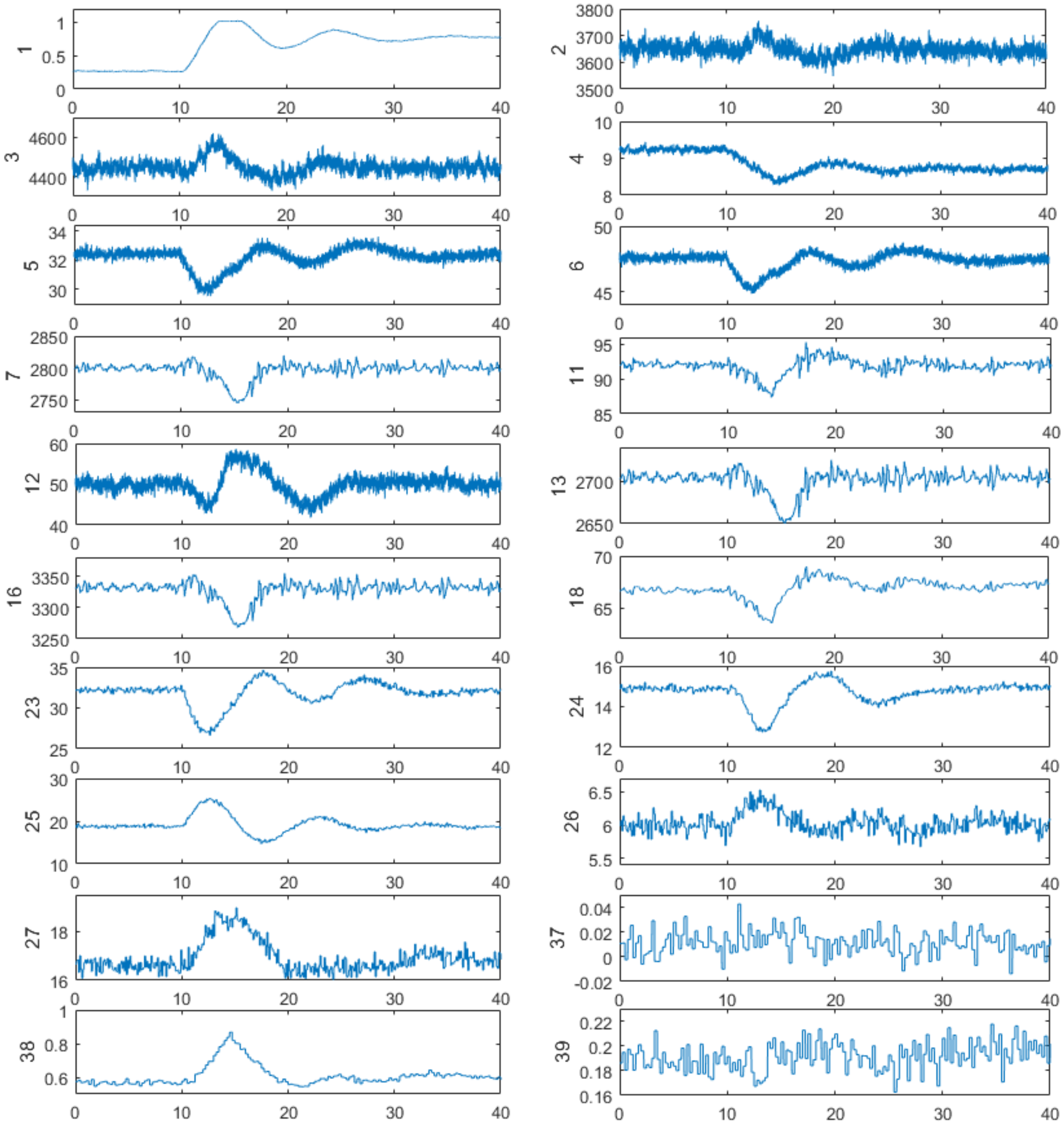

IDV1

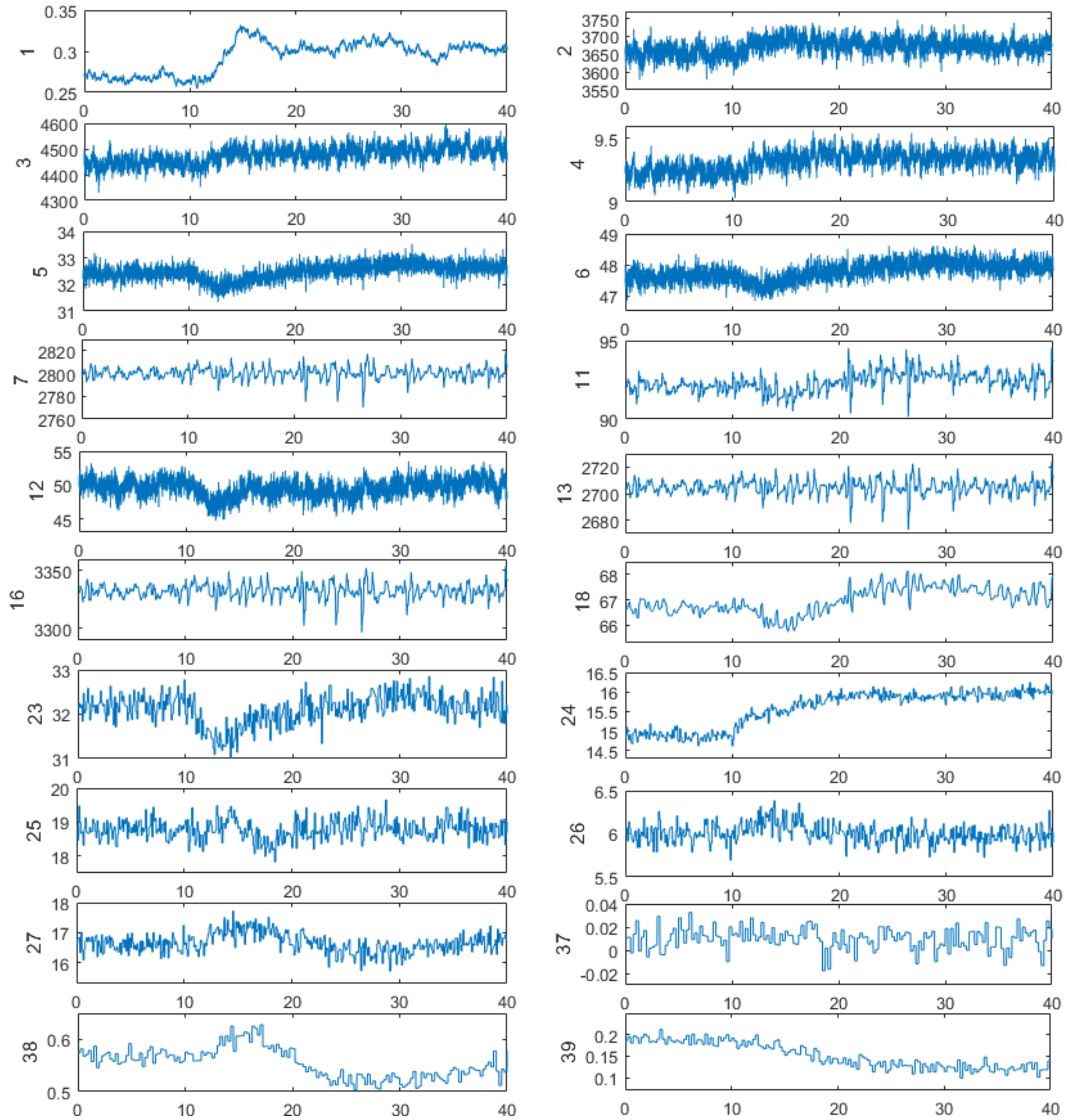
1 0.35 0.3 0.25
2 3750 3700 3650 3600 3550
3 4600 4500 4400 4300
4 9.5 9
5 34 33 32 31
6 49 48 47
7 2820 2800 2780 2760
11 95 90
12 55 50 45
13 2720 2700 2680
16 3350 3300
18 68 67 66
23 33 32 31
24 16.5 16 15.5 15 14.5
25 20 19 18
26 6.5 6 5.5
27 18 17 16
37 0.04 0.02 0 -0.02
38 0.6 0.5
39 0.2 0.15 0.1

IDV2

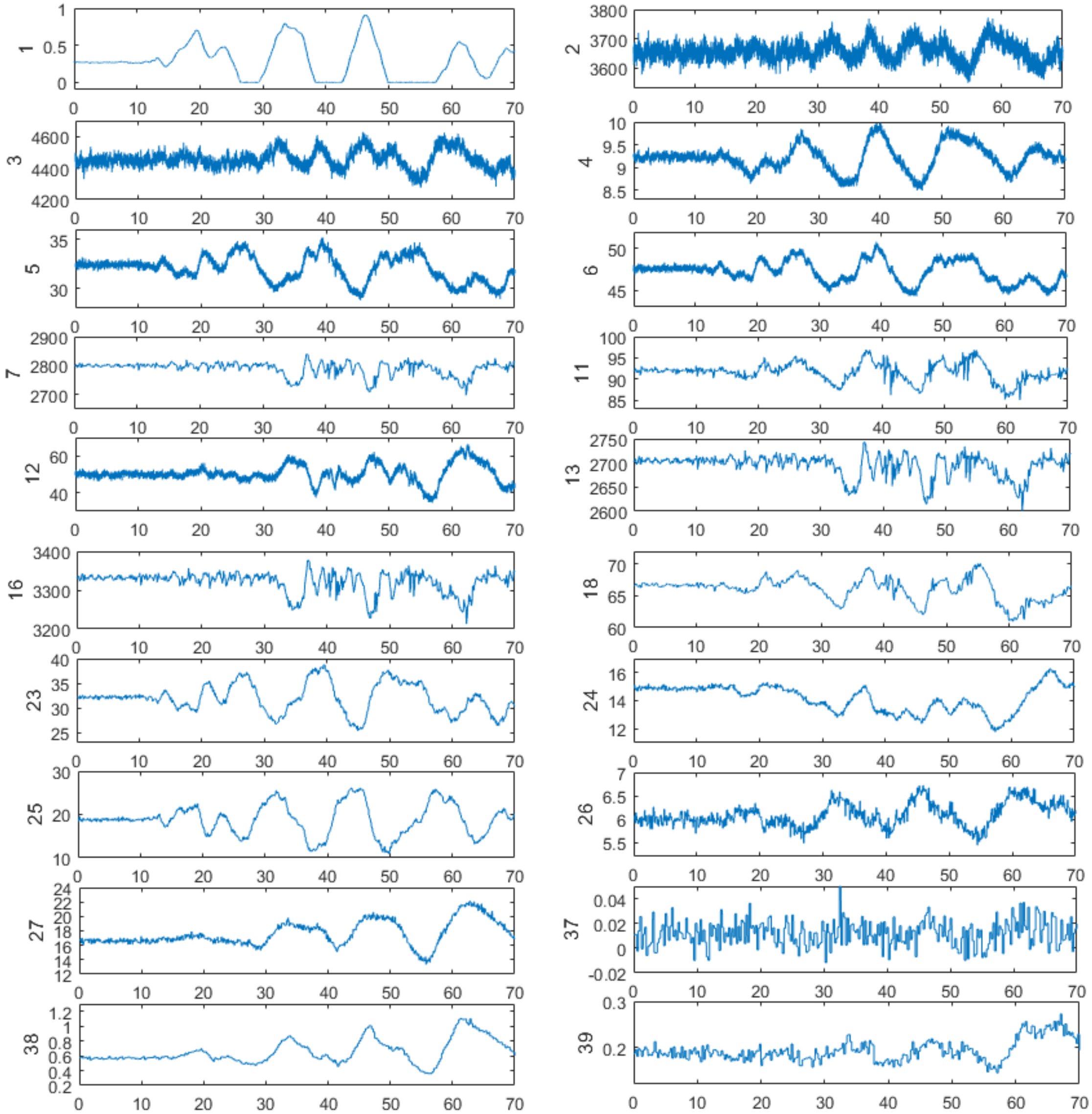

IDV8

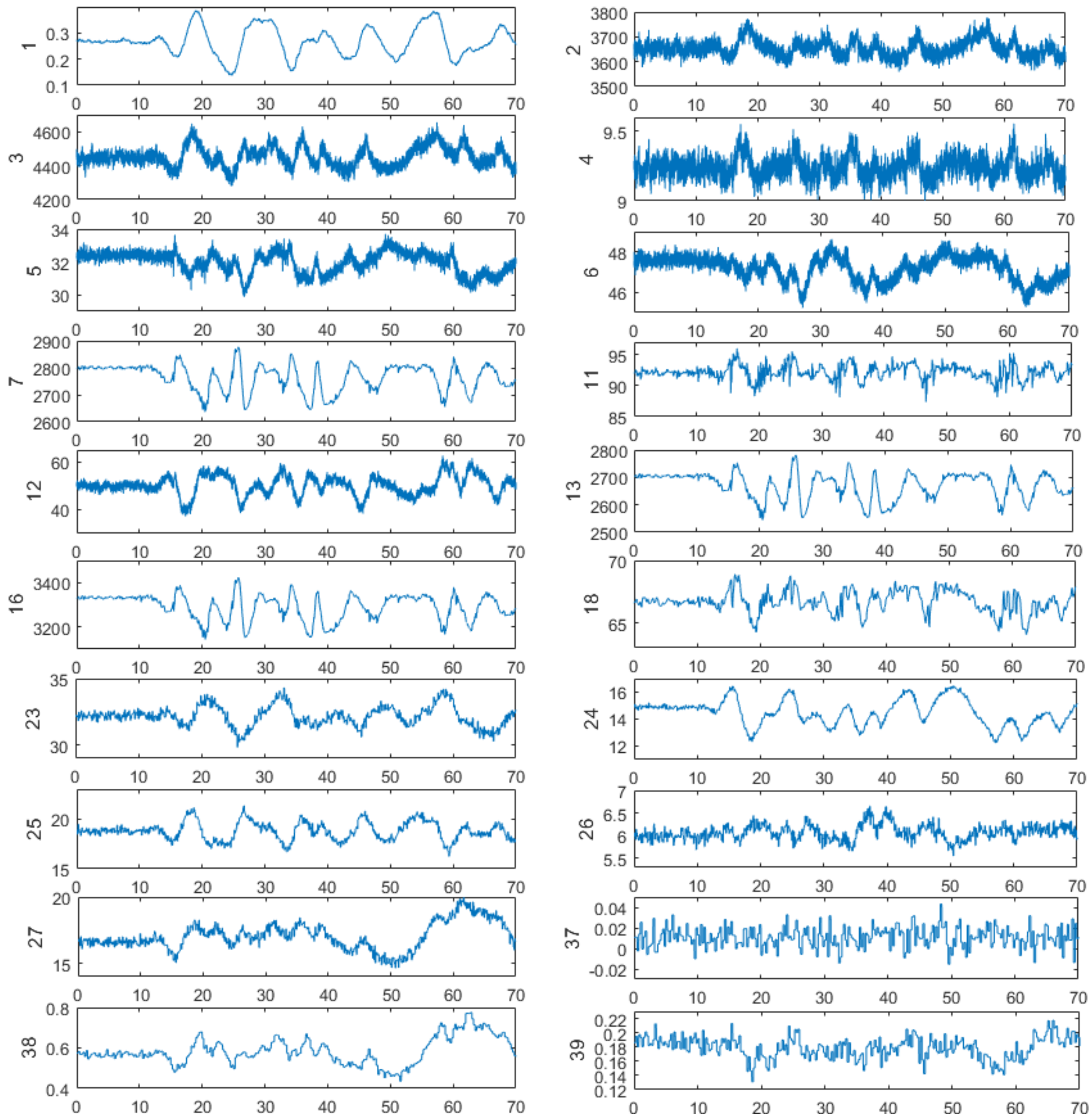

IDV13

Appendix 4. Comparison of PI and MPC

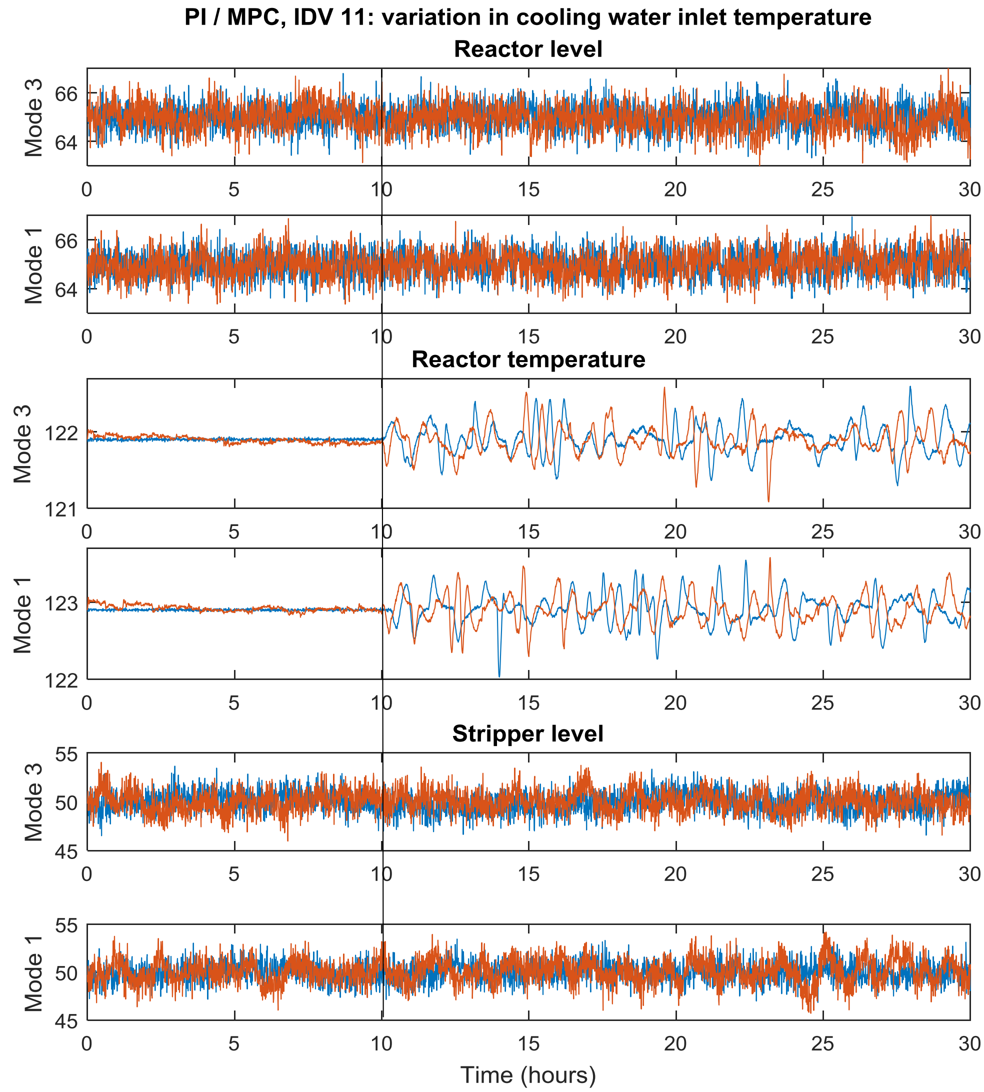

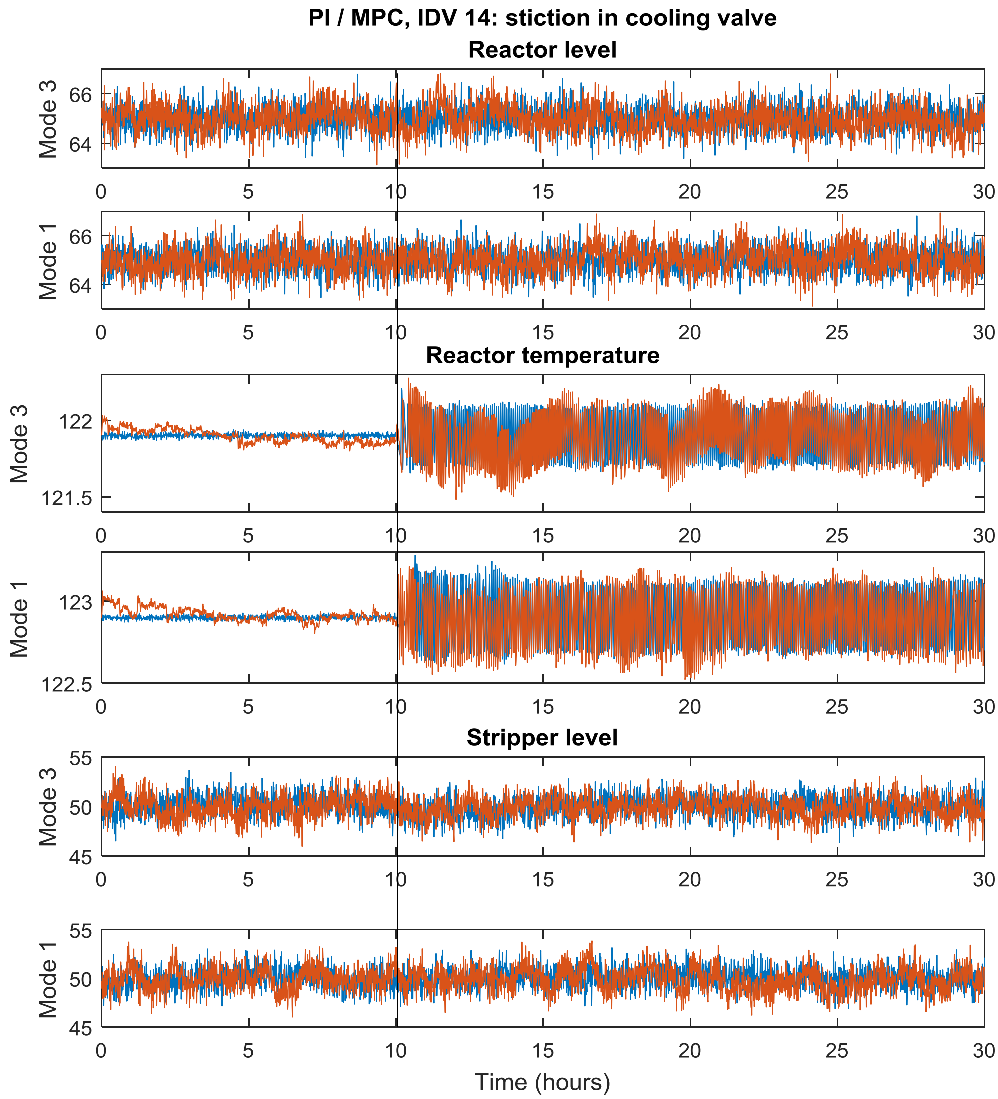
PI / MPC, IDV 14: stiction in cooling valve
Reactor level
Mode 3
Mode 1
Reactor temperature
Mode 3
Mode 1
Stripper level
Mode 3
Mode 1
Time (hours)

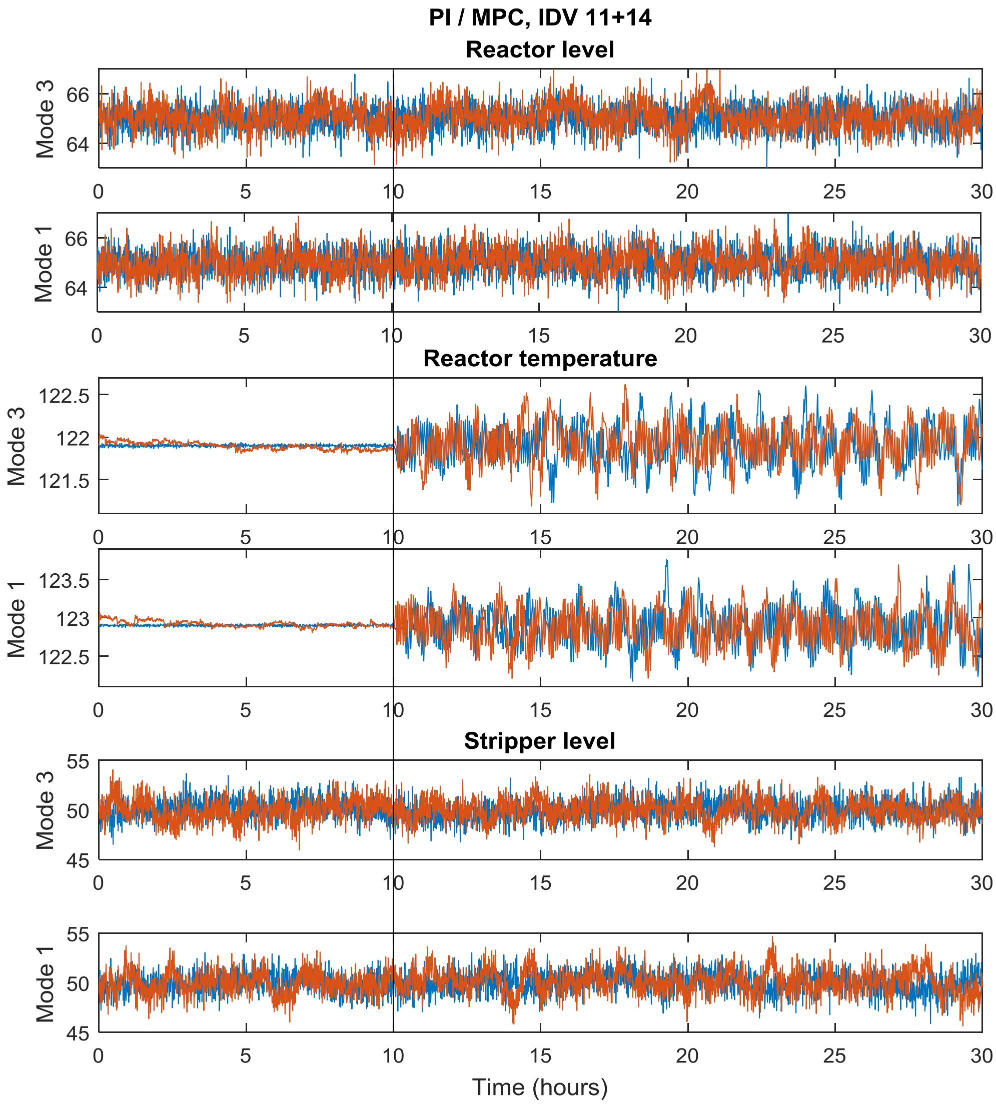
PI / MPC, IDV 11+14
Reactor level
Mode 3
Mode 1
Reactor temperature
Mode 3
Mode 1
Stripper level
Mode 3
Mode 1
Time (hours)

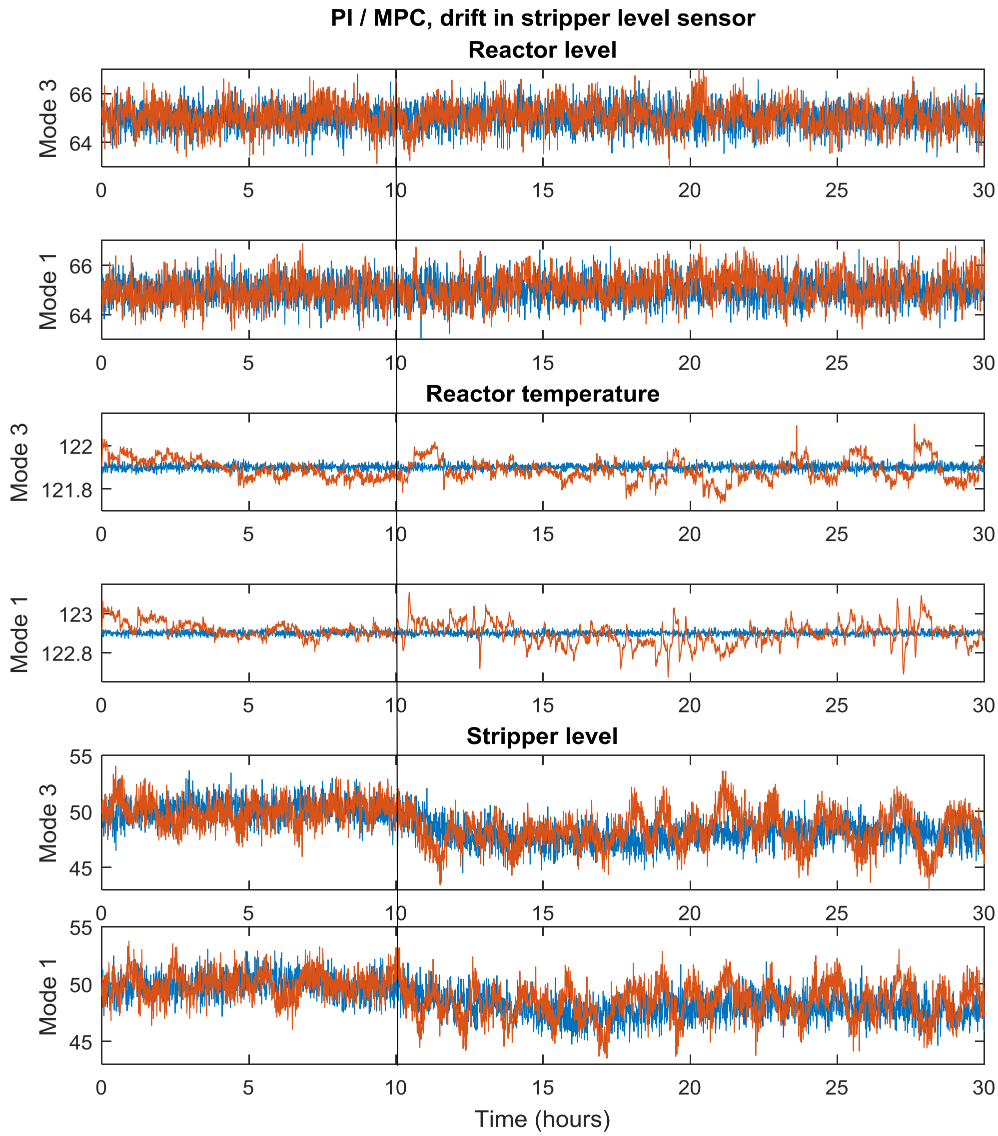
PI / MPC, drift in stripper level sensor
Reactor level
Mode 3
Mode 1
Reactor temperature
Mode 3
Mode 1
Stripper level
Mode 3
Mode 1
Time (hours)